



Paired electron pockets in the hole-doped cuprates

Talk online: sachdev.physics.harvard.edu



Paired electron pockets in the hole-doped cuprates



Hole dynamics in an antiferromagnet across a deconfined quantum critical point, R. K. Kaul, A. Kolezhuk, M. Levin, S. Sachdev, and T. Senthil, *Physical Review B* **75**, 235122 (2007).

Algebraic charge liquids and the underdoped cuprates, R. K. Kaul, Y. B. Kim, S. Sachdev, and T. Senthil, *Nature Physics* **4**, 28 (2008).

Destruction of Neel order in the cuprates by electron doping, R. K. Kaul, M. Metlitski, S. Sachdev, and C. Xu, *Physical Review B* **78**, 045110 (2008).

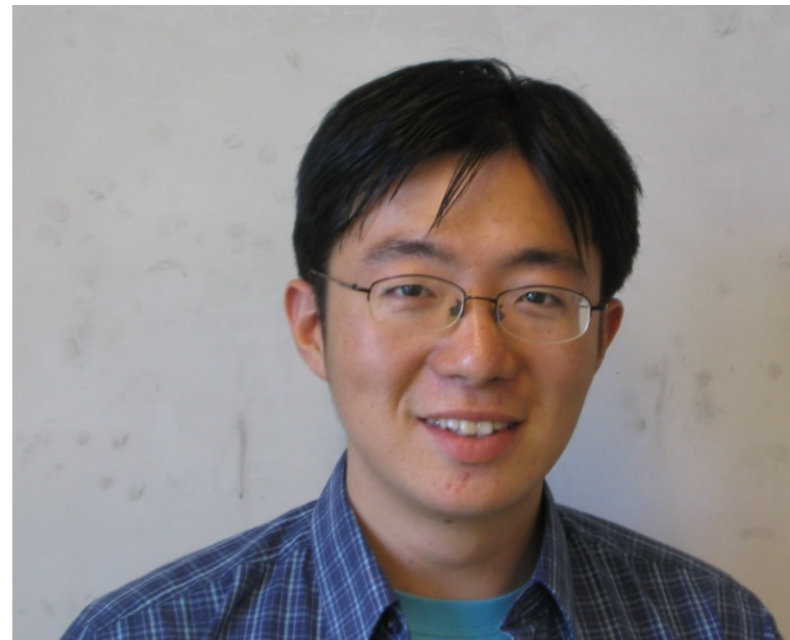
Paired electron pockets in the underdoped cuprates, V. Galitski and S. Sachdev, [arXiv:0901.0005](https://arxiv.org/abs/0901.0005)



Ribhu Kaul
UCSB



Victor Galitski
Maryland



Cenke Xu
Harvard

Outline

1. Nodal-anti-nodal dichotomy in the cuprates
Survey of recent experiments
2. Spin density wave theory of normal metal
From a “large” Fermi surface to electron and hole pockets
3. Algebraic charge liquids
Pairing by gauge forces, d-wave superconductivity, and the nodal-anti-nodal dichotomy

Outline

1. Nodal-anti-nodal dichotomy in the cuprates

Survey of recent experiments

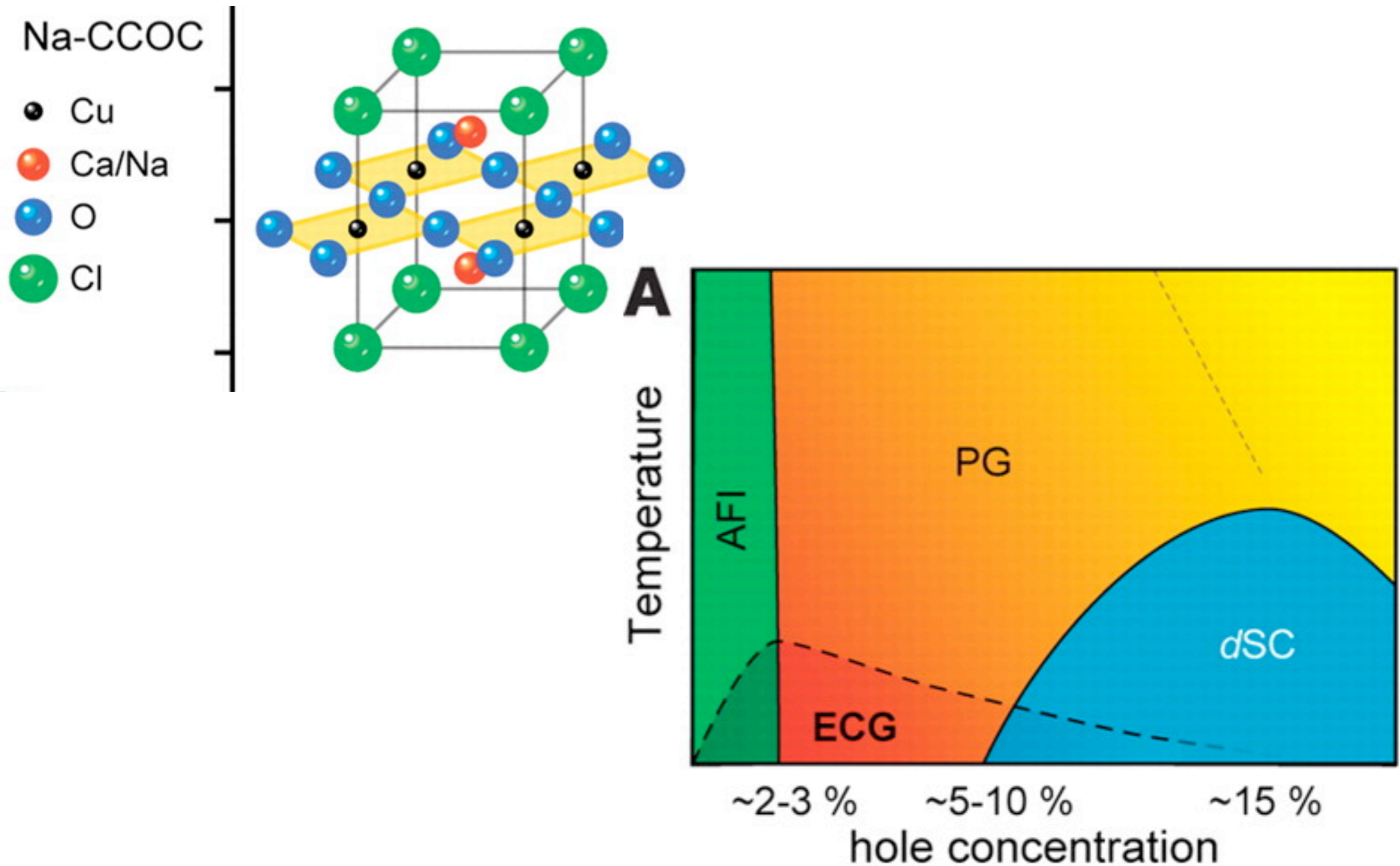
2. Spin density wave theory of normal metal

From a “large” Fermi surface to electron and hole pockets

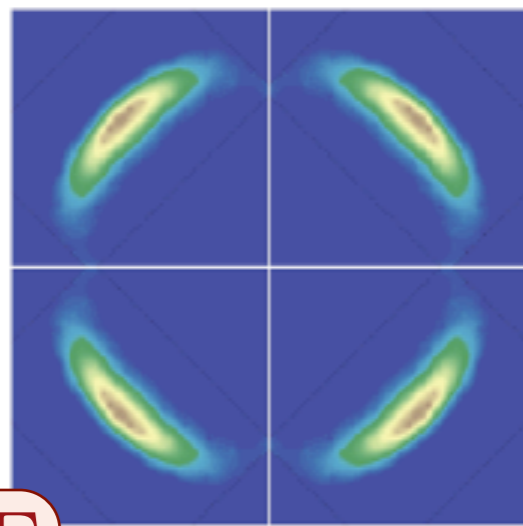
3. Algebraic charge liquids

Pairing by gauge forces, d-wave superconductivity, and the nodal-anti-nodal dichotomy

The cuprate superconductors

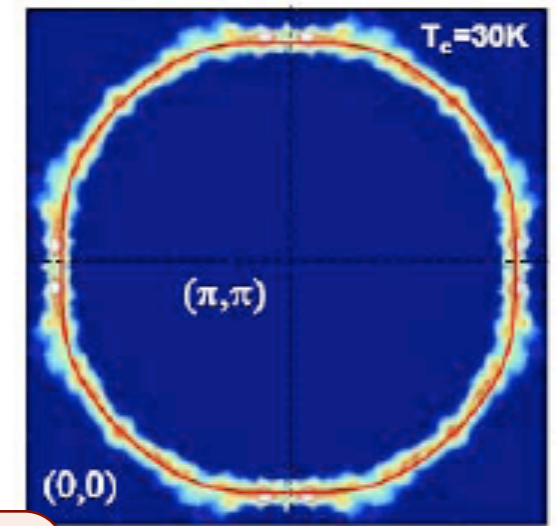
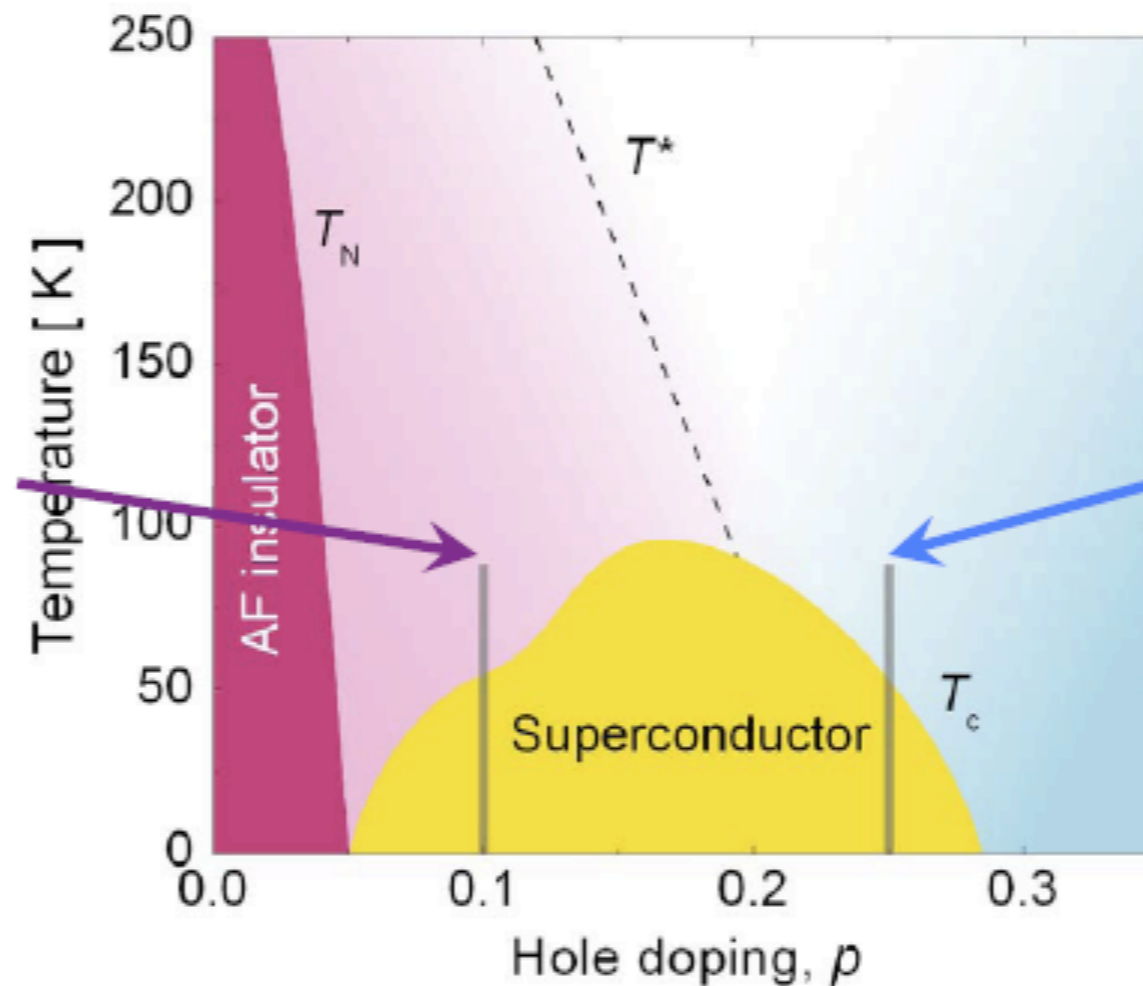


Evolution of the (ARPES) Fermi surface on the cuprate phase diagram



Γ

K.M. Shen et al., Science 2005



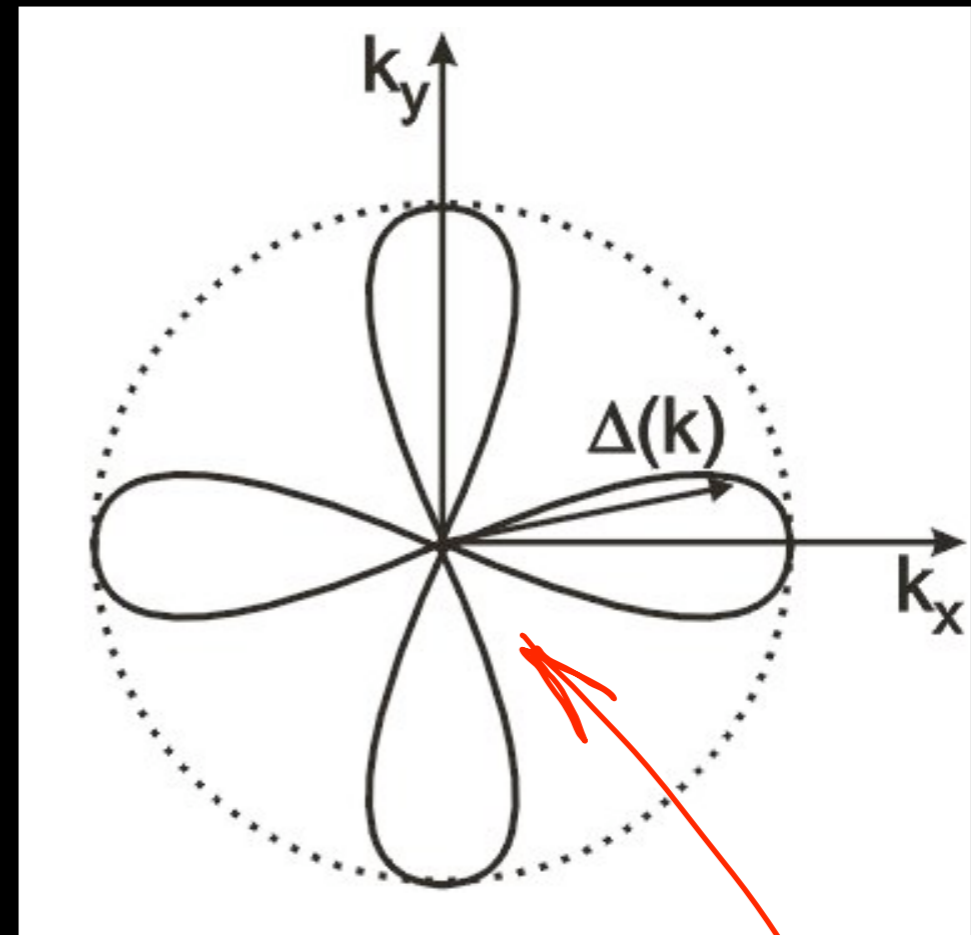
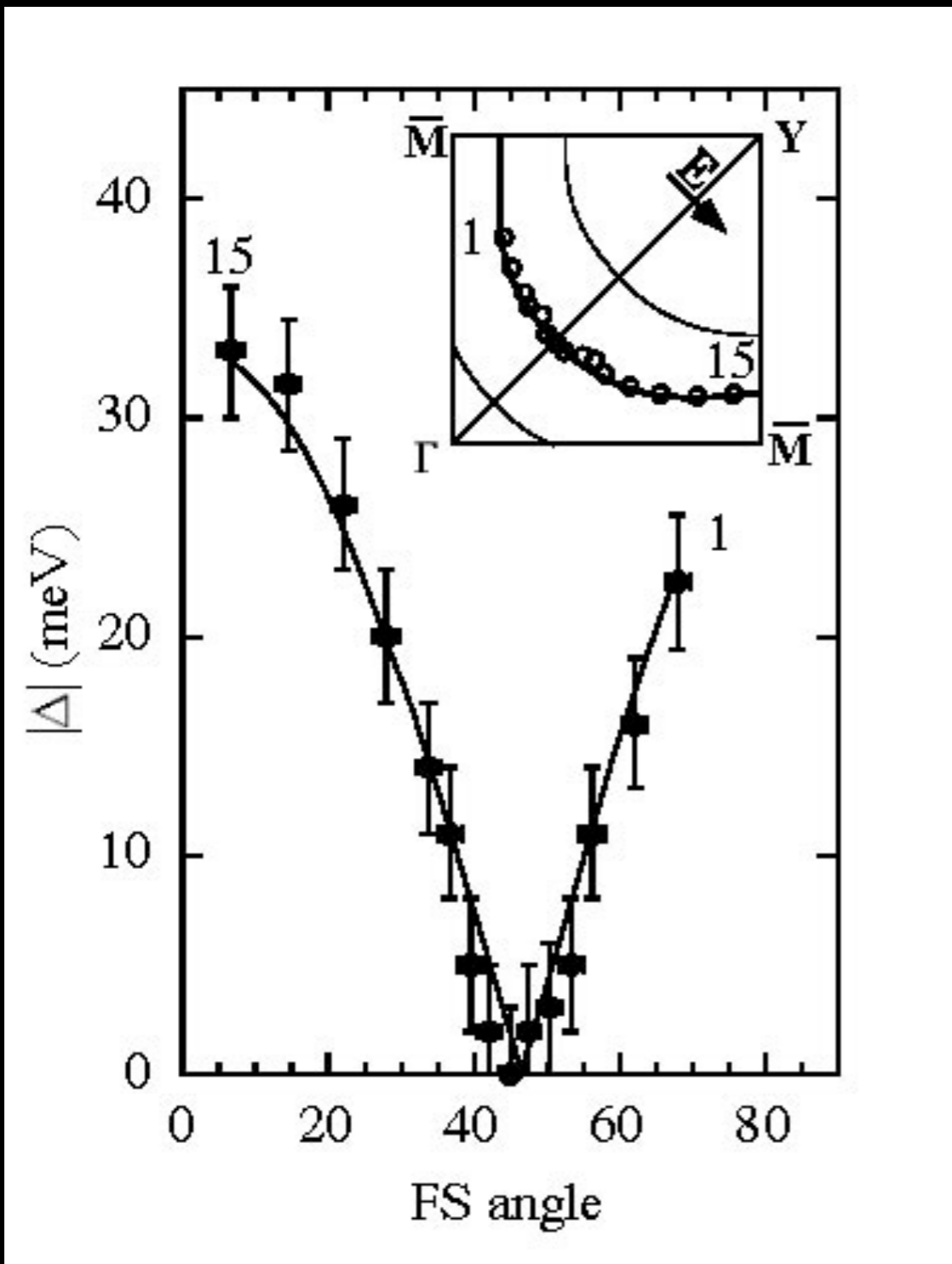
Γ

M. Platié et al., PRL 2005

Smaller hole
Fermi-pockets

Large hole
Fermi surface

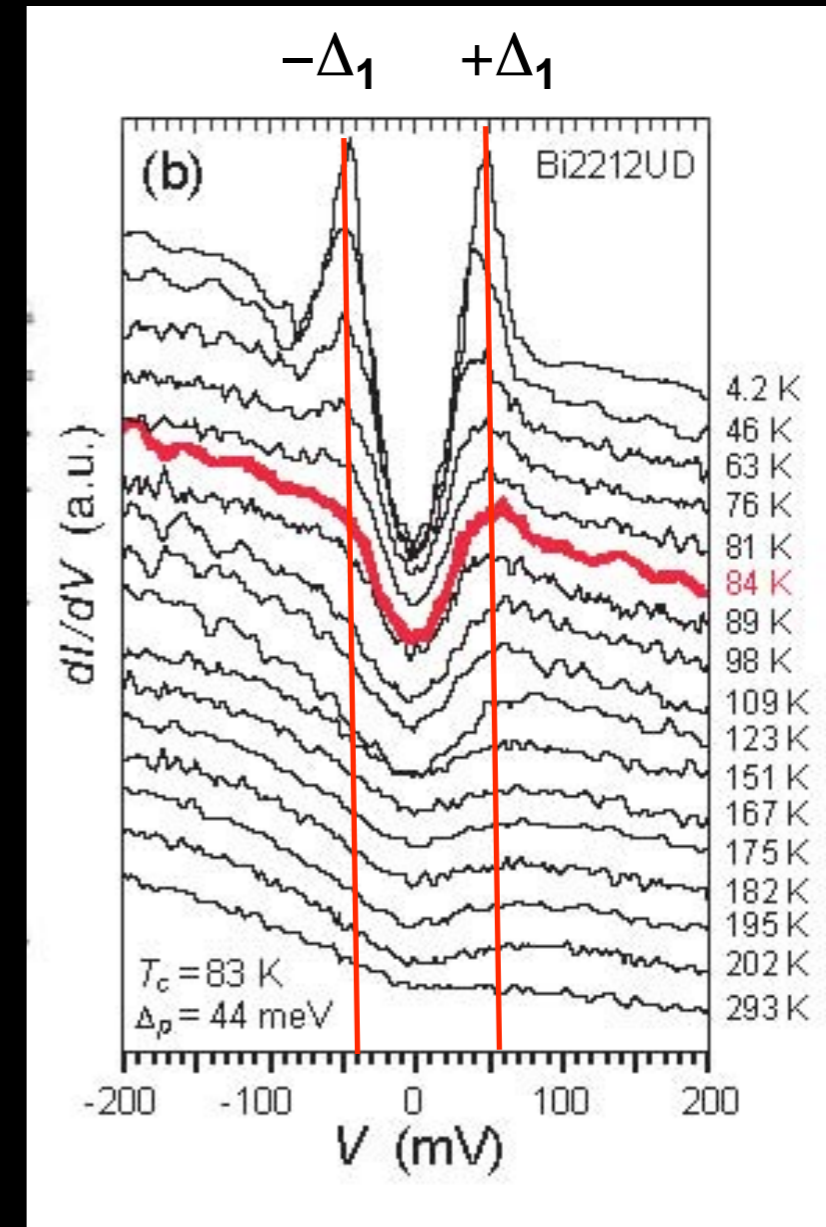
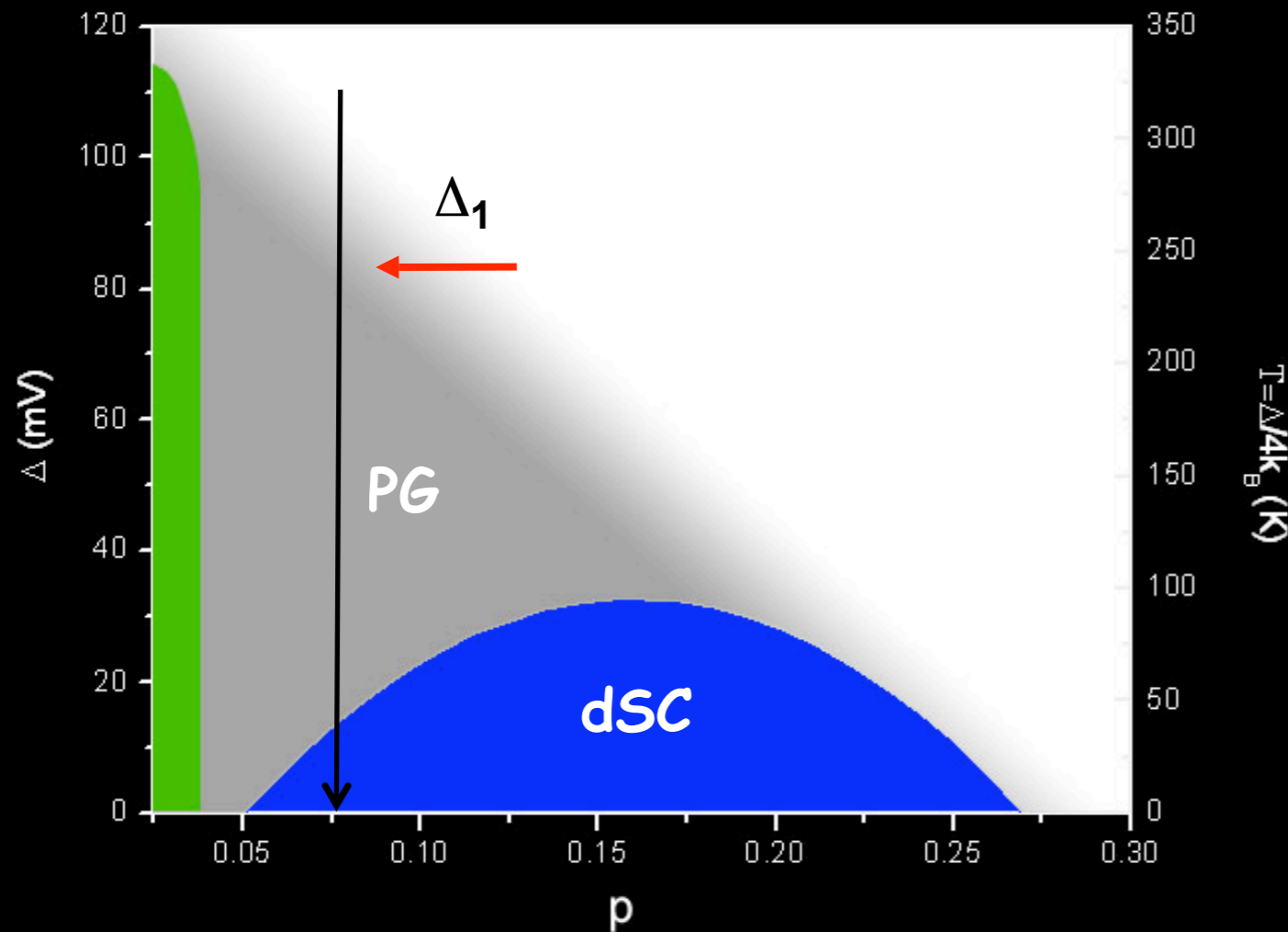
Overdoped SC State: Momentum-dependent Pair Energy Gap $\Delta(\vec{k})$



The SC energy gap $\Delta(\vec{k})$ has four nodes.

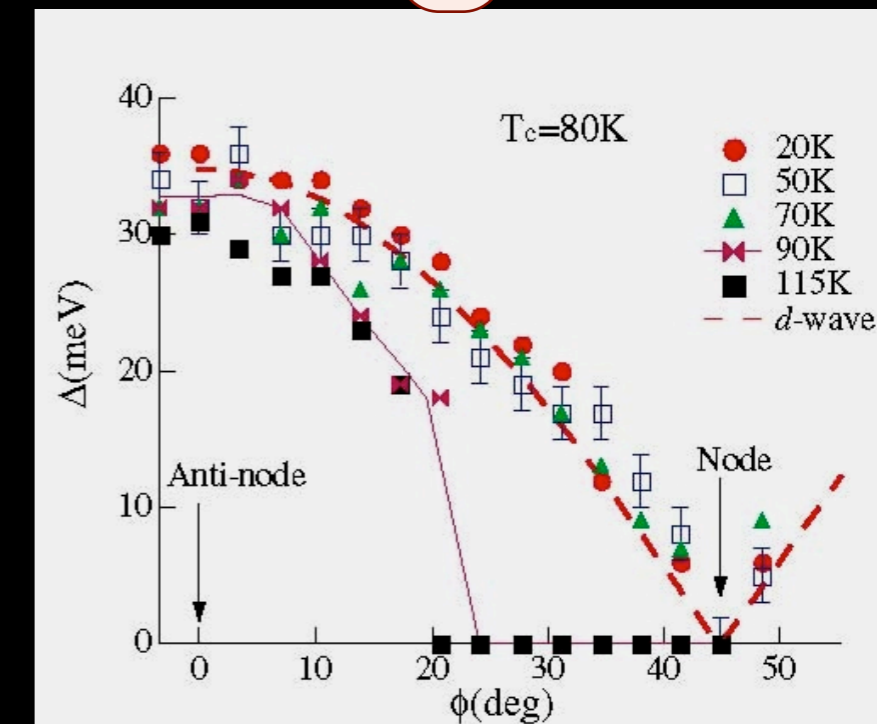
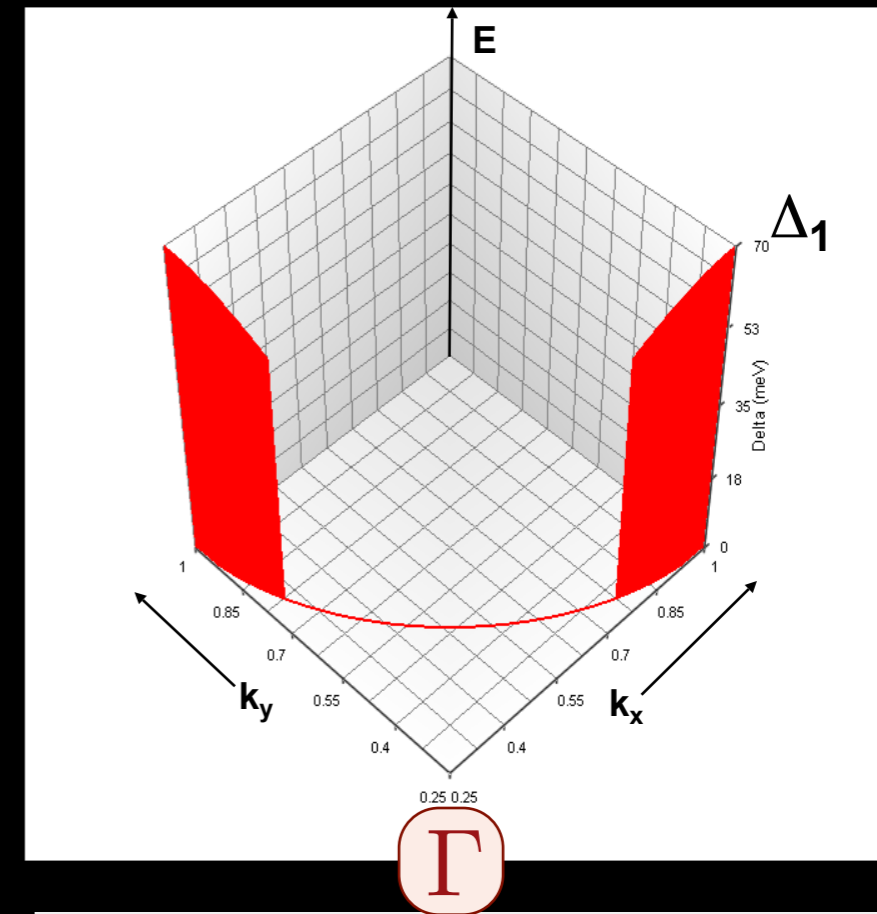
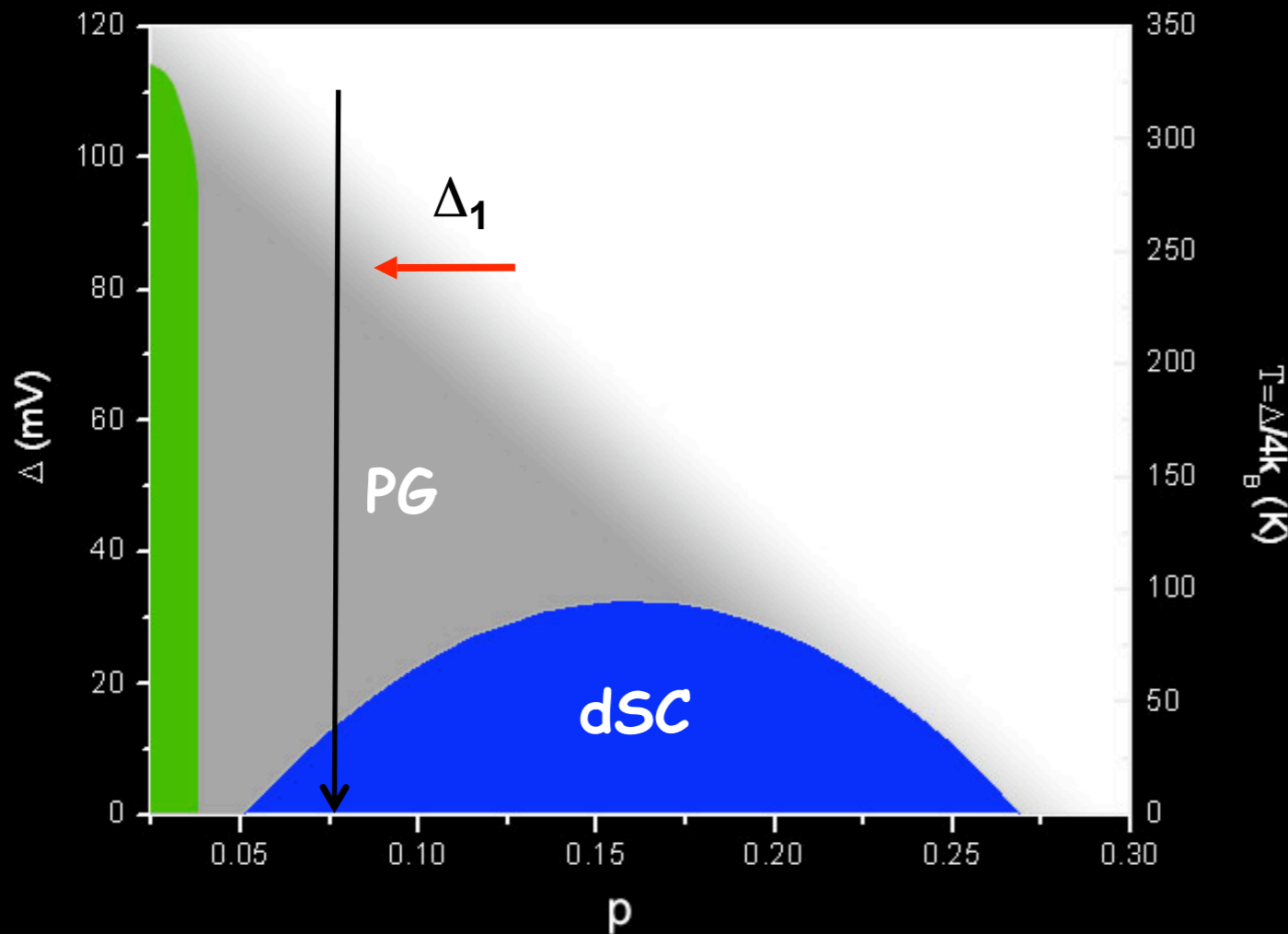
- Shen et al PRL 70, 3999 (1993)
- Ding et al PRB 54 9678 (1996)
- Mesot et al PRL 83 840 (1999)

Pseudogap: Temperature-independent energy gap exists $T \gg T_c$



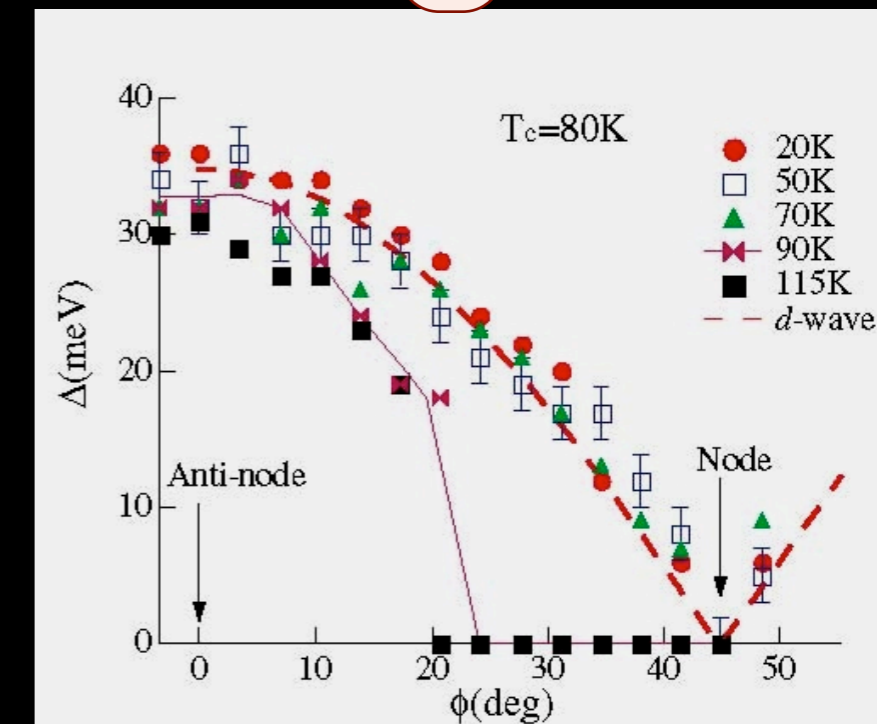
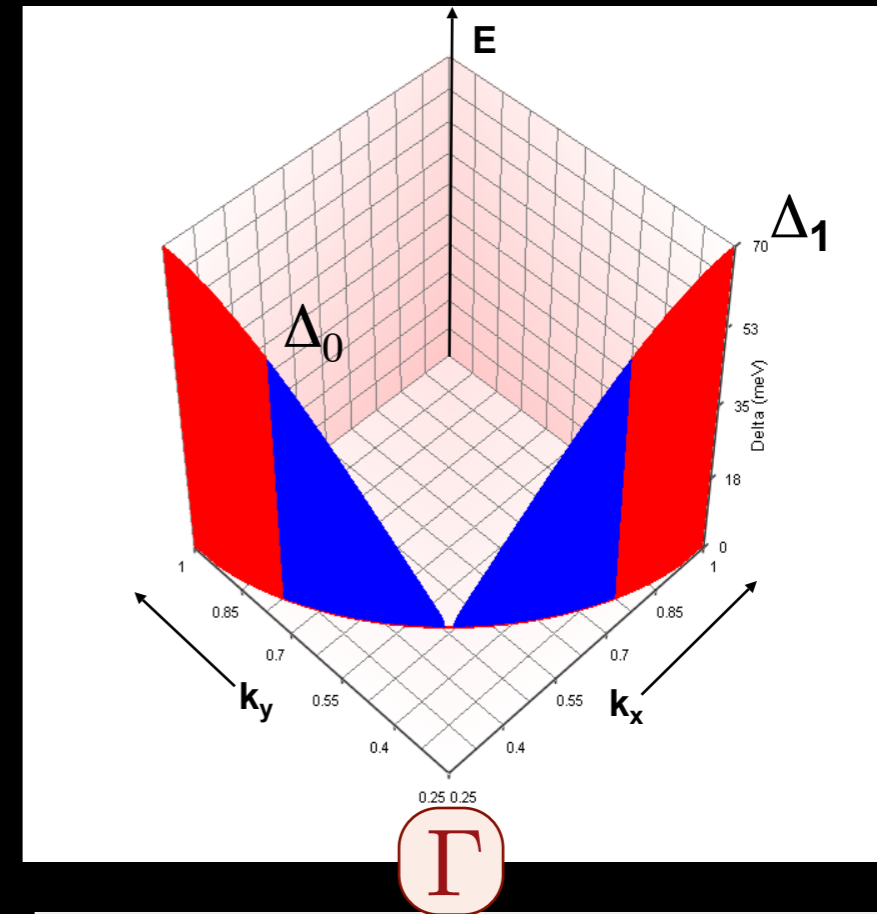
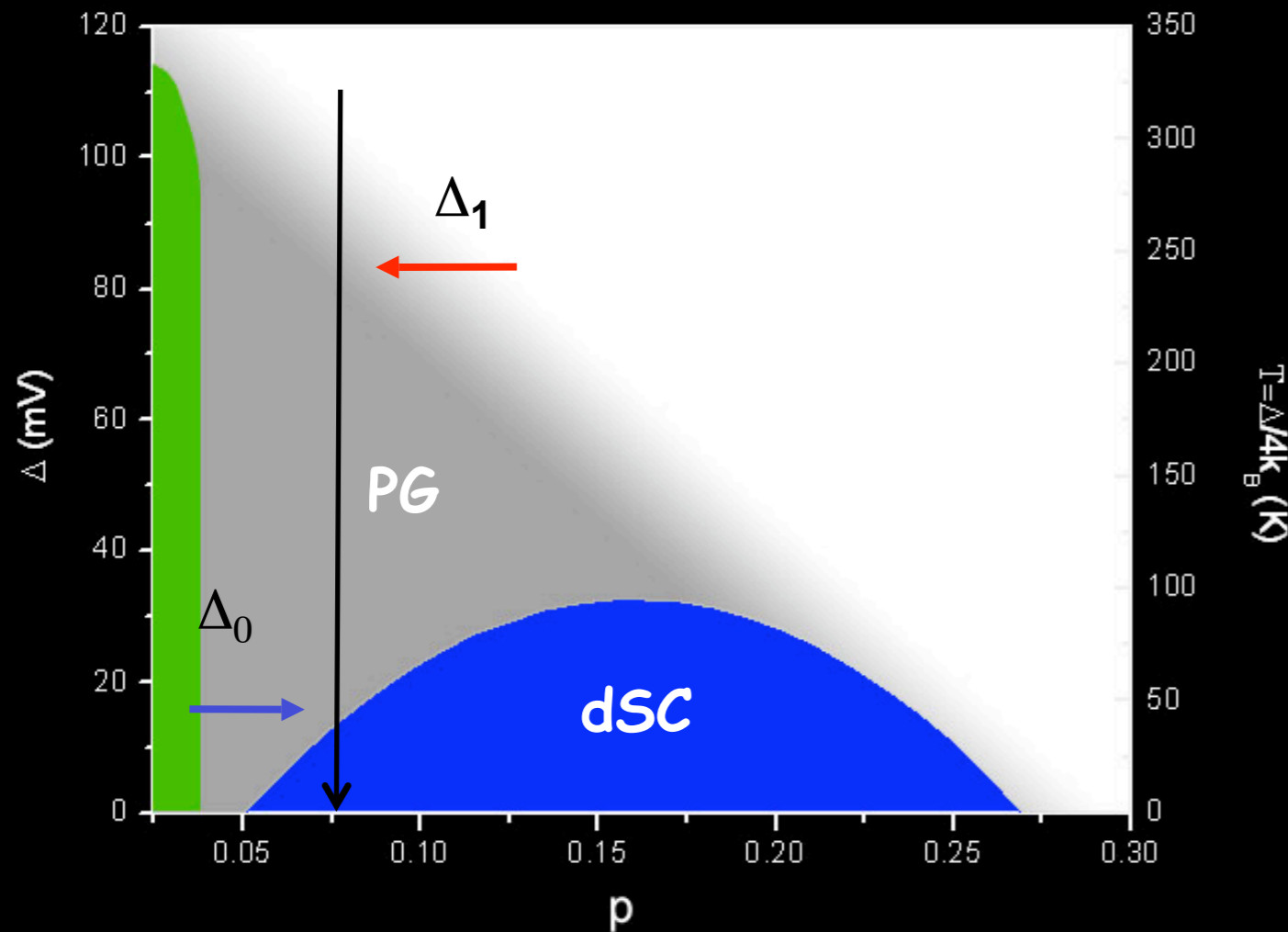
Ch. Renner et al, PRL 80, 149 (1998)
 Ø. Fischer et al, RMP 79, 353 (2007)

Pseudogap: Temperature-independent energy gap near $k \sim (\pi, 0)$



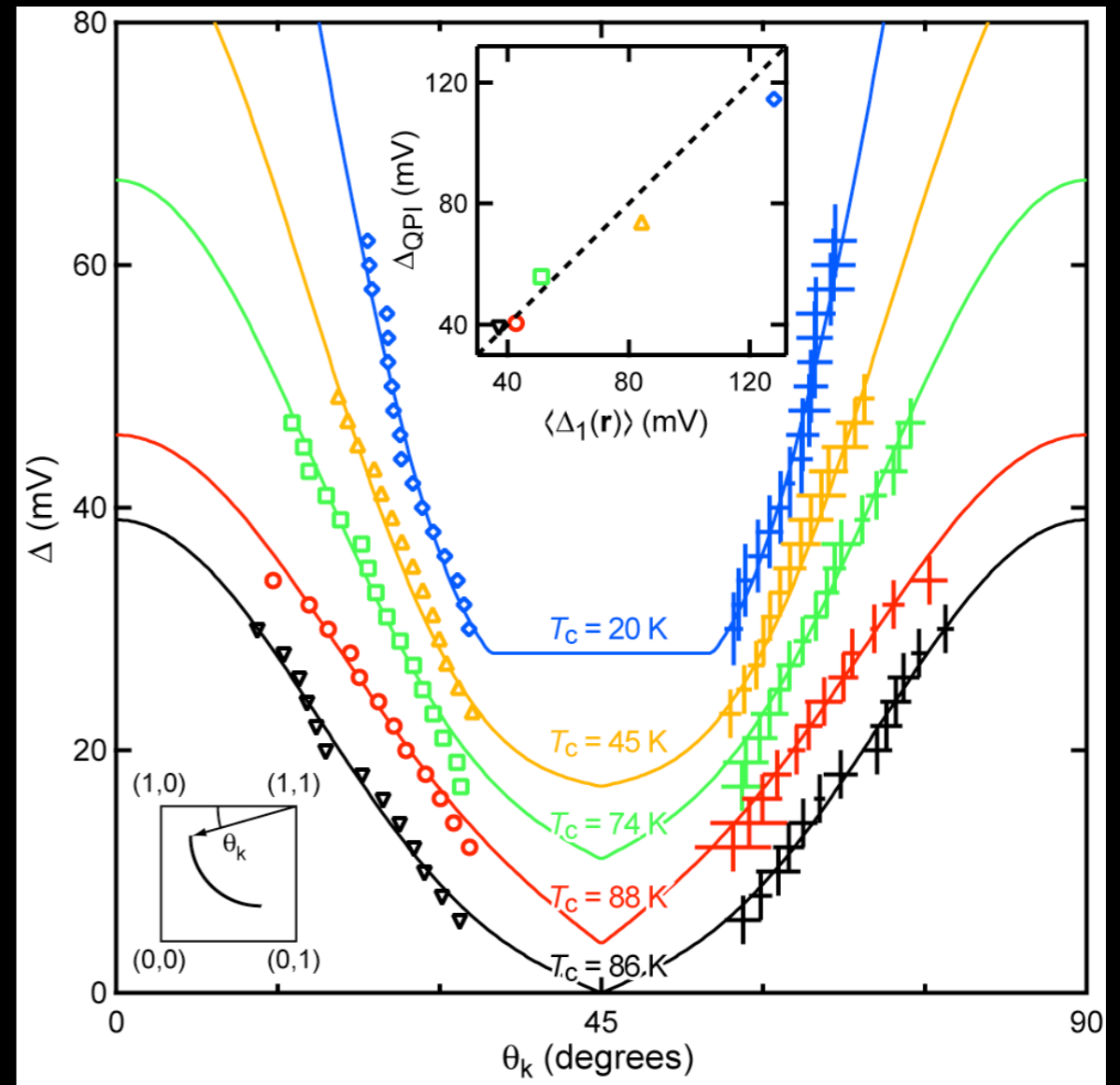
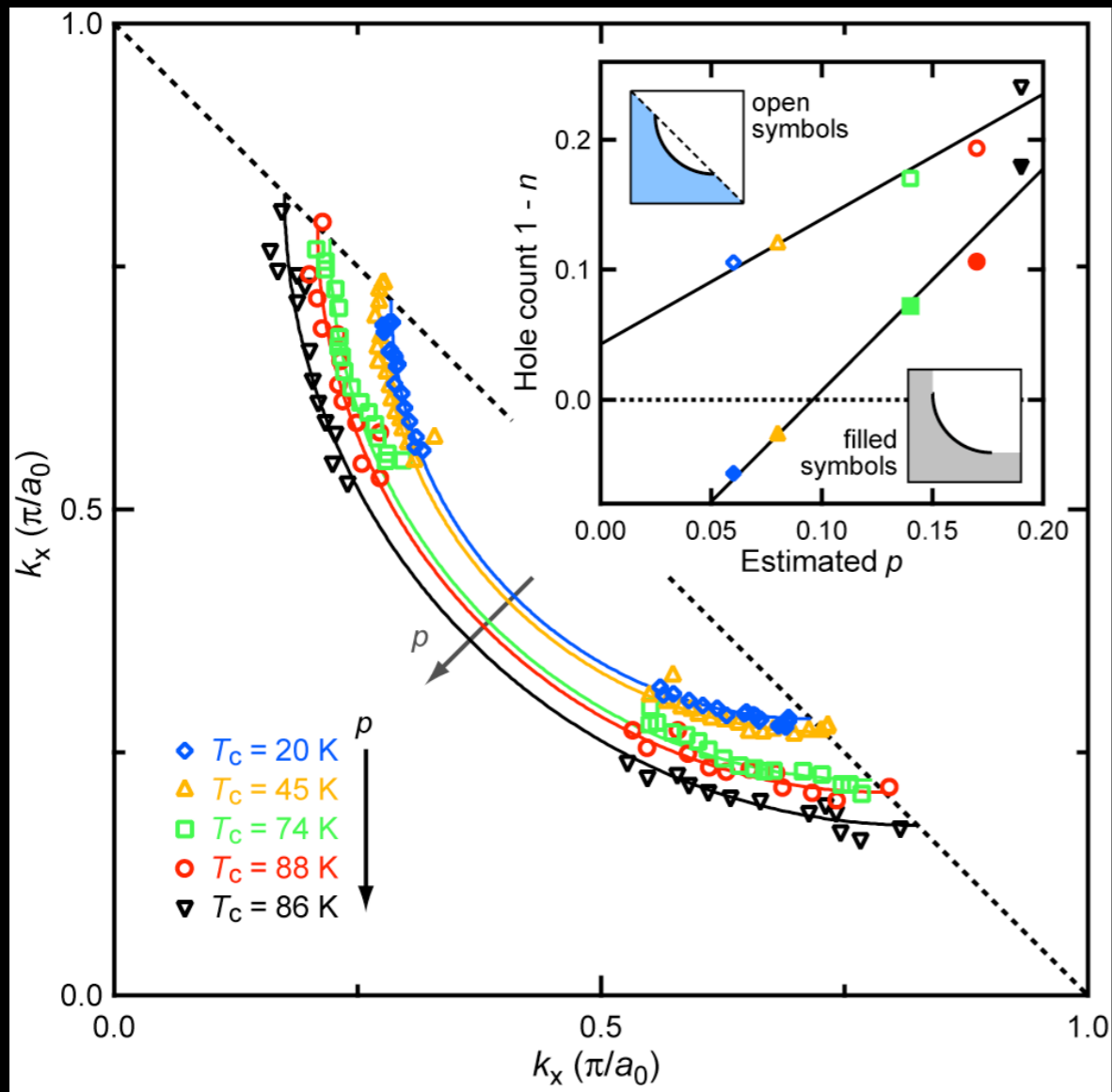
- Loeser et al, Science 273 325 (1996)
- Ding et al, Nature 382 51, (1996)
- Norman et al, Nature 392, 157 (1998)
- Shen et al Science 307, 902 (2005)
- Kanigel et al, Nature Physics 2, 447 (2006)
- Tanaka et al, Science 314, 1912 (2006)

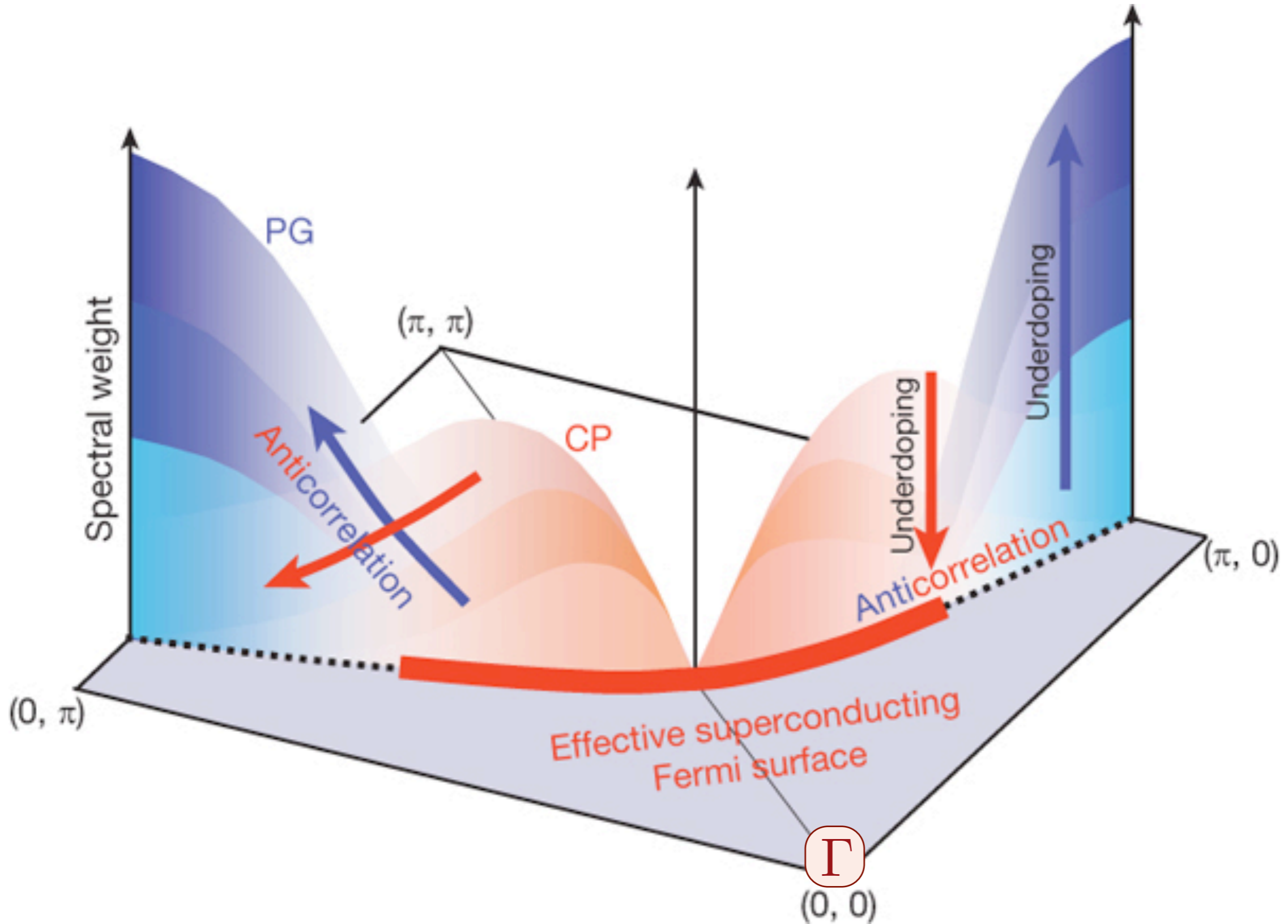
Pseudogap: Temperature-dependent energy gap near node



- Loeser et al, Science 273 325 (1996)
- Ding et al, Nature 382 51, (1996)
- Norman et al, Nature 392, 157 (1998)
- Shen et al Science 307, 902 (2005)
- Kanigel et al, Nature Physics 2, 447 (2006)
- Tanaka et al, Science 314, 1912 (2006)

Development of Fermi arc with underdoping





Competition between the pseudogap and superconductivity in the high- T_c copper oxides

T. Kondo, R. Khasanov, T. Takeuchi, J. Schmalian, A. Kaminski, *Nature* **457**, 296 (2009)

Nodal-anti-nodal dichotomy in the underdoped cuprates

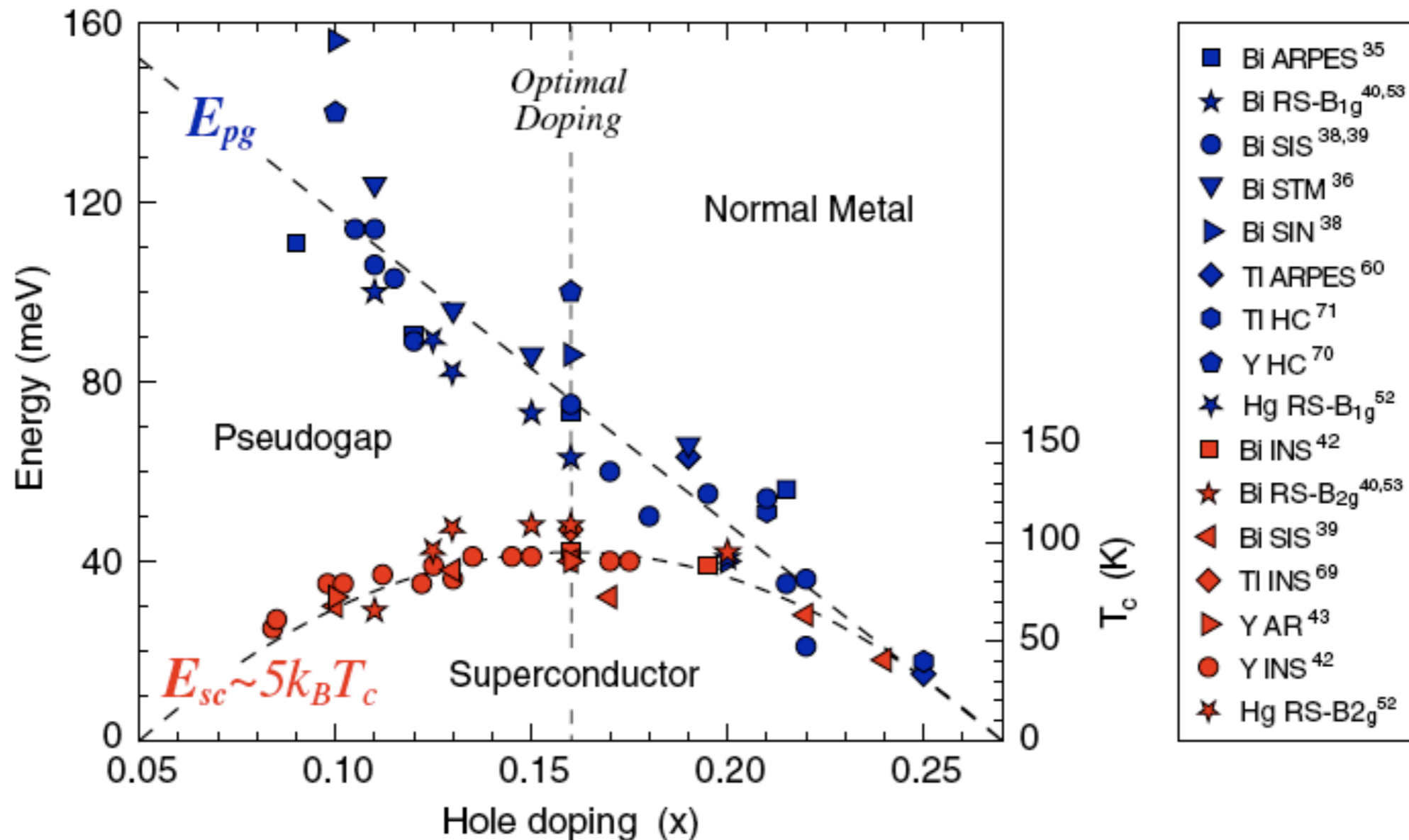


Figure 2. Pseudogap ($E_{pg} = 2\Delta_{pg}$) and superconducting ($E_{sc} \sim 5k_B T_c$) energy scales for a number of HTSCs with $T_c^{\max} \sim 95$ K (Bi2212, Y123, Tl2201 and Hg1201). The datapoints were obtained, as a function of hole doping x , by angle-resolved photoemission spectroscopy (ARPES), tunneling (STM, SIN, SIS), Andreev reflection (AR), Raman scattering (RS) and heat conductivity (HC). On the same plot we are also including the energy Ω_r of the magnetic resonance mode measured by inelastic neutron scattering (INS), which we identify with E_{sc} because of the striking quantitative correspondence as a function of T_c . The data fall on two universal curves given by $E_{pg} = E_{pg}^{\max} (0.27 - x)/0.22$ and $E_{sc} = E_{sc}^{\max} [1 - 82.6(0.16 - x)^2]$, with $E_{pg}^{\max} = E_{pg}(x = 0.05) = 152 \pm 8$ meV and $E_{sc}^{\max} = E_{sc}(x = 0.16) = 42 \pm 2$ meV (the statistical errors refer to the fit of the selected datapoints; however, the spread of all available data would be more appropriately described by ± 20 and ± 10 meV, respectively).

Superconductivity in a system with preformed pairs

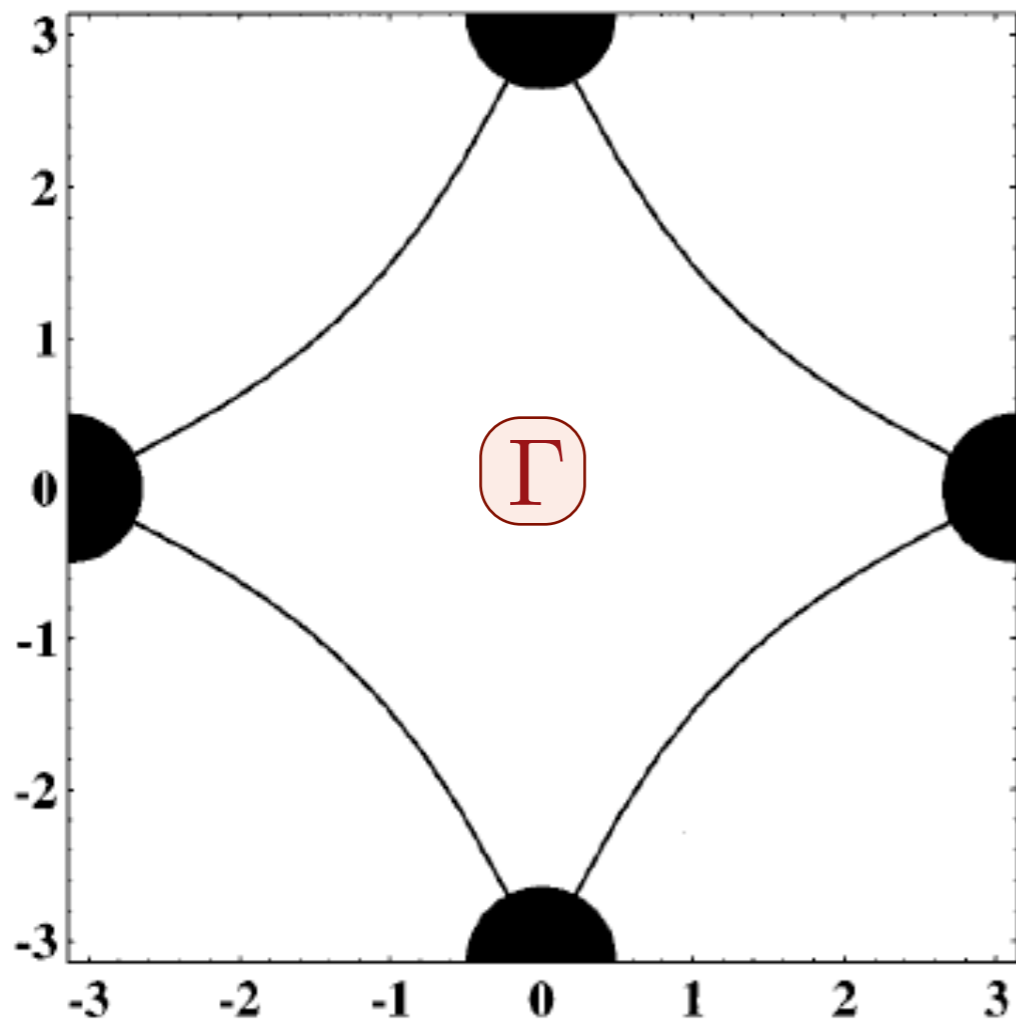


FIG. 1. Sketch of the Fermi line and region of the momentum space where pseudogap pairs is formed. The Fermi line shown here was obtained in the tight binding model with diagonal hopping $t' = -0.3t$; it is similar to the Fermi line observed in the underdoped $\text{Bi}_2\text{Sr}_2\text{CaCu}_2\text{O}_{8+\delta}$ (Ref. 5). The shaded disks denote the part of the momentum space where a pseudogap was observed in the experiment. We shall assume that the fermions in these regions are paired into the bosons.

$$H = \sum_q \varepsilon b_q^\dagger b_q + \sum_{p,q}' V_{p,q} (b_q^\dagger c_{p\uparrow} c_{q-p\downarrow} + \text{H.c.})$$

$$+ \sum_p \xi_p c_{p,\sigma}^\dagger c_{p,\sigma};$$

$$V_{p,q} = Va^2(p_x^2 - p_y^2)$$

Superconductivity in a system with preformed pairs

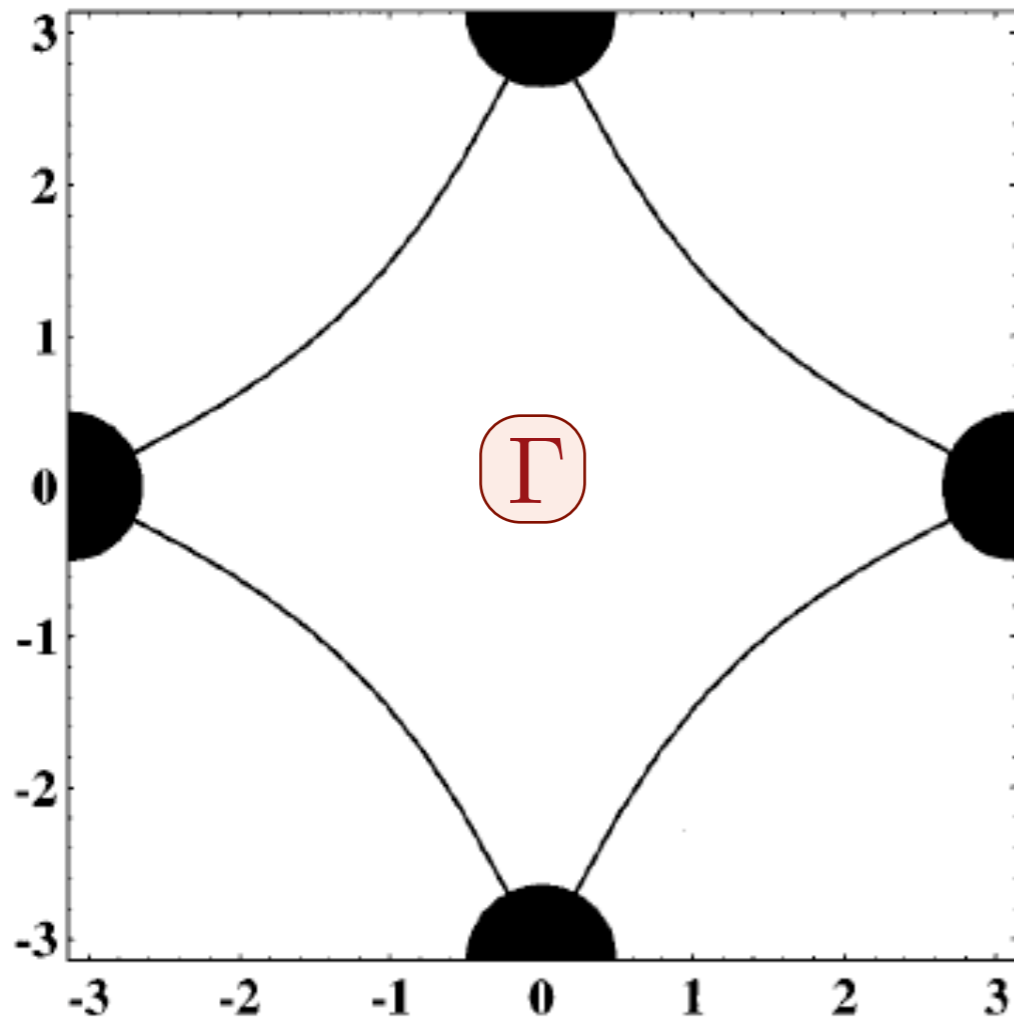


FIG. 1. Sketch of the Fermi line and region of the momentum space where pseudogap pairs is formed. The Fermi line shown here was obtained in the tight binding model with diagonal hopping $t' = -0.3t$; it is similar to the Fermi line observed in the underdoped $\text{Bi}_2\text{Sr}_2\text{CaCu}_2\text{O}_{8+\delta}$ (Ref. 5). The shaded disks denote the part of the momentum space where a pseudogap was observed in the experiment. We shall assume that the fermions in these regions are paired into the bosons.

$$H = \sum_q \varepsilon b_q^\dagger b_q + \sum_{p,q}' V_{p,q} (b_q^\dagger c_{p\uparrow} c_{q-p\downarrow} + \text{H.c.})$$

$$+ \sum_p \xi_p c_{p,\sigma}^\dagger c_{p,\sigma};$$

$$V_{p,q} = Va^2(p_x^2 - p_y^2)$$

Attractive
phenomenological model,
but theoretical and
microscopic basis is unclear

Outline

1. Nodal-anti-nodal dichotomy in the cuprates
Survey of recent experiments
2. Spin density wave theory of normal metal
From a “large” Fermi surface to electron and hole pockets
3. Algebraic charge liquids
Pairing by gauge forces, d-wave superconductivity, and the nodal-anti-nodal dichotomy

Outline

1. Nodal-anti-nodal dichotomy in the cuprates

Survey of recent experiments

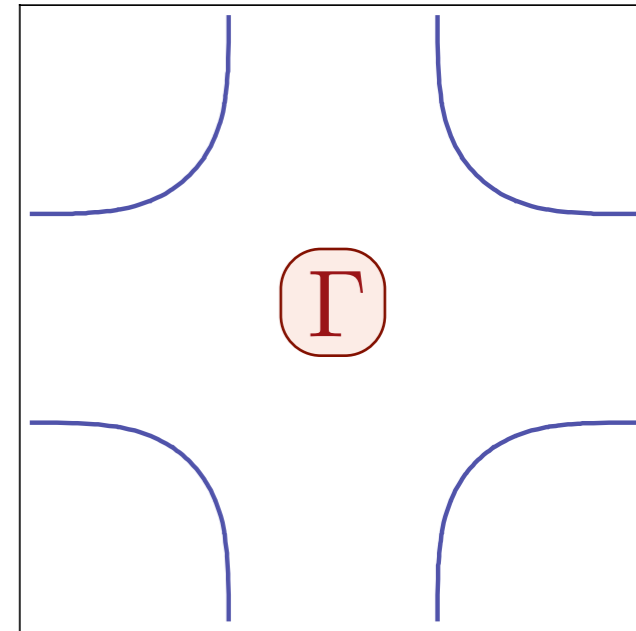
2. Spin density wave theory of normal metal

From a “large” Fermi surface to electron and hole pockets

3. Algebraic charge liquids

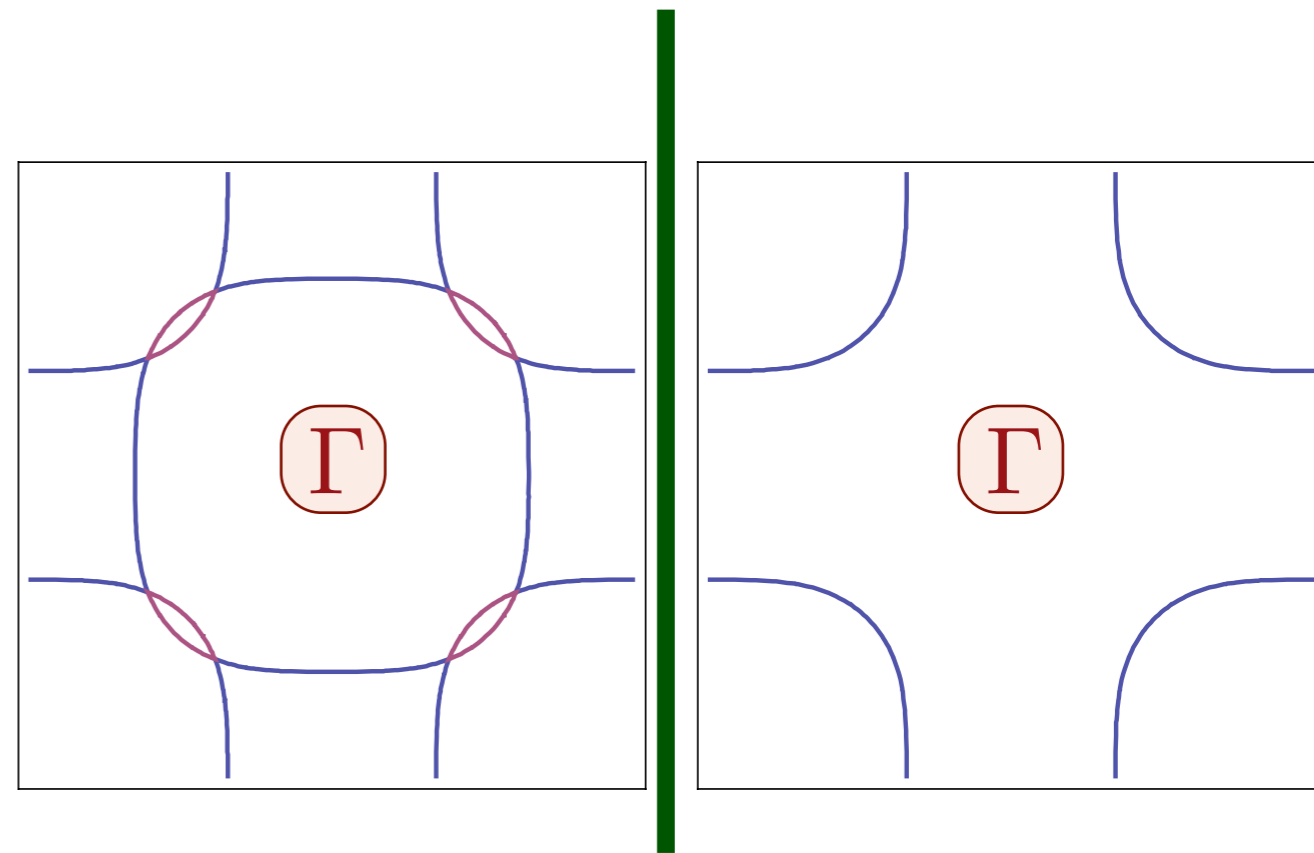
Pairing by gauge forces, d-wave superconductivity, and the nodal-anti-nodal dichotomy

Spin density wave theory in electron-doped cuprates



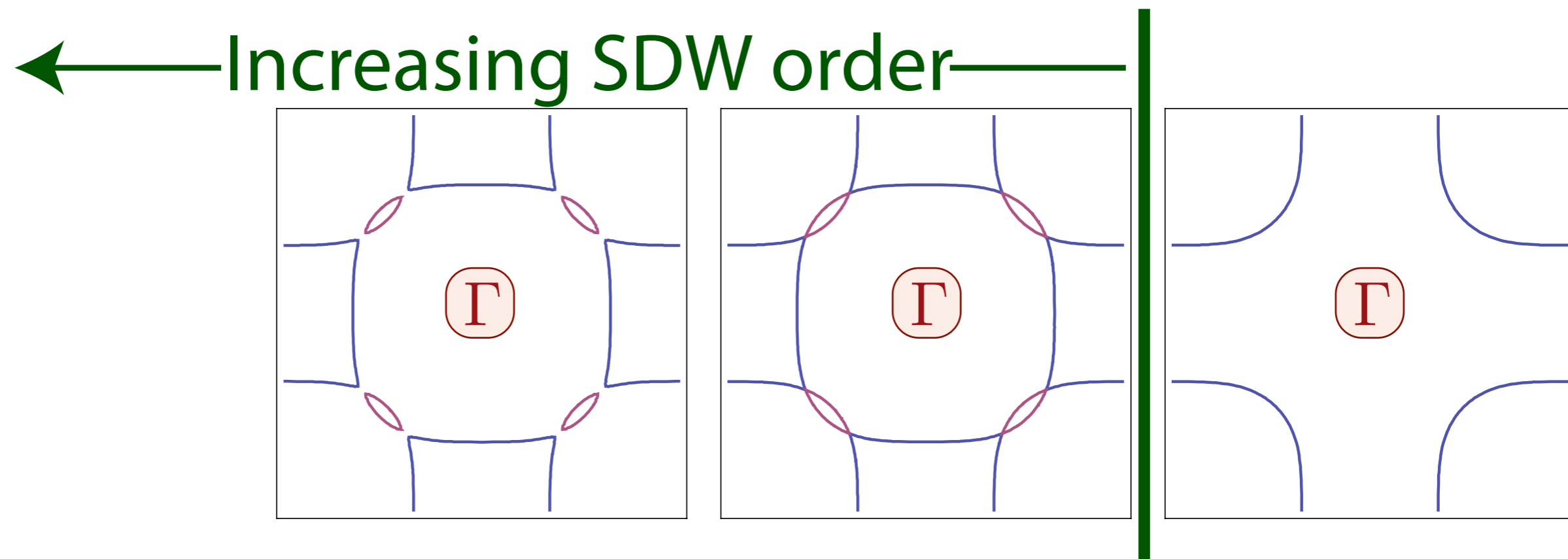
S. Sachdev, A. V. Chubukov, and A. Sokol, *Phys. Rev. B* **51**, 14874 (1995).
A. V. Chubukov and D. K. Morr, *Physics Reports* **288**, 355 (1997).

Spin density wave theory in electron-doped cuprates



S. Sachdev, A. V. Chubukov, and A. Sokol, *Phys. Rev. B* **51**, 14874 (1995).
A. V. Chubukov and D. K. Morr, *Physics Reports* **288**, 355 (1997).

Spin density wave theory in electron-doped cuprates

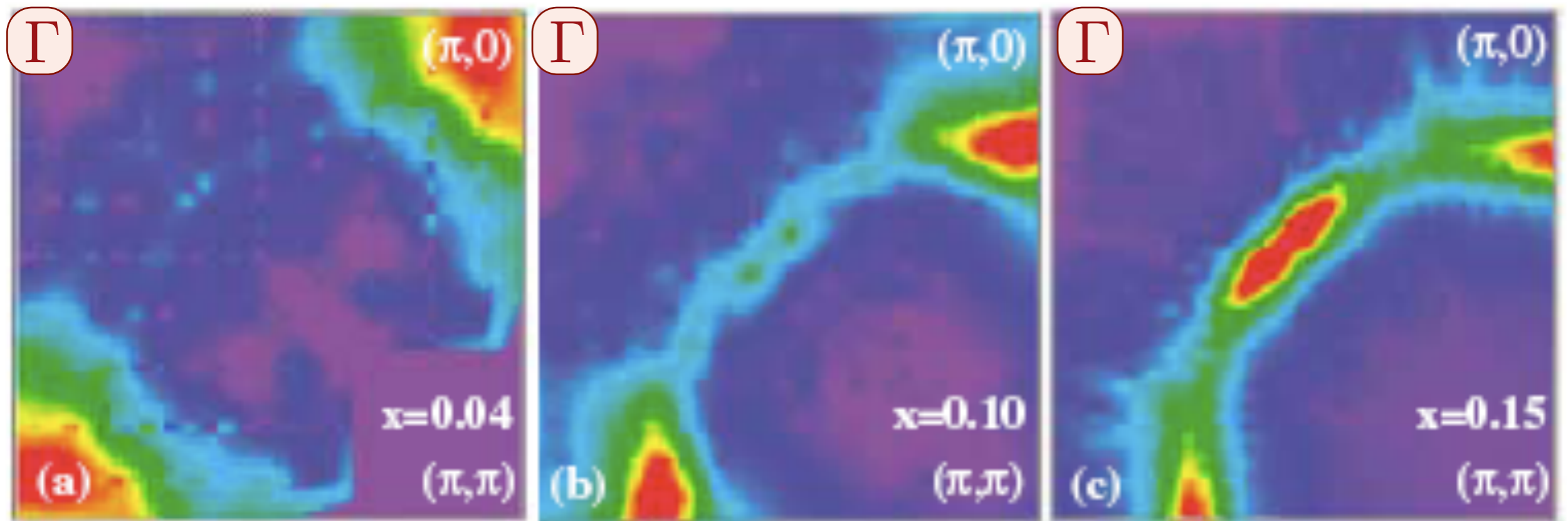


SDW order parameter is a vector, $\vec{\varphi}$, whose amplitude vanishes at the transition to the Fermi liquid.

S. Sachdev, A. V. Chubukov, and A. Sokol, *Phys. Rev. B* **51**, 14874 (1995).

A. V. Chubukov and D. K. Morr, *Physics Reports* **288**, 355 (1997).

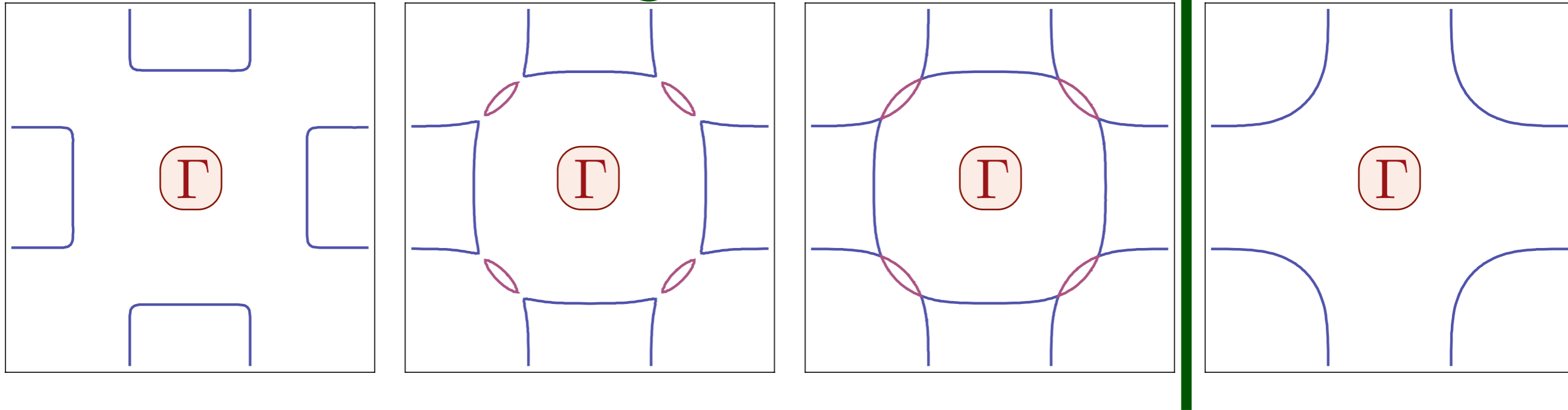
Photoemission in NCCO (electron-doped)



N. P. Armitage *et al.*, Phys. Rev. Lett. **88**, 257001 (2002).

Spin density wave theory in electron-doped cuprates

← Increasing SDW order →

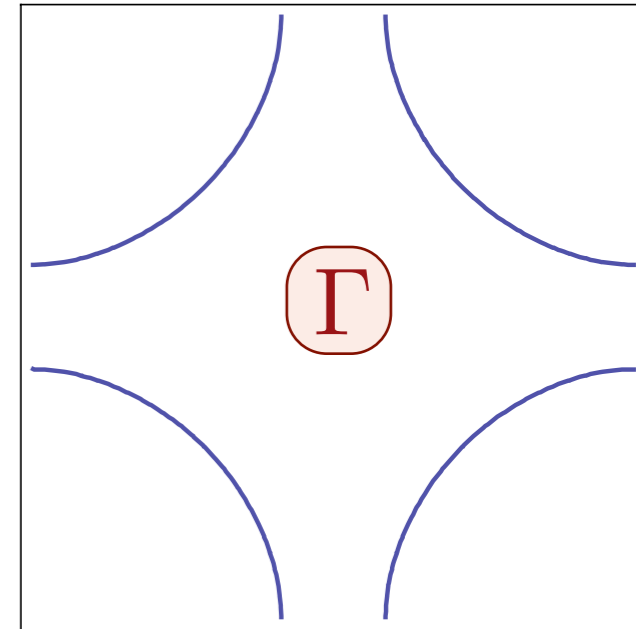


SDW order parameter is a vector, $\vec{\varphi}$,
whose amplitude vanishes at the transition
to the Fermi liquid.

S. Sachdev, A. V. Chubukov, and A. Sokol, *Phys. Rev. B* **51**, 14874 (1995).

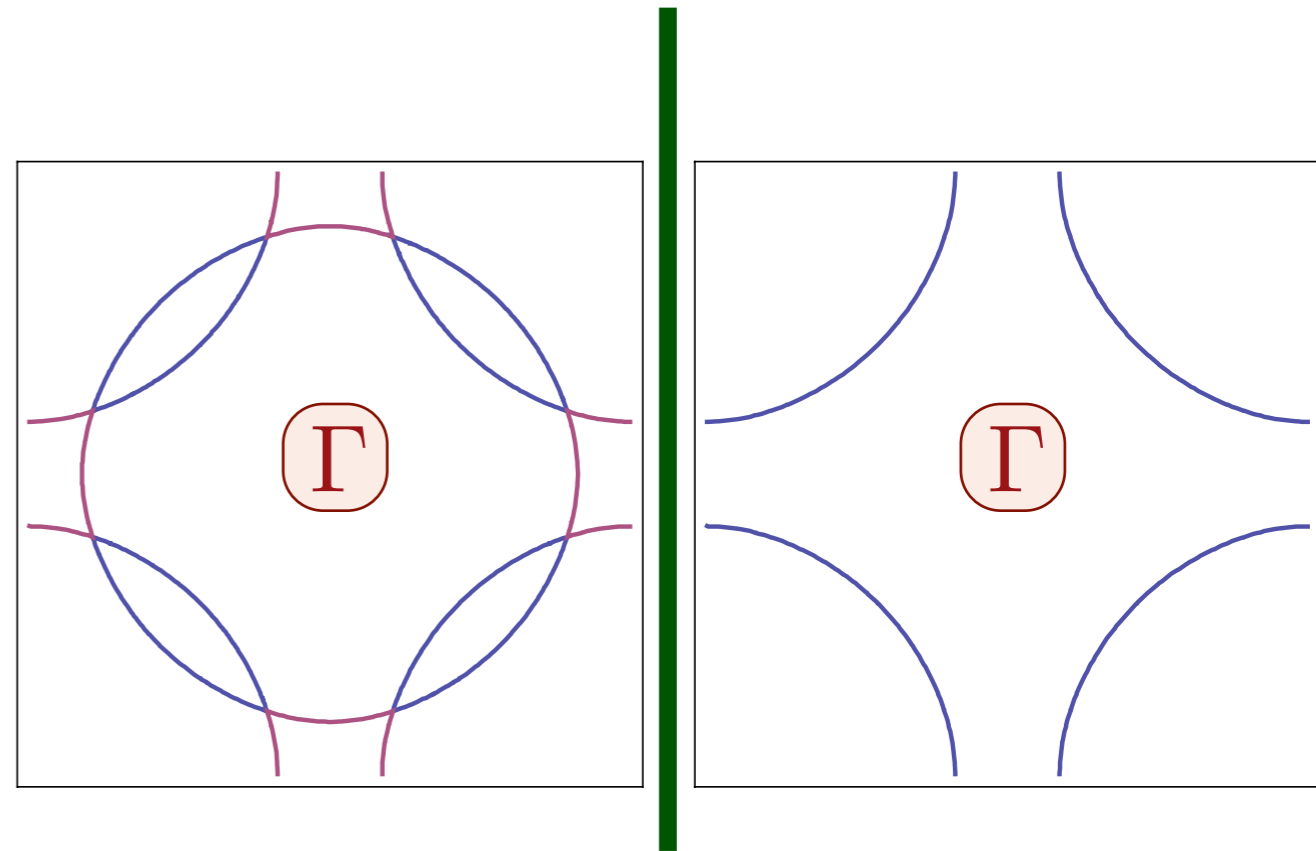
A. V. Chubukov and D. K. Morr, *Physics Reports* **288**, 355 (1997).

Spin density wave theory in hole-doped cuprates



S. Sachdev, A. V. Chubukov, and A. Sokol, *Phys. Rev. B* **51**, 14874 (1995).
A. V. Chubukov and D. K. Morr, *Physics Reports* **288**, 355 (1997).

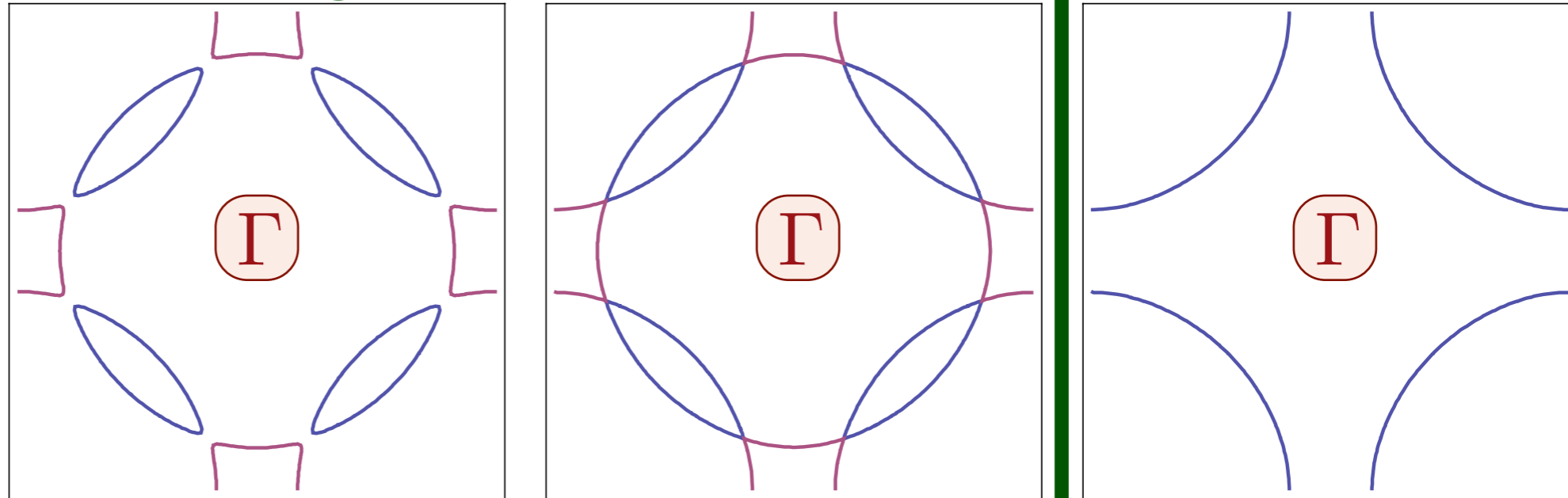
Spin density wave theory in hole-doped cuprates



S. Sachdev, A. V. Chubukov, and A. Sokol, *Phys. Rev. B* **51**, 14874 (1995).
A. V. Chubukov and D. K. Morr, *Physics Reports* **288**, 355 (1997).

Spin density wave theory in hole-doped cuprates

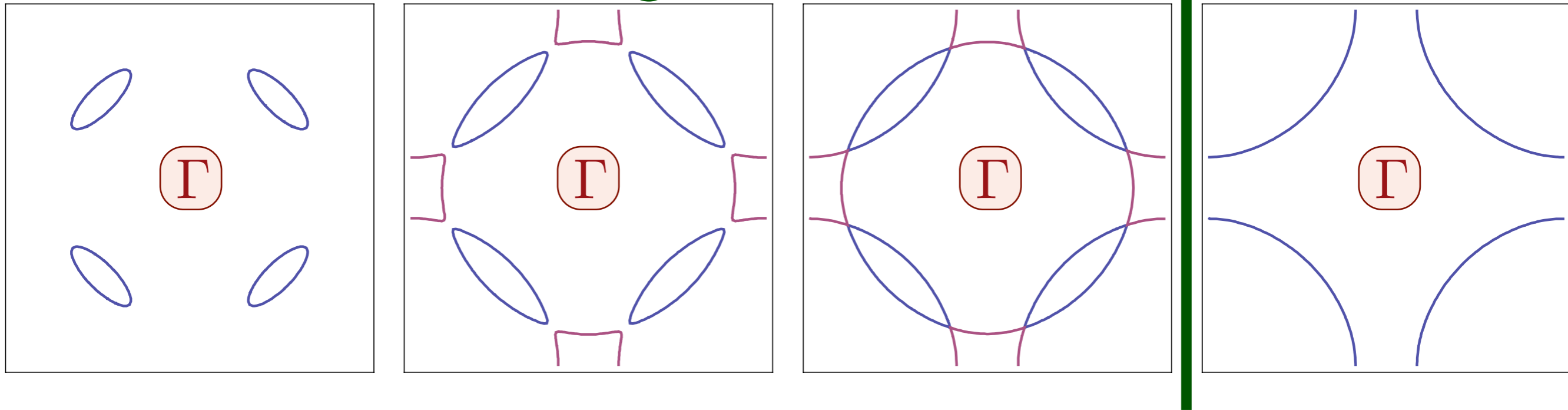
← Increasing SDW order →



S. Sachdev, A. V. Chubukov, and A. Sokol, *Phys. Rev. B* **51**, 14874 (1995).
A. V. Chubukov and D. K. Morr, *Physics Reports* **288**, 355 (1997).

Spin density wave theory in hole-doped cuprates

← Increasing SDW order →

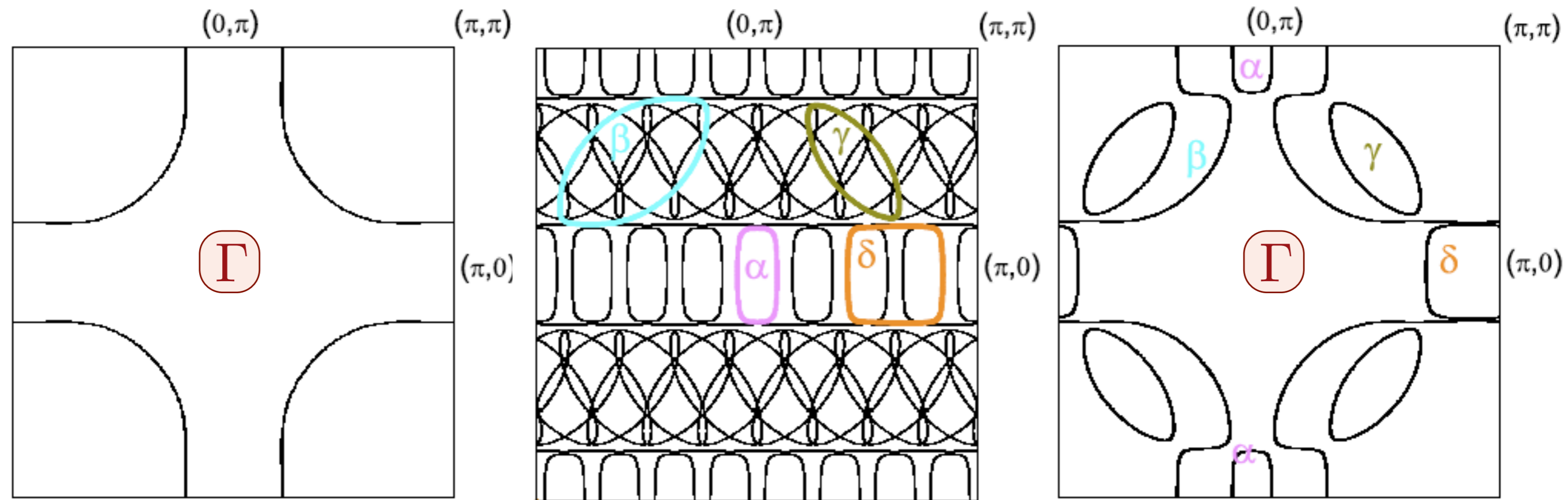


SDW order parameter is a vector, $\vec{\varphi}$, whose amplitude vanishes at the transition to the Fermi liquid.

S. Sachdev, A. V. Chubukov, and A. Sokol, *Phys. Rev. B* **51**, 14874 (1995).

A. V. Chubukov and D. K. Morr, *Physics Reports* **288**, 355 (1997).

Spin density wave theory in hole-doped cuprates

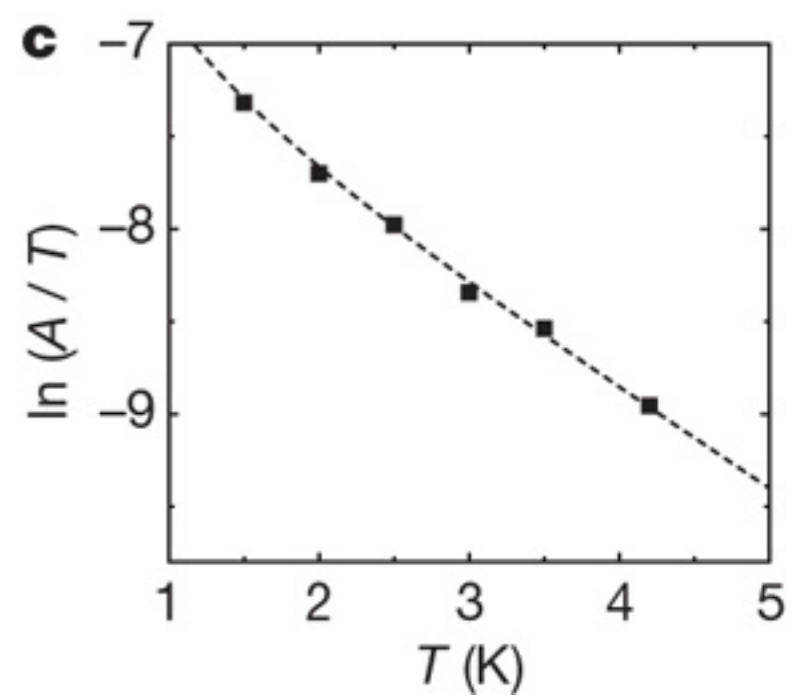
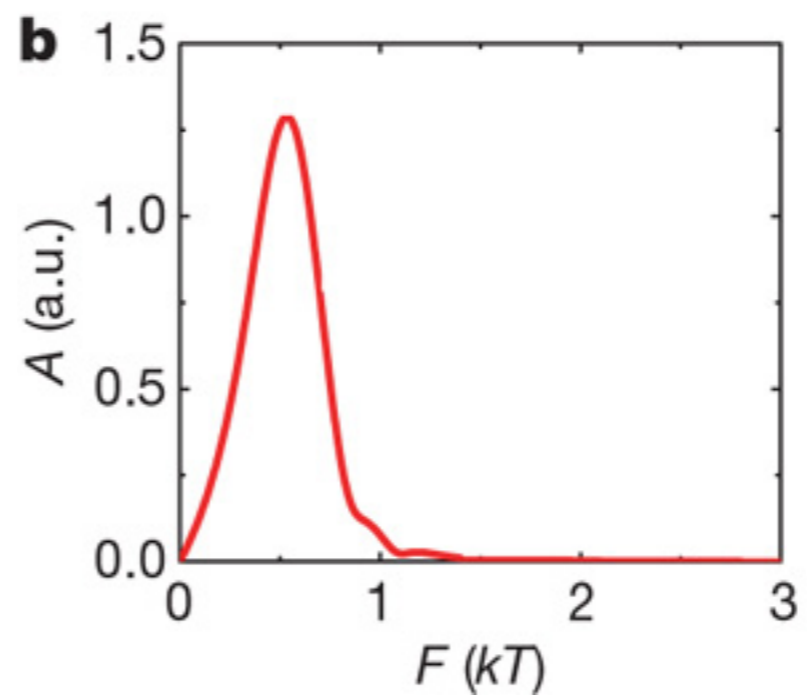
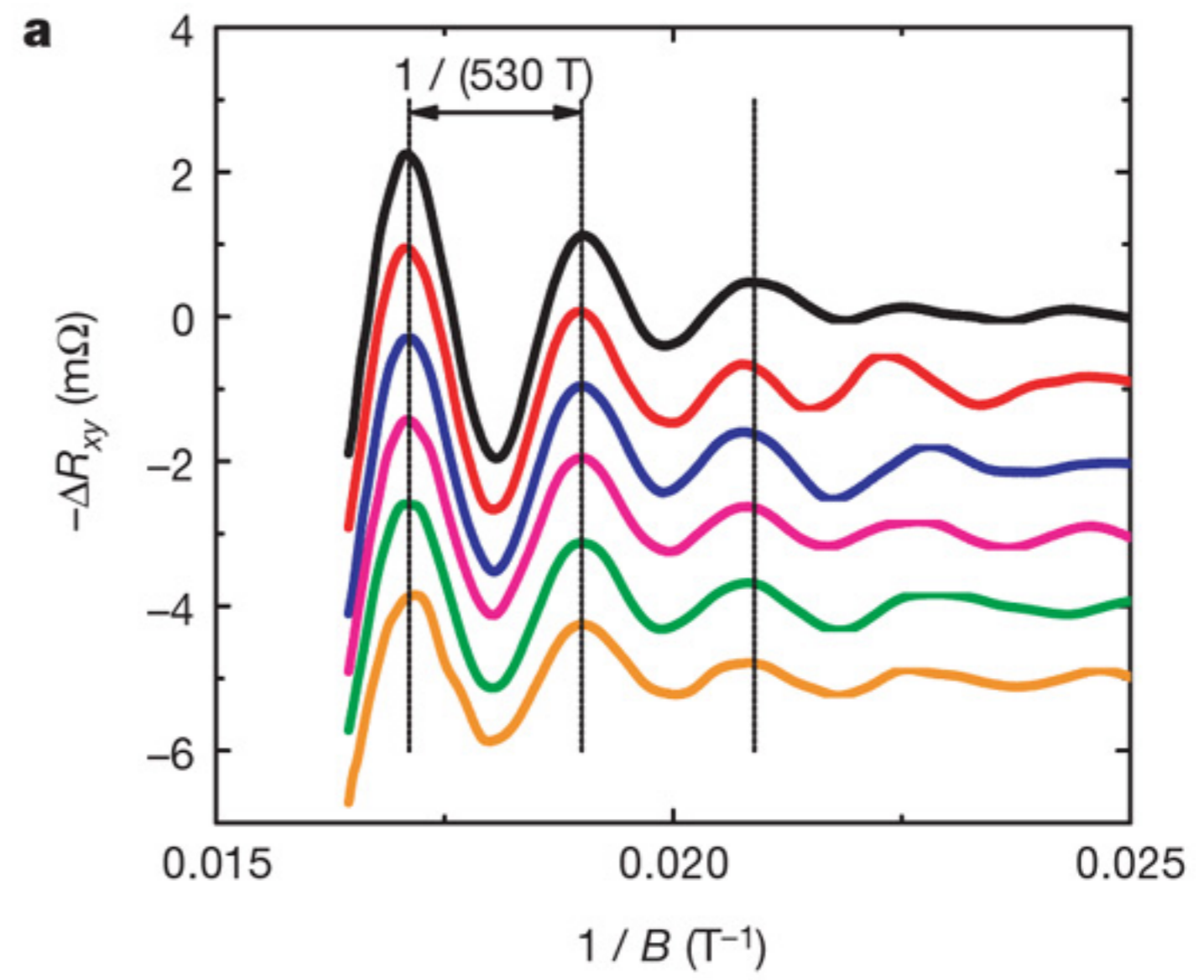


Incommensurate order in $\text{YBa}_2\text{Cu}_3\text{O}_{6+x}$

N. Harrison, arXiv:0902.2741.

Quantum oscillations and the Fermi surface in an underdoped high T_c superconductor (ortho-II ordered $\text{YBa}_2\text{Cu}_3\text{O}_{6.5}$). The period corresponds to a carrier density ≈ 0.076 .

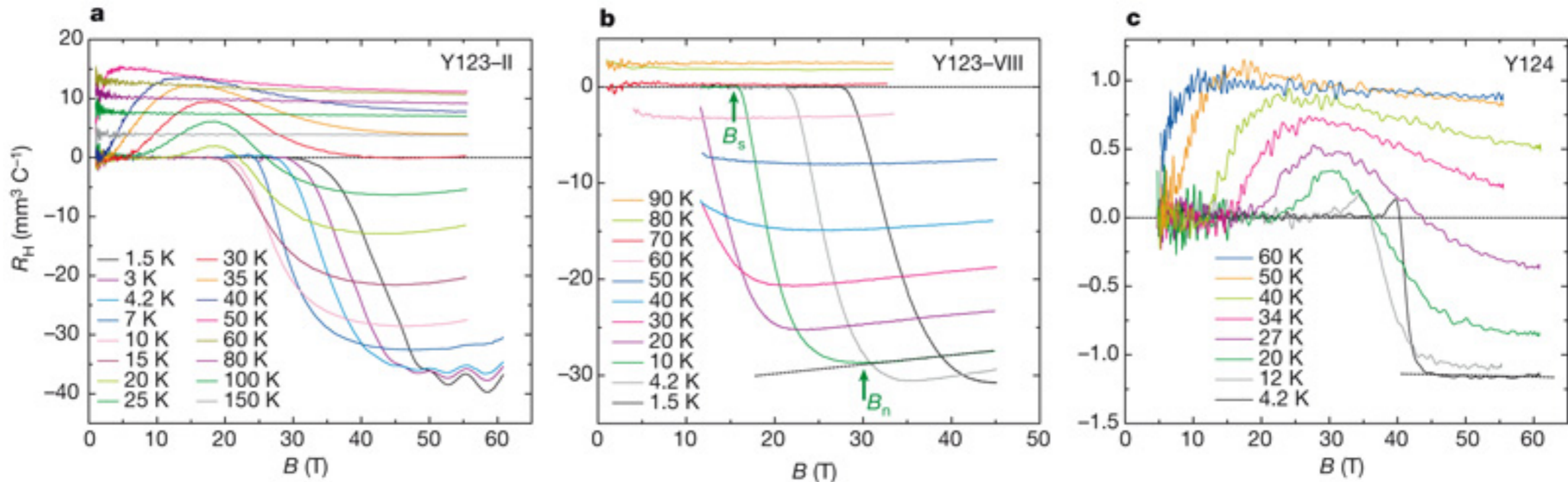
N. Doiron-Leyraud, C. Proust, D. LeBoeuf, J. Levallois, J.-B. Bonnemaïson, R. Liang, D. A. Bonn, W. N. Hardy, and L. Taillefer, *Nature* **447**, 565 (2007)



Electron pockets in the Fermi surface of hole-doped high- T_c superconductors

David LeBoeuf¹, Nicolas Doiron-Leyraud¹, Julien Levallois², R. Daou¹, J.-B. Bonnemaïson¹, N. E. Hussey³, L. Balicas⁴, B. J. Ramshaw⁵, Ruixing Liang^{5,6}, D. A. Bonn^{5,6}, W. N. Hardy^{5,6}, S. Adachi⁷, Cyril Proust² & Louis Taillefer^{1,6}

Nature **450**, 533 (2007)



Outline

1. Nodal-anti-nodal dichotomy in the cuprates
Survey of recent experiments
2. Spin density wave theory of normal metal
From a “large” Fermi surface to electron and hole pockets
3. Algebraic charge liquids
Pairing by gauge forces, d-wave superconductivity, and the nodal-anti-nodal dichotomy

Outline

1. Nodal-anti-nodal dichotomy in the cuprates

Survey of recent experiments

2. Spin density wave theory of normal metal

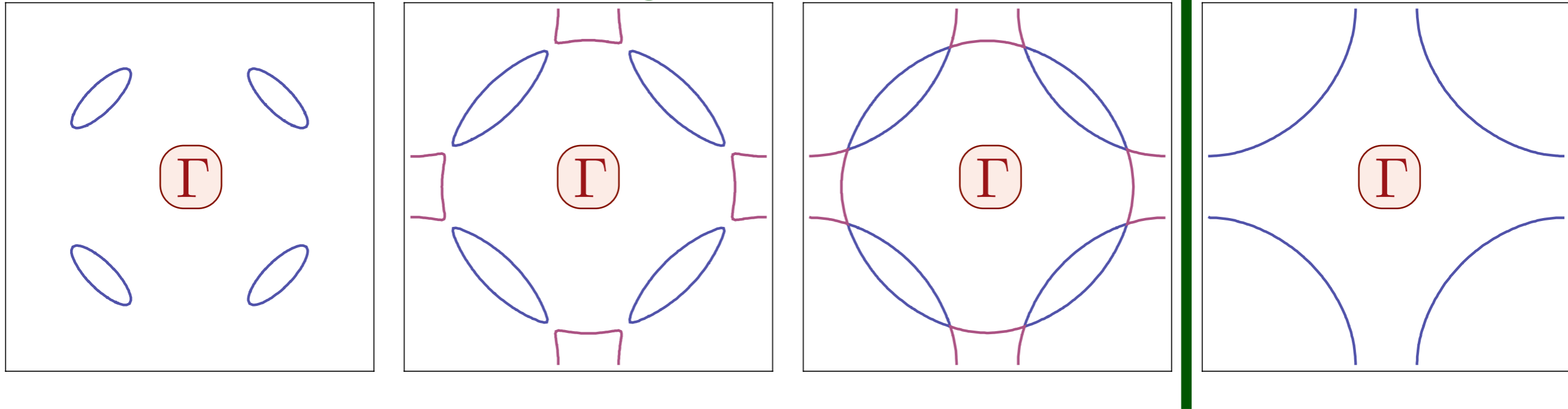
From a “large” Fermi surface to electron and hole pockets

3. Algebraic charge liquids

Pairing by gauge forces, d-wave superconductivity, and the nodal-anti-nodal dichotomy

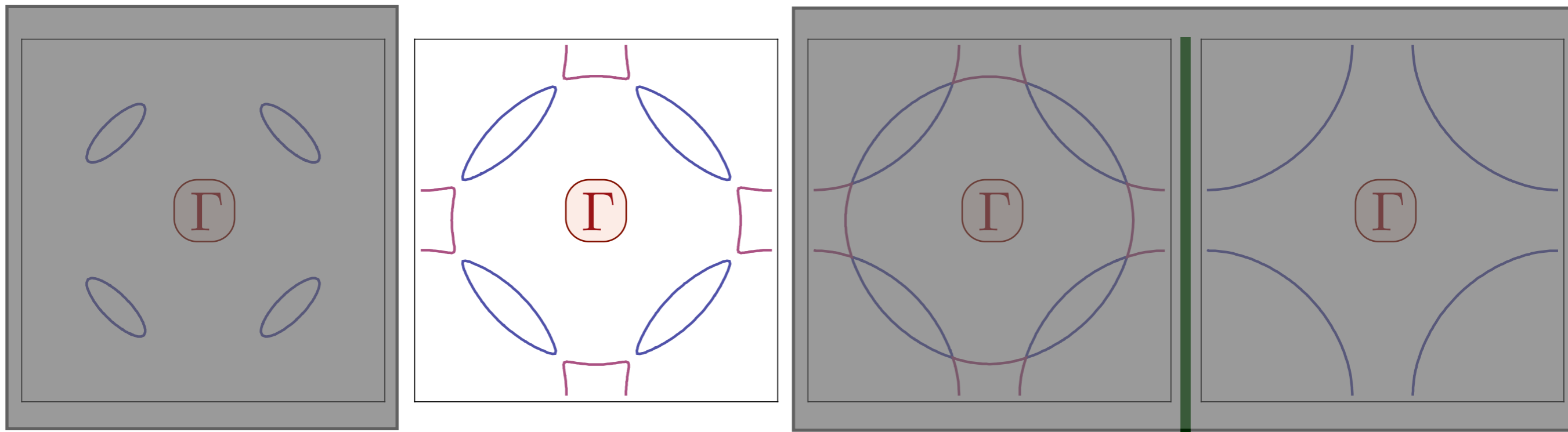
Spin density wave theory in hole-doped cuprates

← Increasing SDW order →



SDW order parameter is a vector, $\vec{\varphi}$,
whose amplitude vanishes at the transition
to the Fermi liquid.

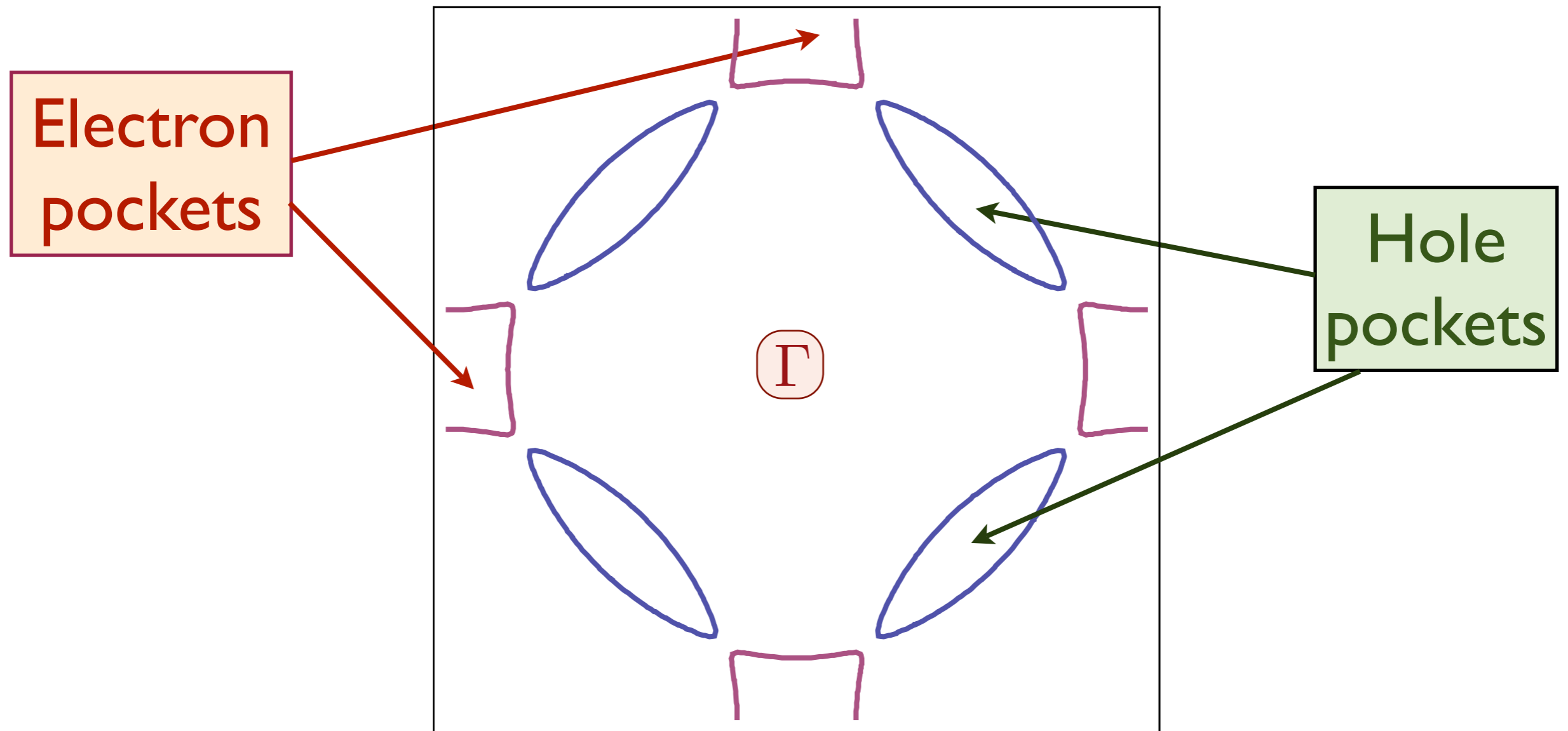
Fermi pockets in hole-doped cuprates



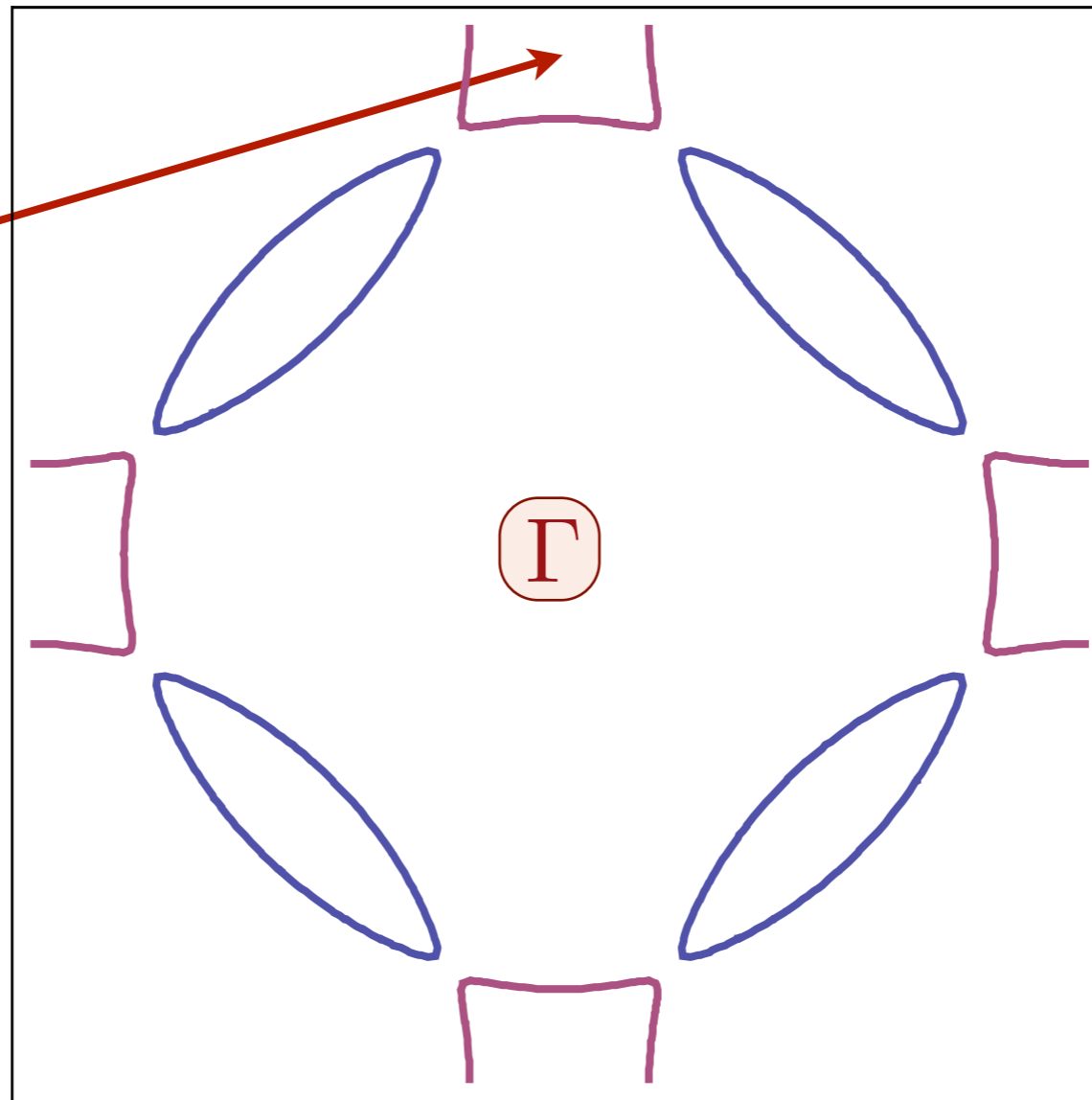
Begin with SDW ordered state, and focus on fluctuations in the *orientation* of $\vec{\varphi}$, by using a unit-length bosonic spinor z_α

$$\vec{\varphi} = z_\alpha^* \vec{\sigma}_{\alpha\beta} z_\beta$$

Charge carriers in the lightly-doped cuprates with Neel order



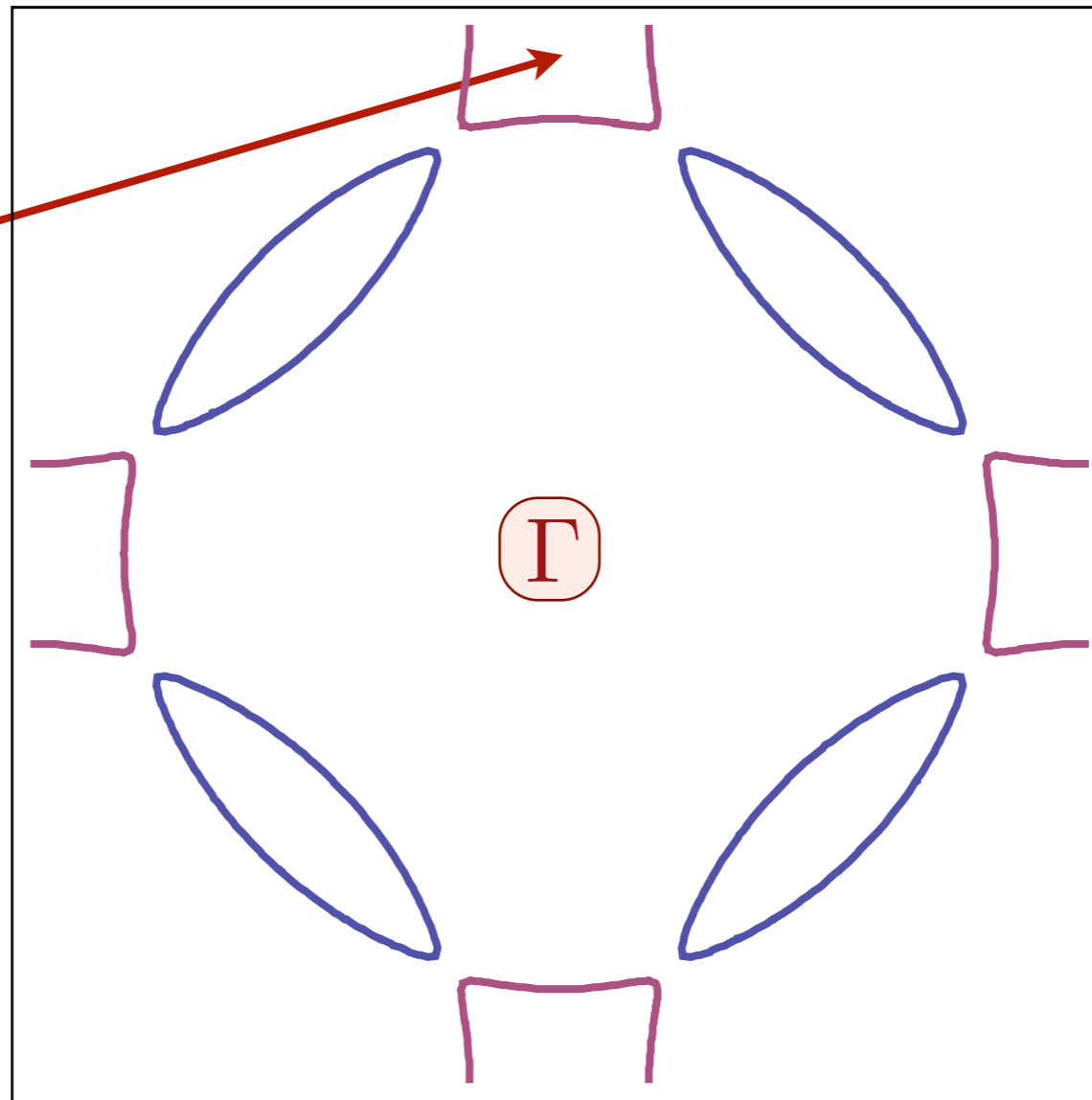
Electron
operator
 $c_{1\alpha}$



For a uniform SDW order with $\vec{\varphi} \propto (0, 0, 1)$, write

$$\begin{pmatrix} c_{1\uparrow} \\ c_{1\downarrow} \end{pmatrix} = \begin{pmatrix} g_+ \\ g_- \end{pmatrix}$$

Electron
operator
 $c_{1\alpha}$

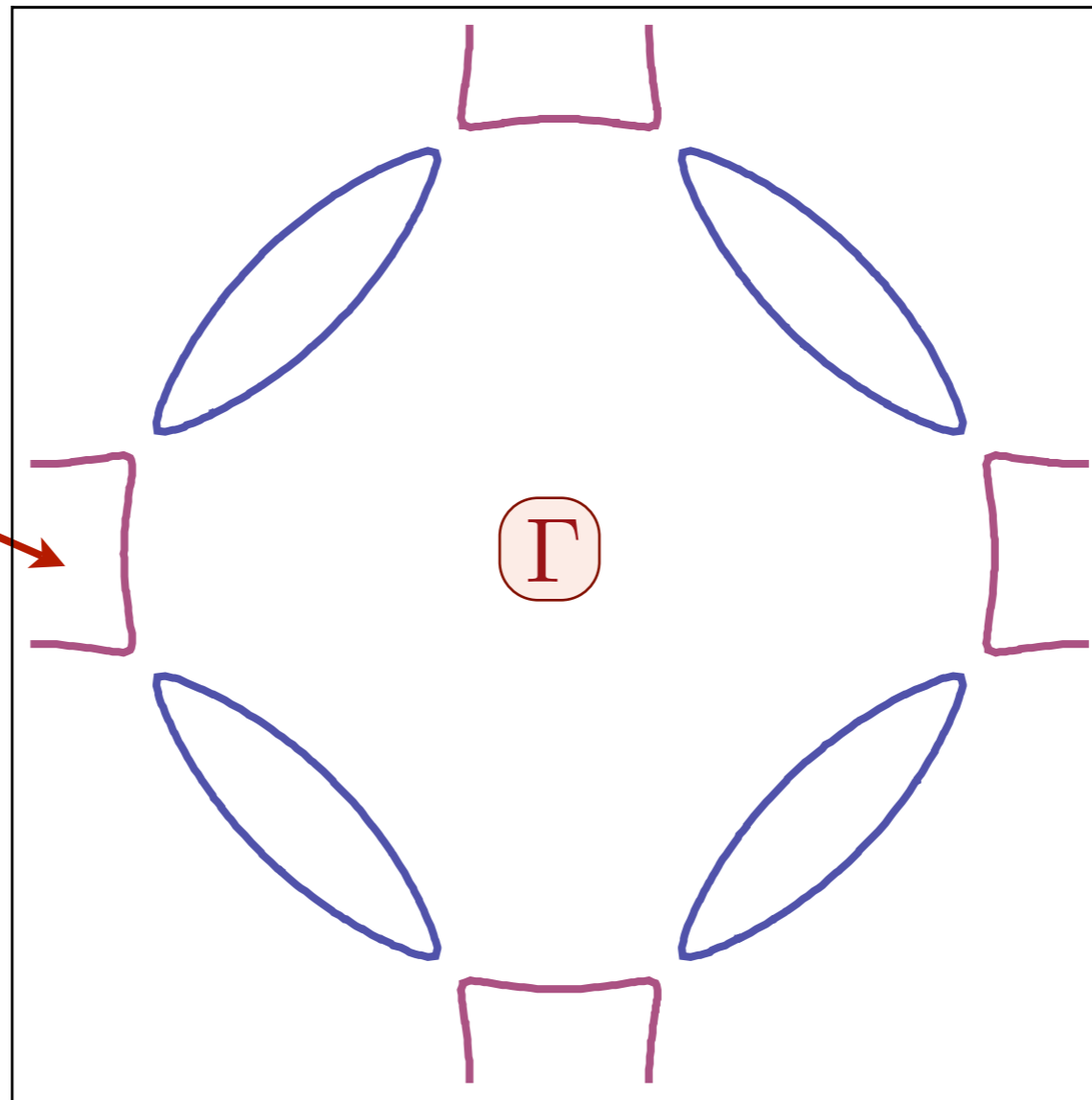


For a spacetime dependent SDW order, $\vec{\varphi} = z_{\alpha}^* \vec{\sigma}_{\alpha\beta} z_{\beta}$,

$$\begin{pmatrix} c_{1\uparrow} \\ c_{1\downarrow} \end{pmatrix} = \mathcal{R}_z \begin{pmatrix} g_+ \\ g_- \end{pmatrix} \quad ; \quad \mathcal{R}_z \equiv \begin{pmatrix} z_{\uparrow} & -z_{\downarrow}^* \\ z_{\downarrow} & z_{\uparrow}^* \end{pmatrix}.$$

So g_{\pm} are the “up/down” electron operators in a rotating reference frame defined by the local SDW order

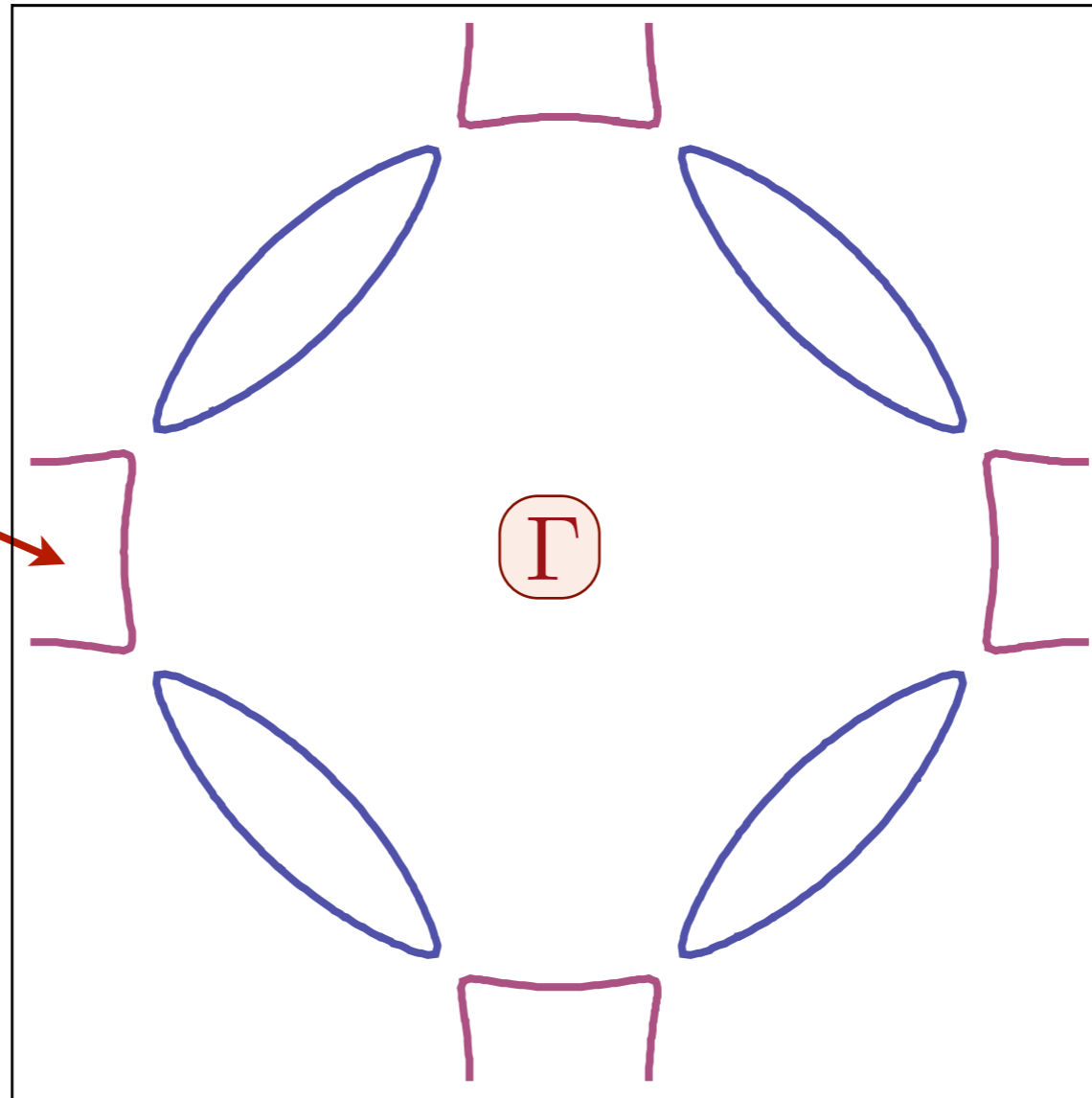
Electron
operator
 $c_{2\alpha}$



SDW theory also specifies electrons
at second pocket for $\vec{\varphi} \propto (0, 0, 1)$

$$\begin{pmatrix} c_{2\uparrow} \\ c_{2\downarrow} \end{pmatrix} = \begin{pmatrix} g_+ \\ -g_- \end{pmatrix}$$

Electron
operator
 $c_{2\alpha}$



For a spacetime dependent SDW order, $\vec{\varphi} = z_{\alpha}^* \vec{\sigma}_{\alpha\beta} z_{\beta}$,

$$\begin{pmatrix} c_{2\uparrow} \\ c_{2\downarrow} \end{pmatrix} = \mathcal{R}_z \begin{pmatrix} g_+ \\ -g_- \end{pmatrix} \quad ; \quad \mathcal{R}_z \equiv \begin{pmatrix} z_{\uparrow} & -z_{\downarrow}^* \\ z_{\downarrow} & z_{\uparrow}^* \end{pmatrix}.$$

Same SU(2) matrix also rotates electrons in second pocket.

Low energy theory for spinless, charge $-e$ fermions g_{\pm} , and spinful, charge 0 bosons z_{α} :

$$\begin{aligned}\mathcal{L} &= \mathcal{L}_z + \mathcal{L}_g \\ \mathcal{L}_z &= \frac{1}{t} \left[|(\partial_{\tau} - iA_{\tau})z_{\alpha}|^2 + c^2 |\nabla - i\mathbf{A})z_{\alpha}|^2 \right] \\ &+ \text{Berry phases of monopoles in } A_{\mu}.\end{aligned}$$

CP^1 field theory for z_{α} and an emergent $\text{U}(1)$ gauge field A_{μ} . Coupling t tunes the strength of SDW orientation fluctuations.

Low energy theory for spinless, charge $-e$ fermions g_{\pm} , and spinful, charge 0 bosons z_{α} :

$$\begin{aligned}\mathcal{L} &= \mathcal{L}_z + \mathcal{L}_g \\ \mathcal{L}_z &= \frac{1}{t} \left[|(\partial_{\tau} - iA_{\tau})z_{\alpha}|^2 + c^2 |\nabla - i\mathbf{A})z_{\alpha}|^2 \right] \\ &+ \text{Berry phases of monopoles in } A_{\mu}.\end{aligned}$$

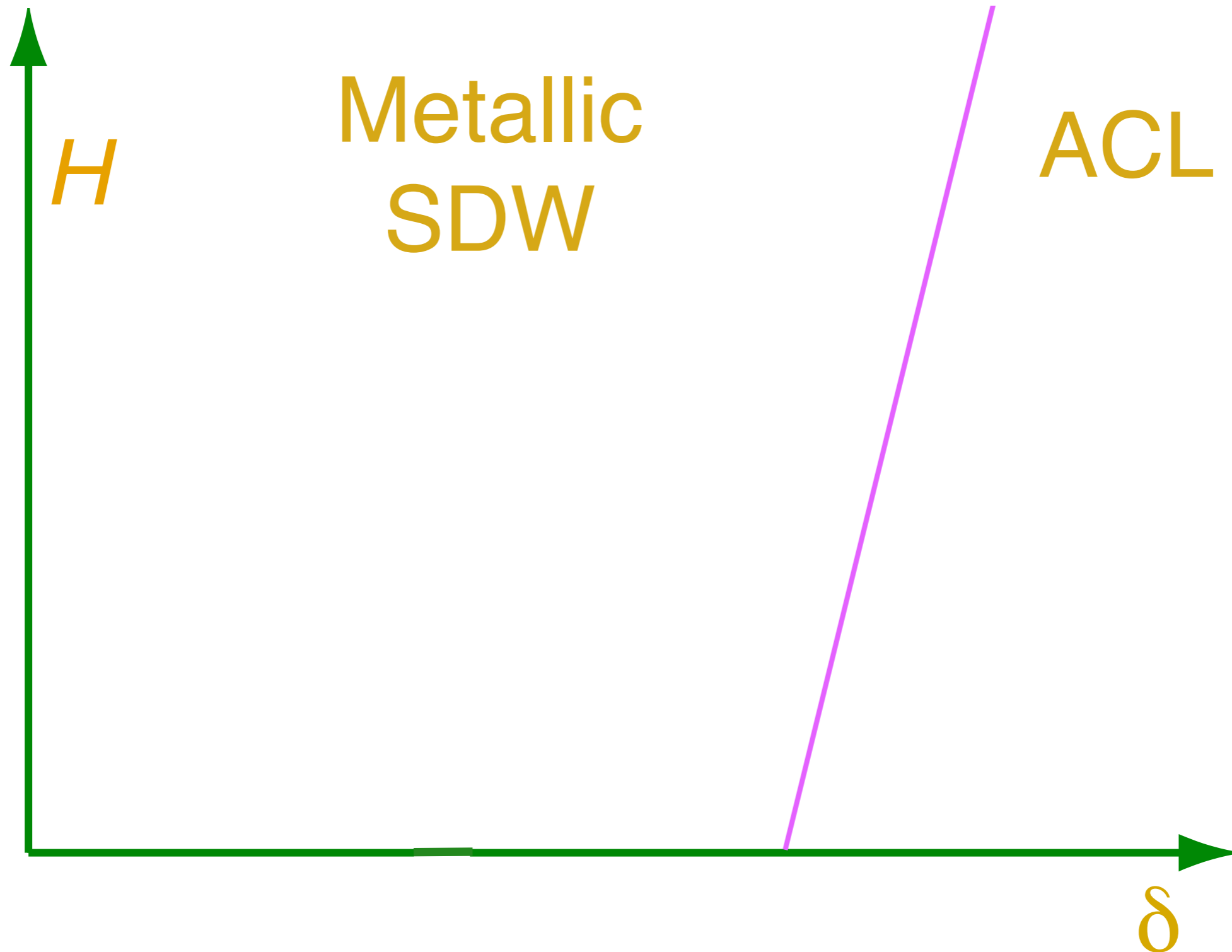
CP^1 field theory for z_{α} and an emergent U(1) gauge field A_{μ} . Coupling t tunes the strength of SDW orientation fluctuations.

$$\begin{aligned}\mathcal{L}_g &= g_{+}^{\dagger} \left[(\partial_{\tau} - iA_{\tau}) - \frac{1}{2m^{*}} (\nabla - i\mathbf{A})^2 - \mu \right] g_{+} \\ &+ g_{-}^{\dagger} \left[(\partial_{\tau} + iA_{\tau}) - \frac{1}{2m^{*}} (\nabla + i\mathbf{A})^2 - \mu \right] g_{-}\end{aligned}$$

Two Fermi surfaces coupled to the emergent U(1) gauge field A_{μ} with opposite charges

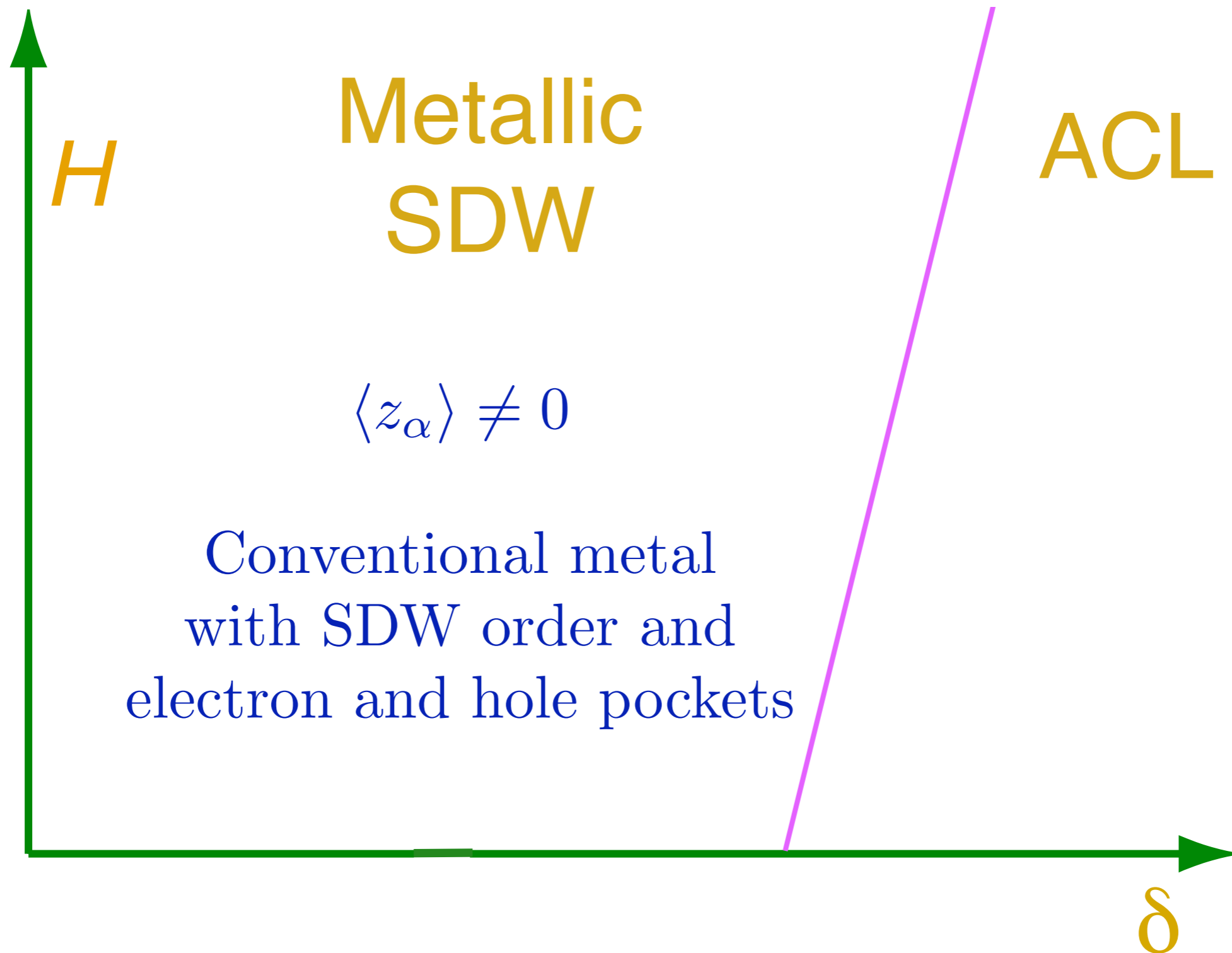
Phase diagram

as a function of hole density $\delta \sim t$ and magnetic field H .



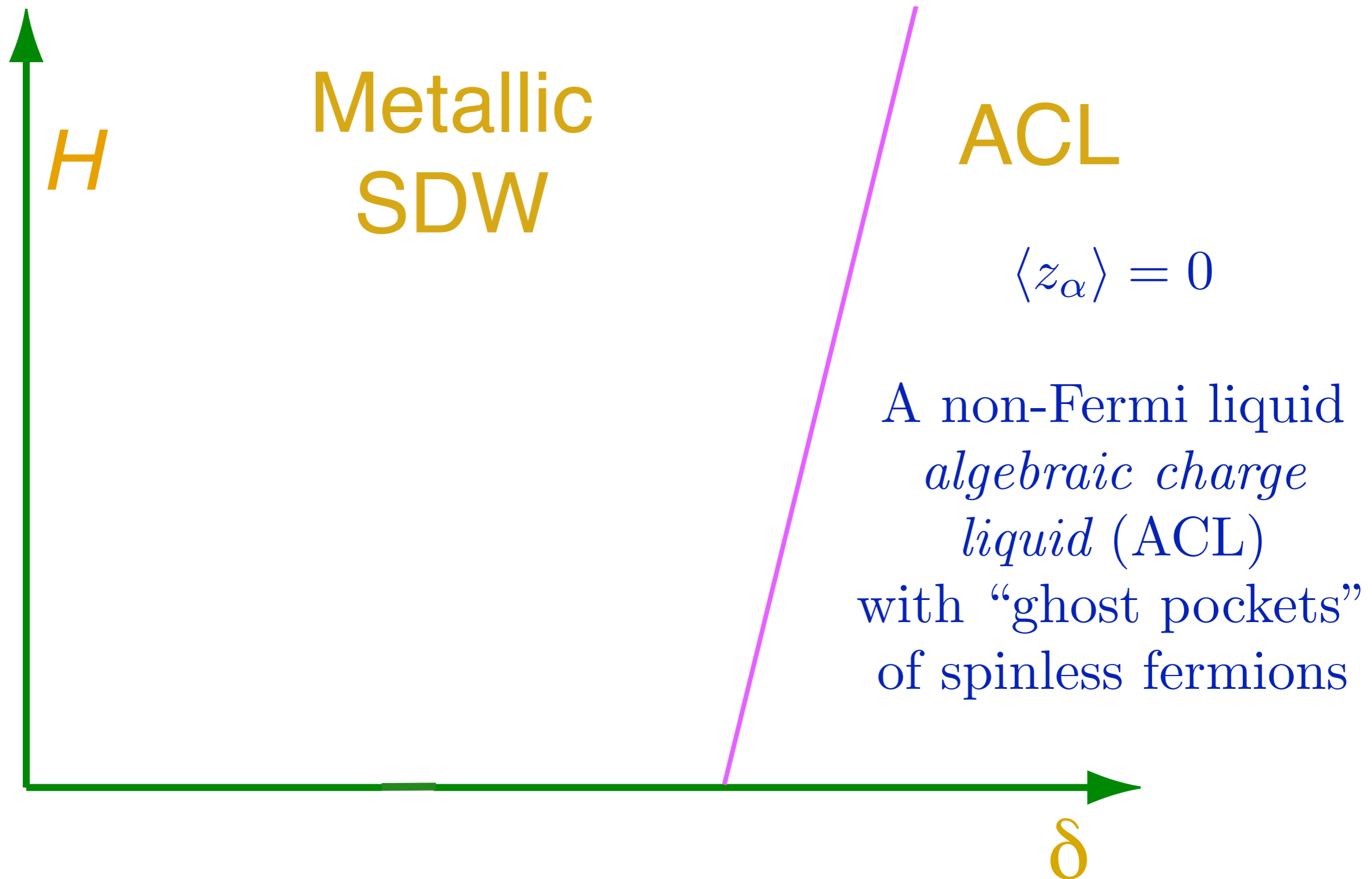
Phase diagram

as a function of hole density $\delta \sim t$ and magnetic field H .



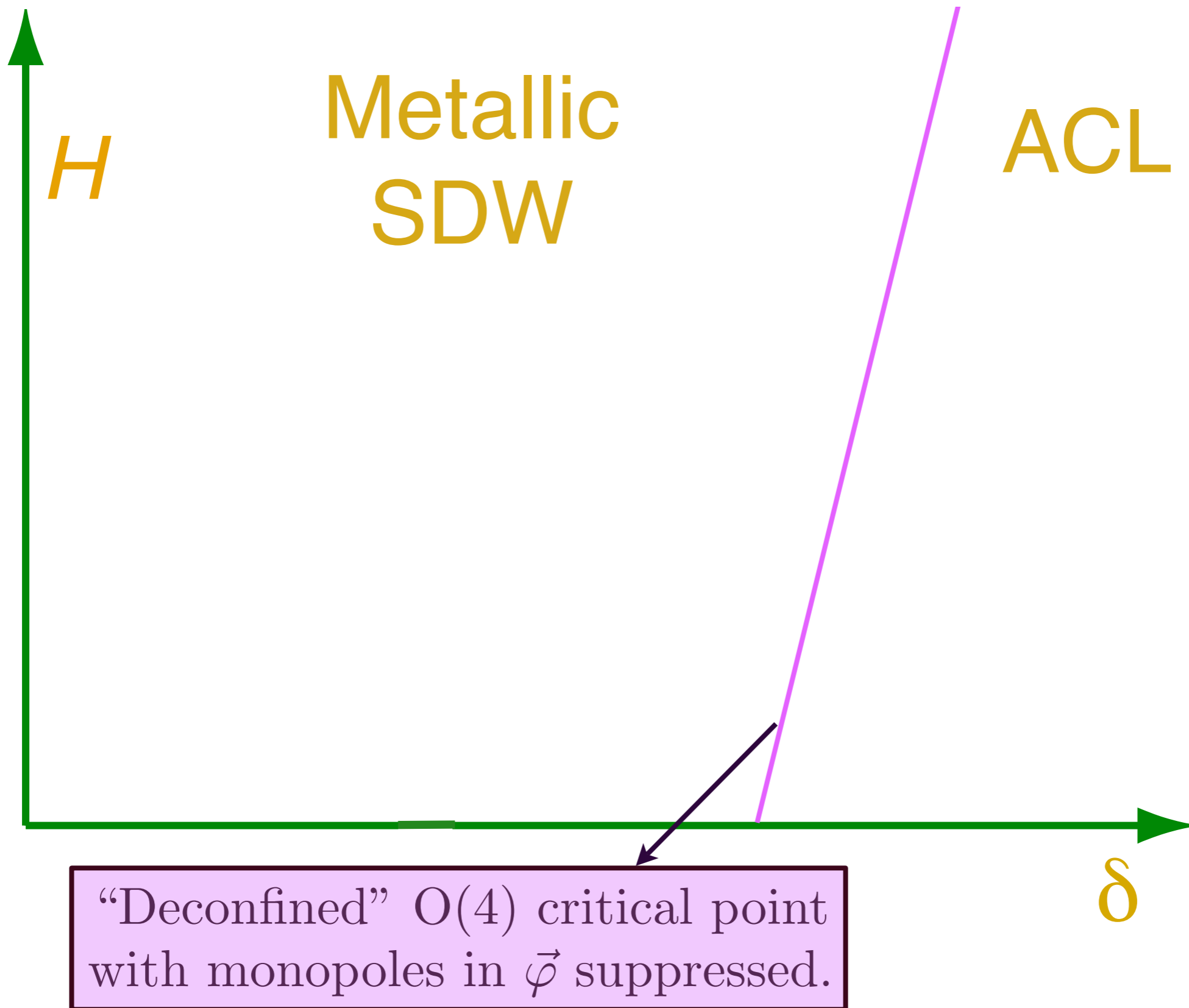
Phase diagram

as a function of hole density $\delta \sim t$ and magnetic field H .



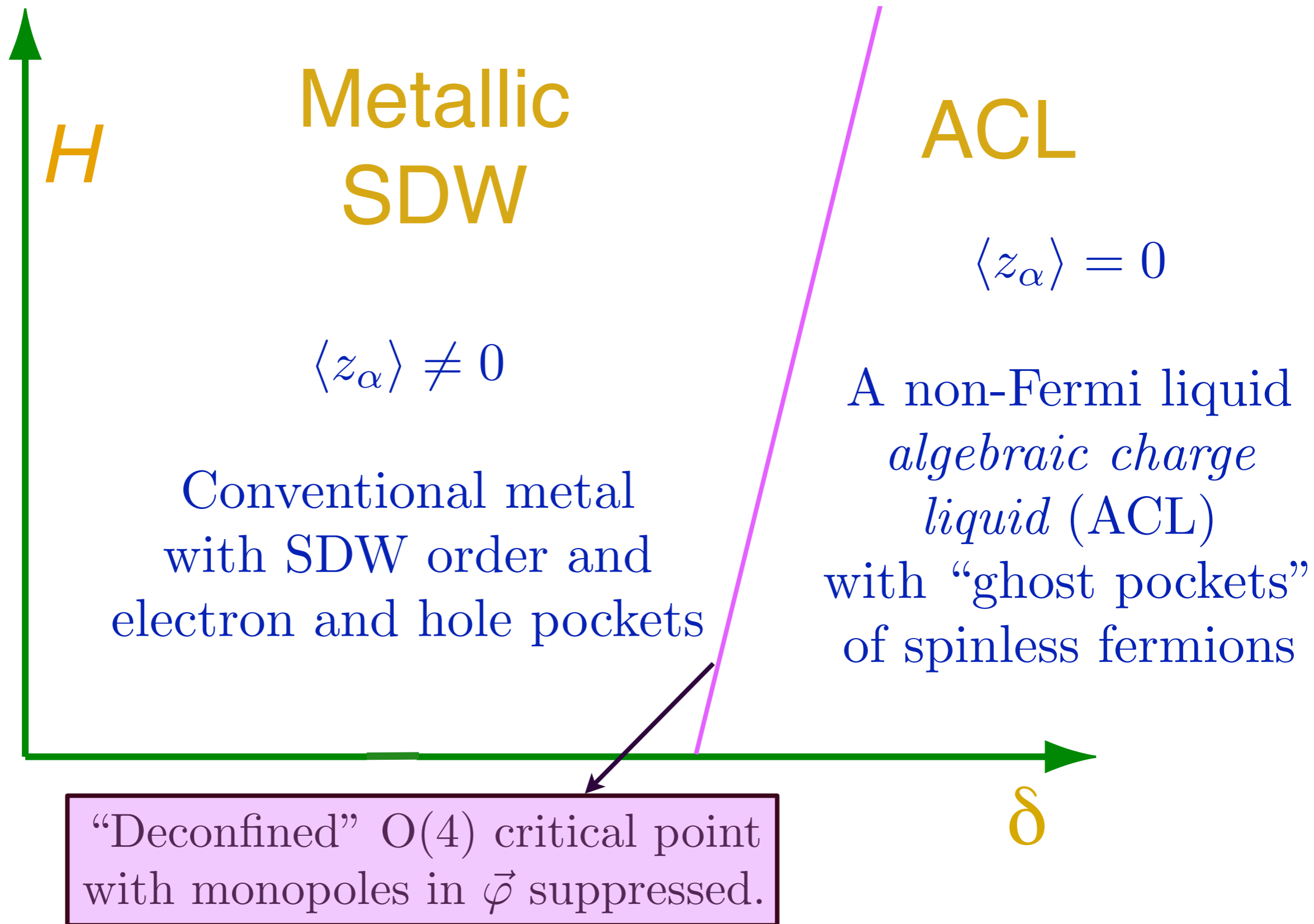
Phase diagram

as a function of hole density $\delta \sim t$ and magnetic field H .



Phase diagram

as a function of hole density $\delta \sim t$ and magnetic field H .



Strong pairing of the g_{\pm} electron pockets

- Problem is similar to double layer quantum Hall systems at total filling fraction $\nu = 1$. At large layer spacing we have 2 composite fermion Fermi surfaces each at filling fraction $\nu = 1/2$. At small layer spacing, there is a paired state formed by attractive interaction mediated by antisymmetric gauge field.

N. E. Bonesteel, I. A. McDonald, and C. Nayak, *Phys. Rev. Lett.* **77**, 3009 (1996).

I. Ussishkin and A. Stern, *Phys. Rev. Lett.* **81**, 3932 (1998).

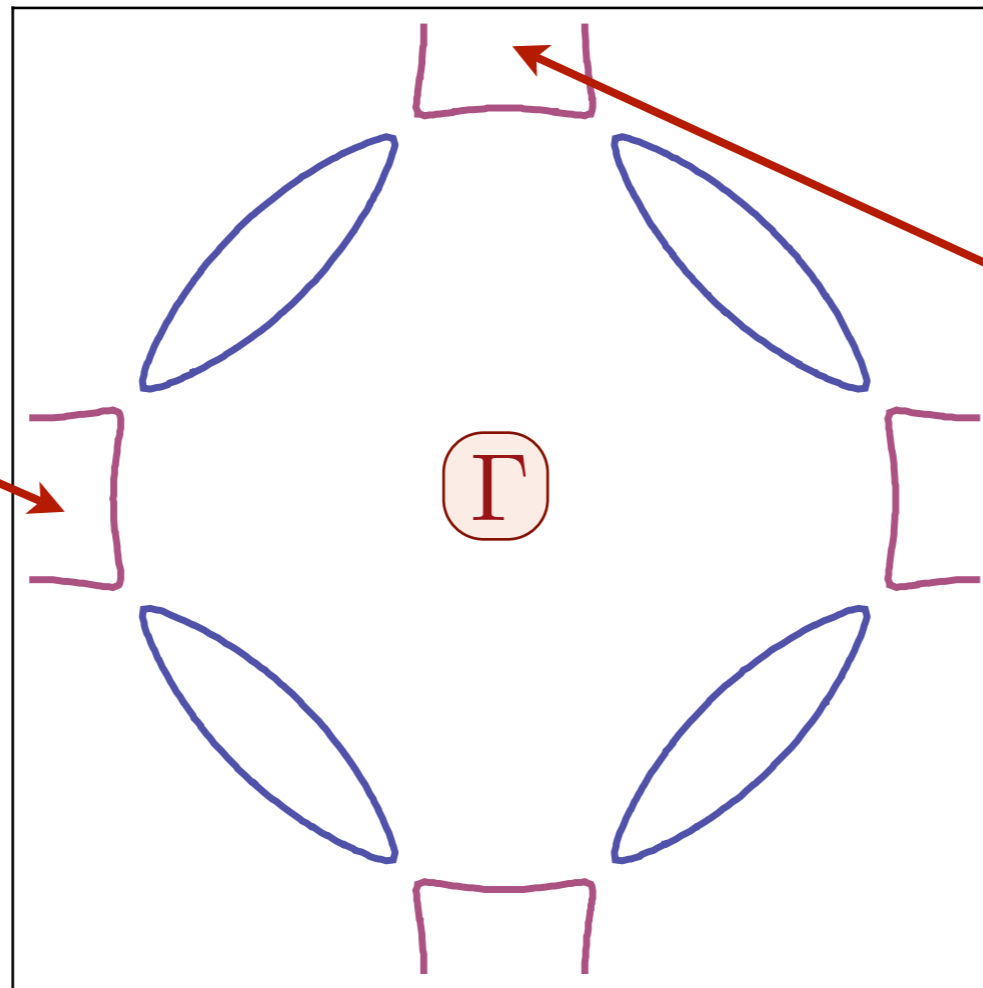
Strong pairing of the g_{\pm} electron pockets

- Problem is similar to double layer quantum Hall systems at total filling fraction $\nu = 1$. At large layer spacing we have 2 composite fermion Fermi surfaces each at filling fraction $\nu = 1/2$. At small layer spacing, there is a paired state formed by attractive interaction mediated by antisymmetric gauge field.
- Gauge forces lead to a s -wave paired state with a T_c of order the Fermi energy of the pockets. Inelastic scattering from low energy gauge modes lead to very singular g_{\pm} self energy, but is *not* pair-breaking.

$$\langle g_+ g_- \rangle = \Delta$$

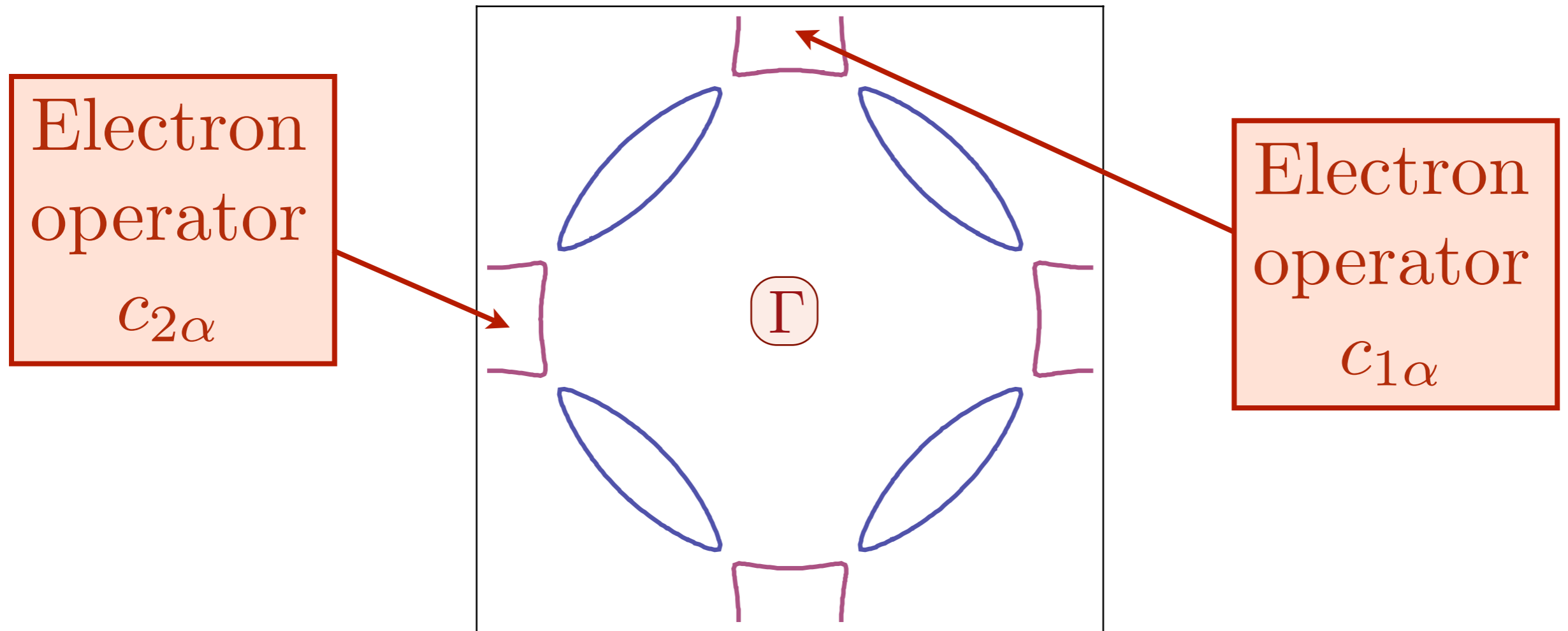
Strong pairing of the g_{\pm} electron pockets

Electron operator
 $c_{2\alpha}$



Electron operator
 $c_{1\alpha}$

Strong pairing of the g_{\pm} electron pockets

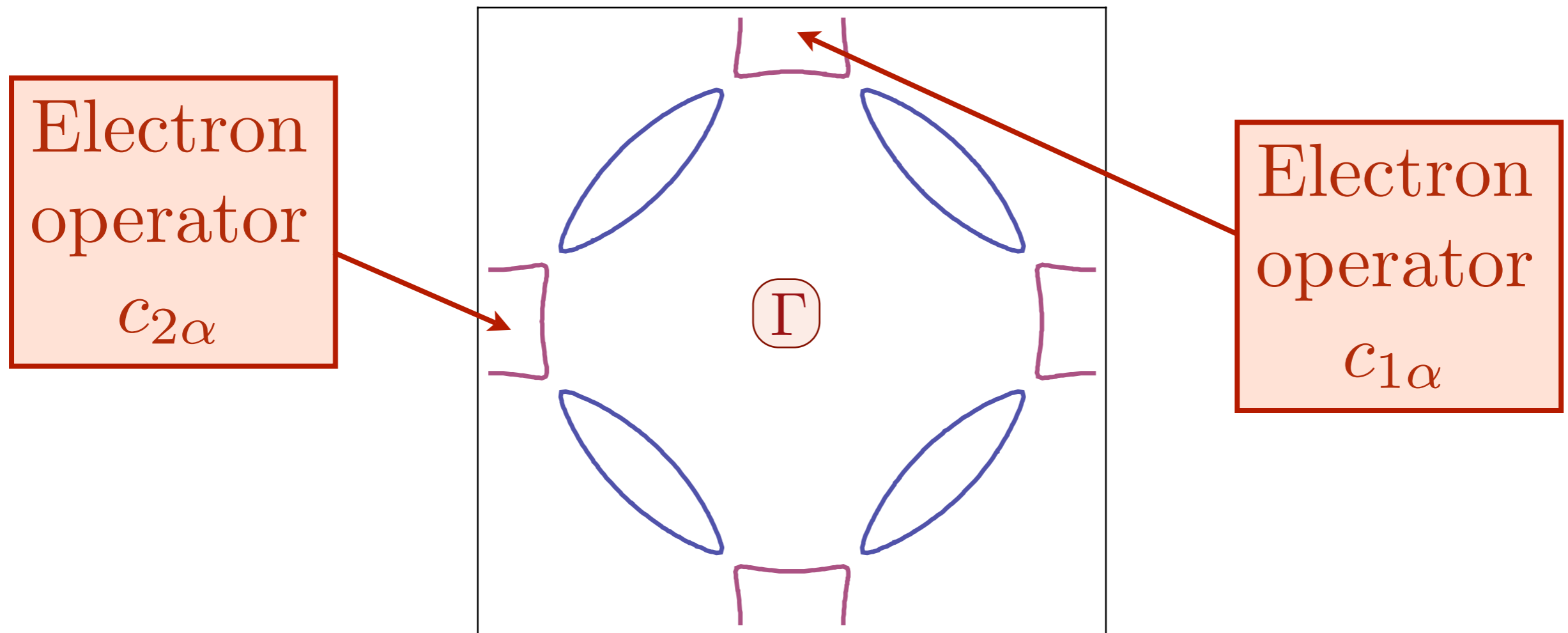


- Transforming back to the physical fermions:

$$\begin{pmatrix} c_{1\uparrow} \\ c_{1\downarrow} \end{pmatrix} = \begin{pmatrix} z_{\uparrow} & -z_{\downarrow}^* \\ z_{\downarrow} & z_{\uparrow}^* \end{pmatrix} \begin{pmatrix} g_+ \\ g_- \end{pmatrix} \quad ; \quad \begin{pmatrix} c_{2\uparrow} \\ c_{2\downarrow} \end{pmatrix} = \begin{pmatrix} z_{\uparrow} & -z_{\downarrow}^* \\ z_{\downarrow} & z_{\uparrow}^* \end{pmatrix} \begin{pmatrix} g_+ \\ -g_- \end{pmatrix},$$

we find: $\langle c_{1\uparrow} c_{1\downarrow} \rangle = -\langle c_{2\uparrow} c_{2\downarrow} \rangle \sim \langle |z_{\uparrow}|^2 + |z_{\downarrow}|^2 \rangle \langle g_+ g_- \rangle;$

Strong pairing of the g_{\pm} electron pockets



- Transforming back to the physical fermions:

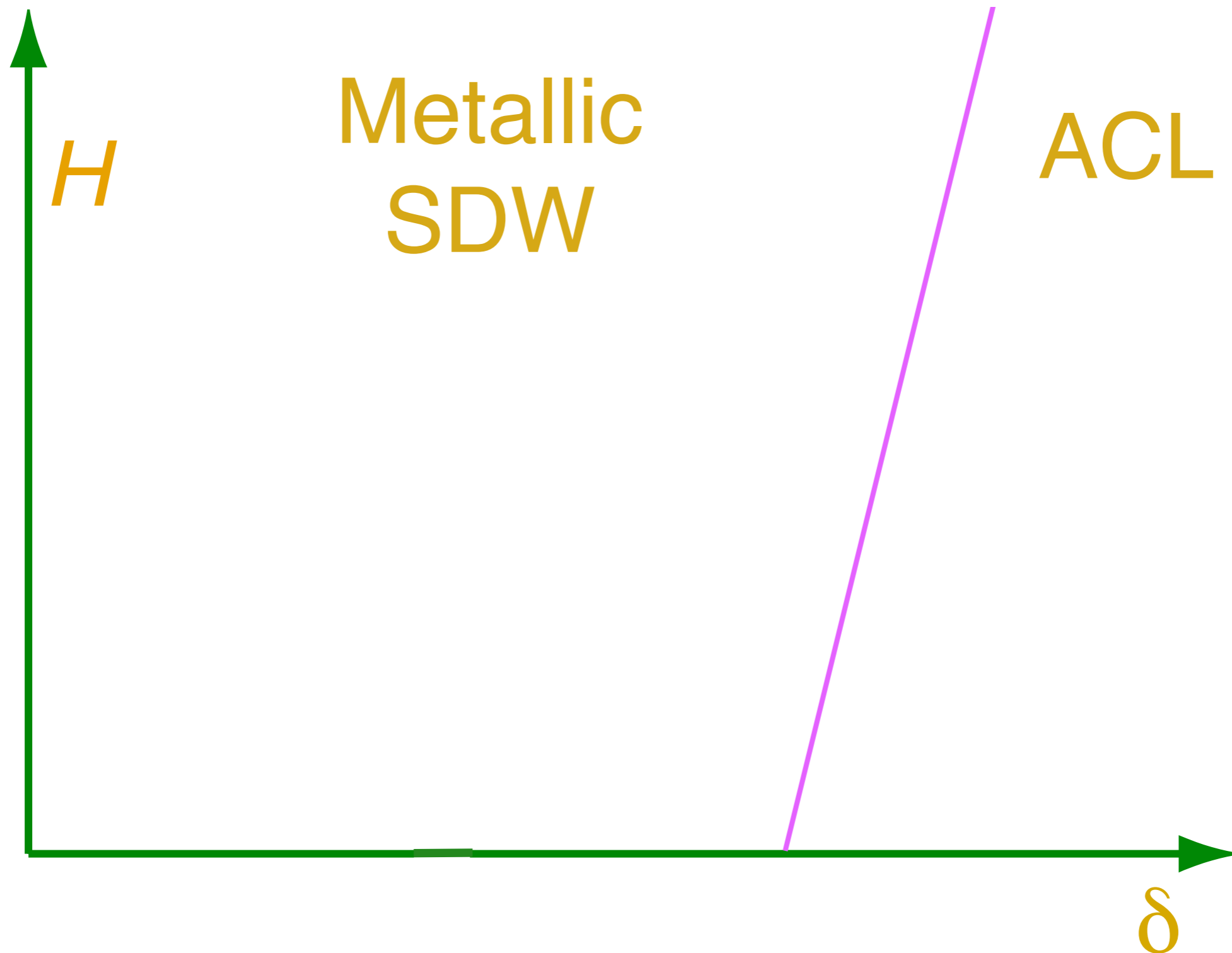
$$\begin{pmatrix} c_{1\uparrow} \\ c_{1\downarrow} \end{pmatrix} = \begin{pmatrix} z_{\uparrow} & -z_{\downarrow}^* \\ z_{\downarrow} & z_{\uparrow}^* \end{pmatrix} \begin{pmatrix} g_+ \\ g_- \end{pmatrix} ; \quad \begin{pmatrix} c_{2\uparrow} \\ c_{2\downarrow} \end{pmatrix} = \begin{pmatrix} z_{\uparrow} & -z_{\downarrow}^* \\ z_{\downarrow} & z_{\uparrow}^* \end{pmatrix} \begin{pmatrix} g_+ \\ -g_- \end{pmatrix},$$

we find: $\langle c_{1\uparrow} c_{1\downarrow} \rangle = -\langle c_{2\uparrow} c_{2\downarrow} \rangle \sim \langle |z_{\uparrow}|^2 + |z_{\downarrow}|^2 \rangle \langle g_+ g_- \rangle$;

i.e. the pairing signature for the electrons is d -wave.

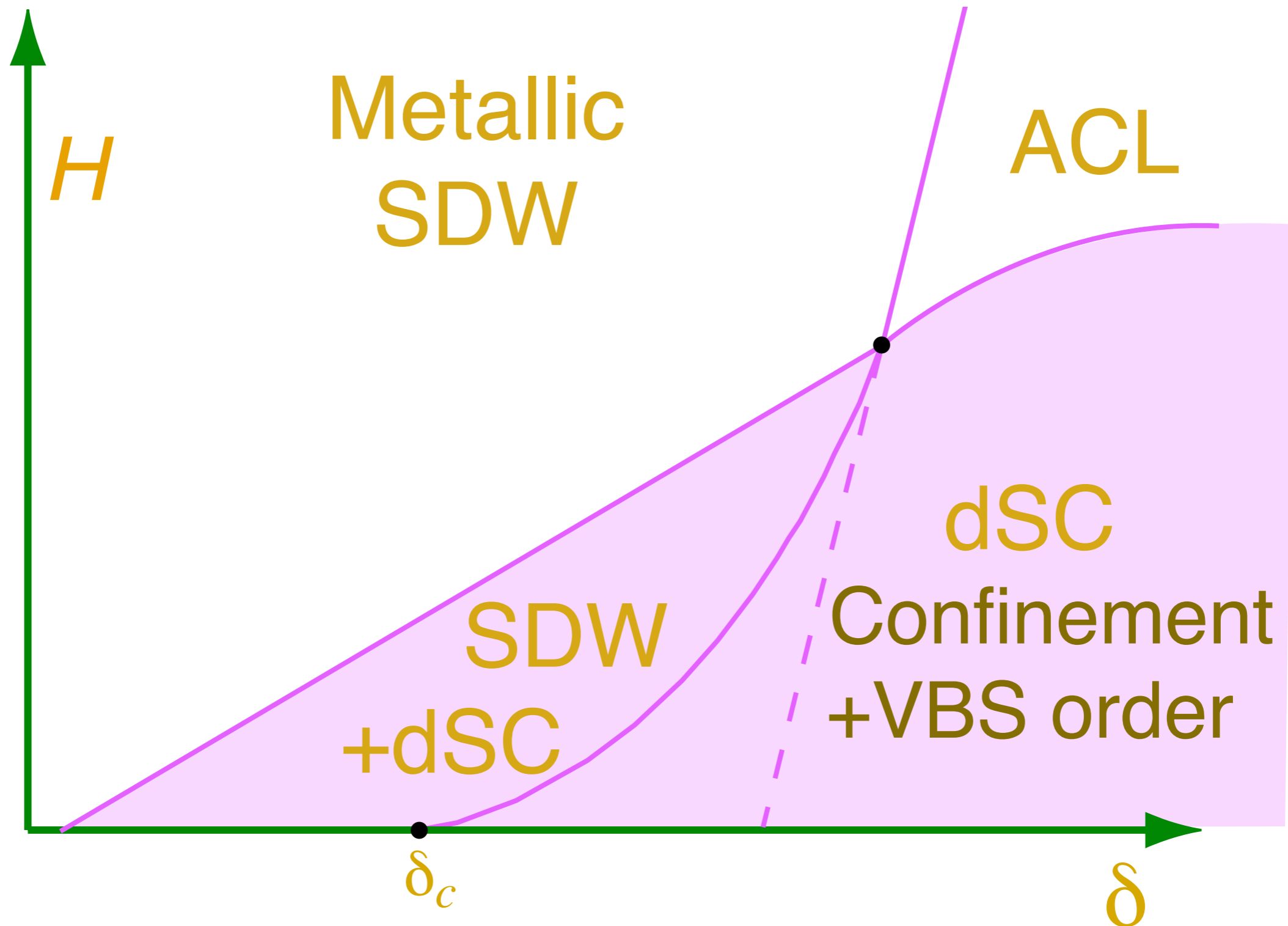
Phase diagram

as a function of hole density $\delta \sim t$ and magnetic field H .



Phase diagram

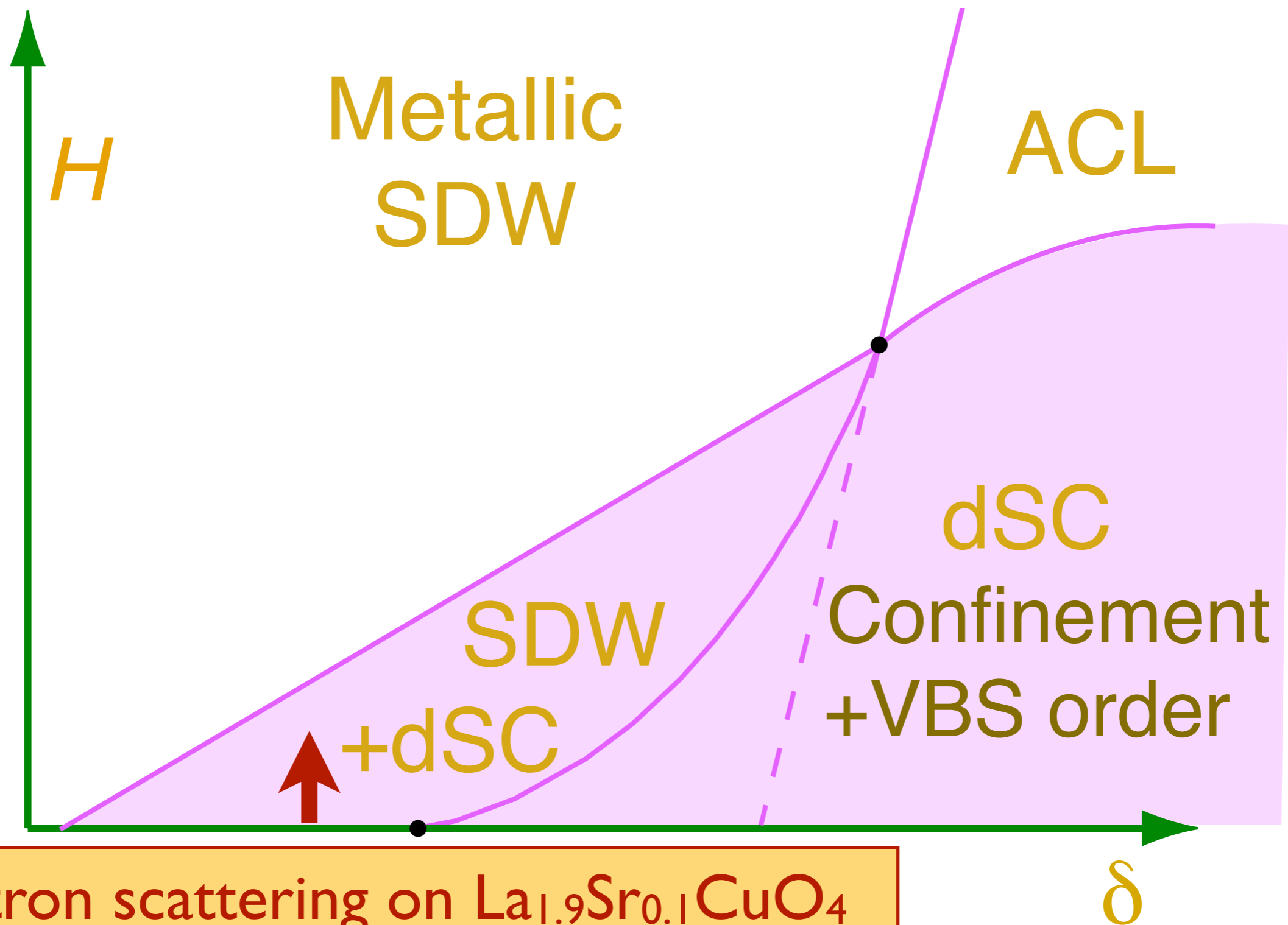
as a function of hole density $\delta \sim t$ and magnetic field H .



Interplay of dSC and SDW order is similar to theory of competing orders

Phase diagram

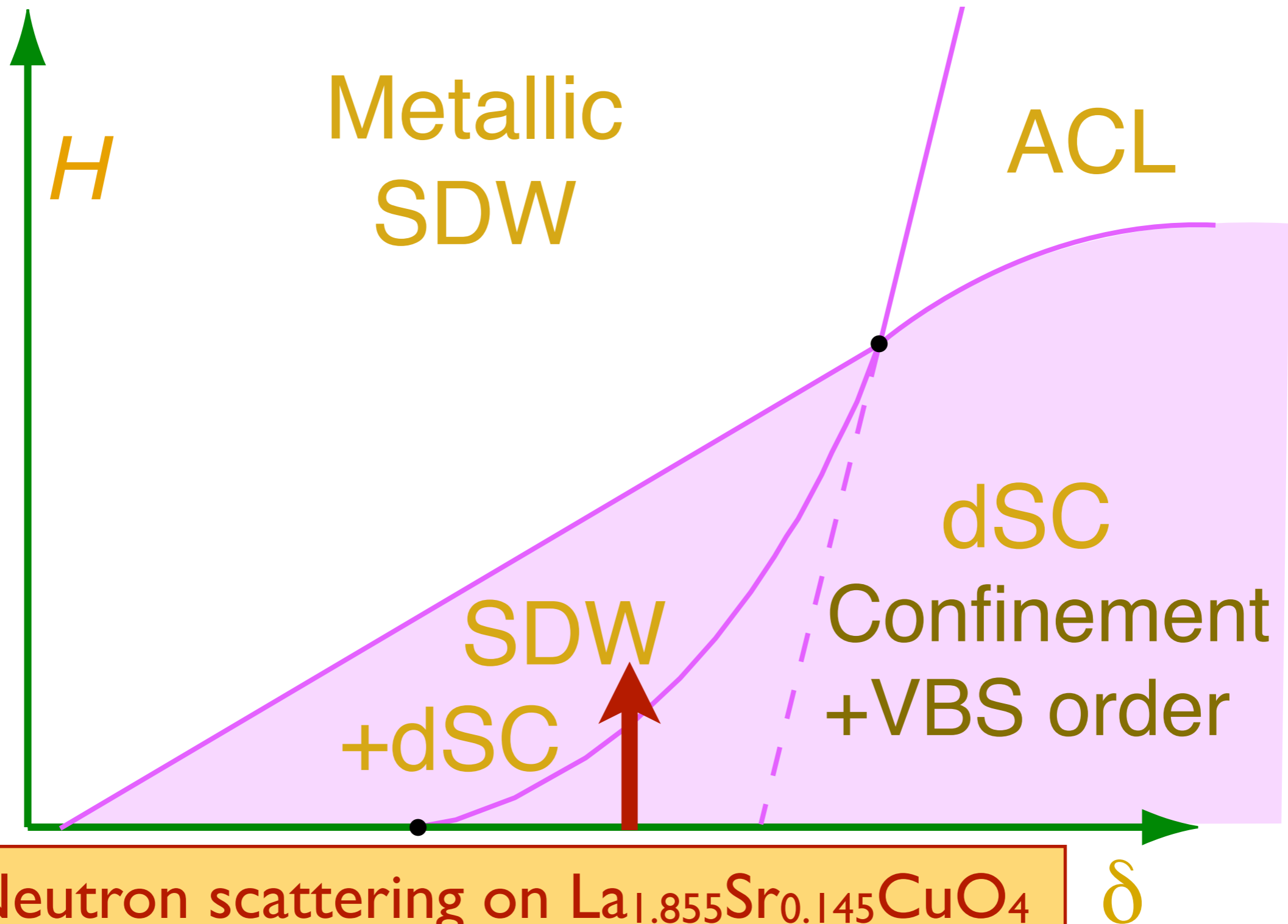
as a function of hole density $\delta \sim t$ and magnetic field H .



Neutron scattering on $\text{La}_{1.9}\text{Sr}_{0.1}\text{CuO}_4$
B. Lake *et al.*, *Nature* **415**, 299 (2002)

Phase diagram

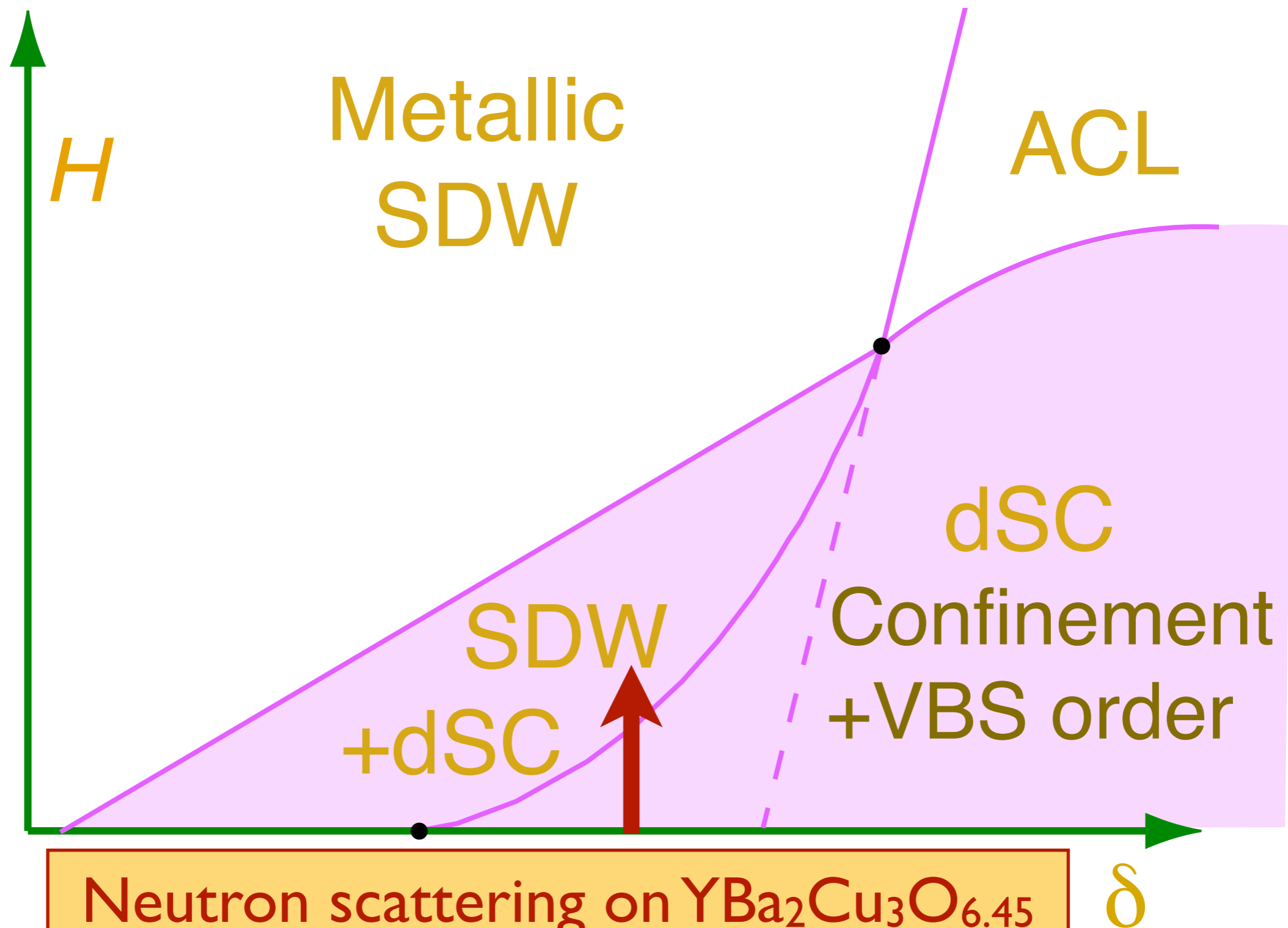
as a function of hole density $\delta \sim t$ and magnetic field H .



Neutron scattering on $\text{La}_{1.855}\text{Sr}_{0.145}\text{CuO}_4$
J. Chang *et al.*, arXiv:0902.1191

Phase diagram

as a function of hole density $\delta \sim t$ and magnetic field H .

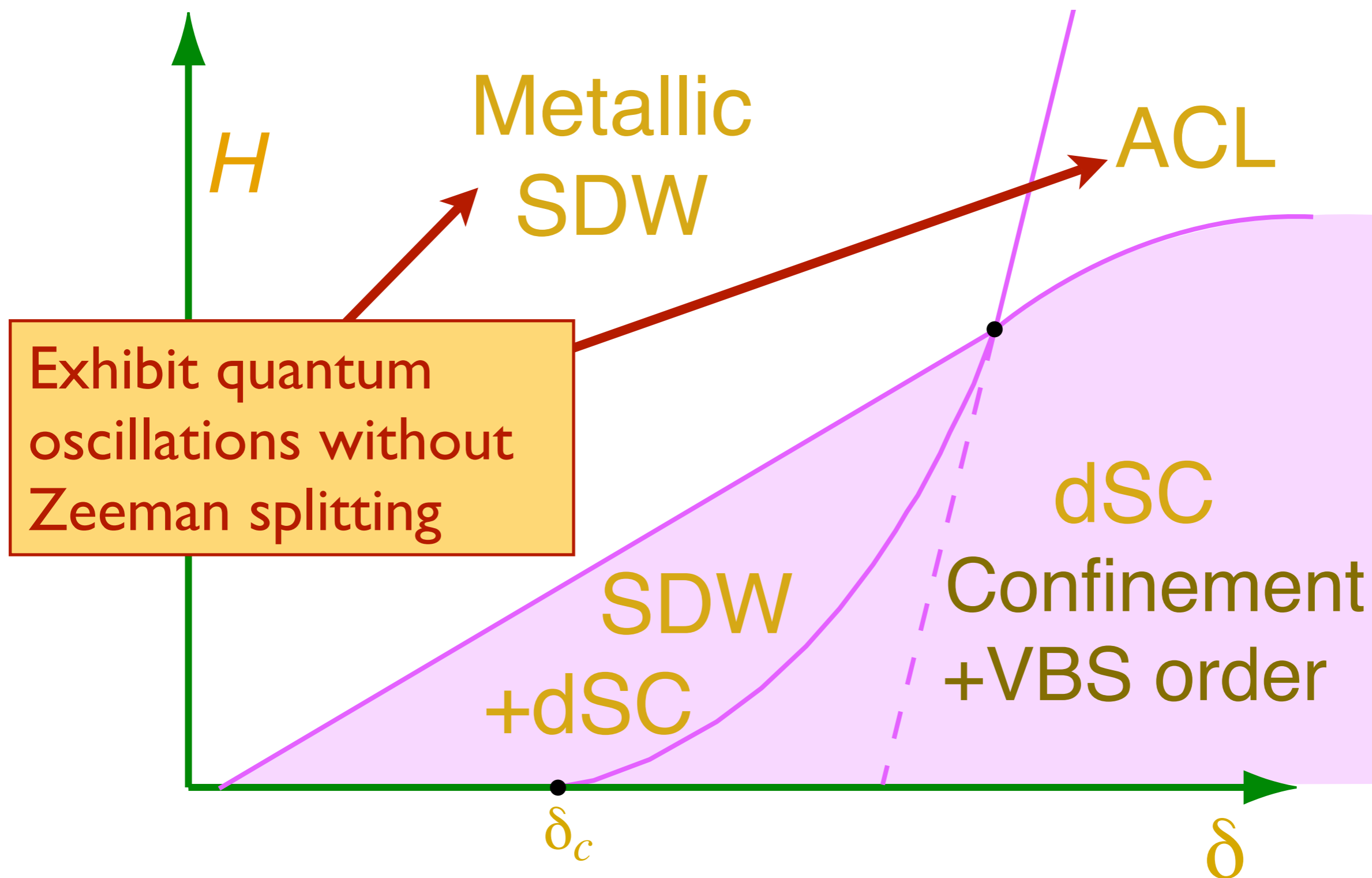


Neutron scattering on $\text{YBa}_2\text{Cu}_3\text{O}_{6.45}$

D. Haug *et al.*, arXiv:0902.3335

Phase diagram

as a function of hole density $\delta \sim t$ and magnetic field H .



Interplay of dSC and SDW order is similar to theory of competing orders

Simple numerical estimates

- Oscillation experiments provide the following information:

1. Effective mass: $m^* \sim (1-3)m_e$
2. Area of the Fermi surface: $A_e \sim 3\%A_{BZ}$
3. Fermi temperature: $T_F \sim (m_e/m^*) 700 \text{ K}$

- The pairing critical field for the e-pocket:

$$H_{p2}(0) \sim H_{\text{onset of oscillations}} \sim 50 \text{ T}$$

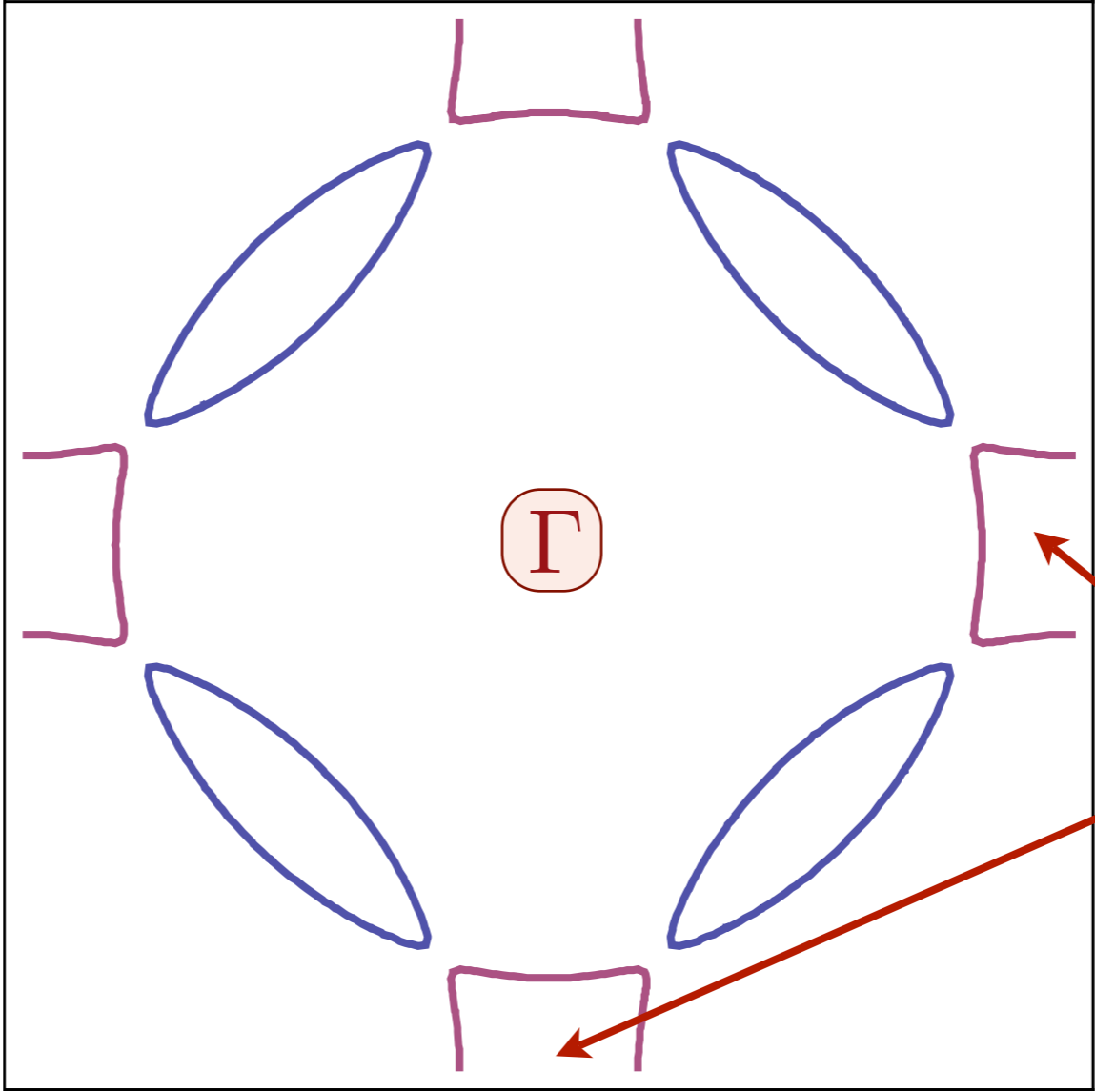
- For numerical estimates, we can use the BCS formula connecting $H_{p2}(0)$ and the pairing temperature:

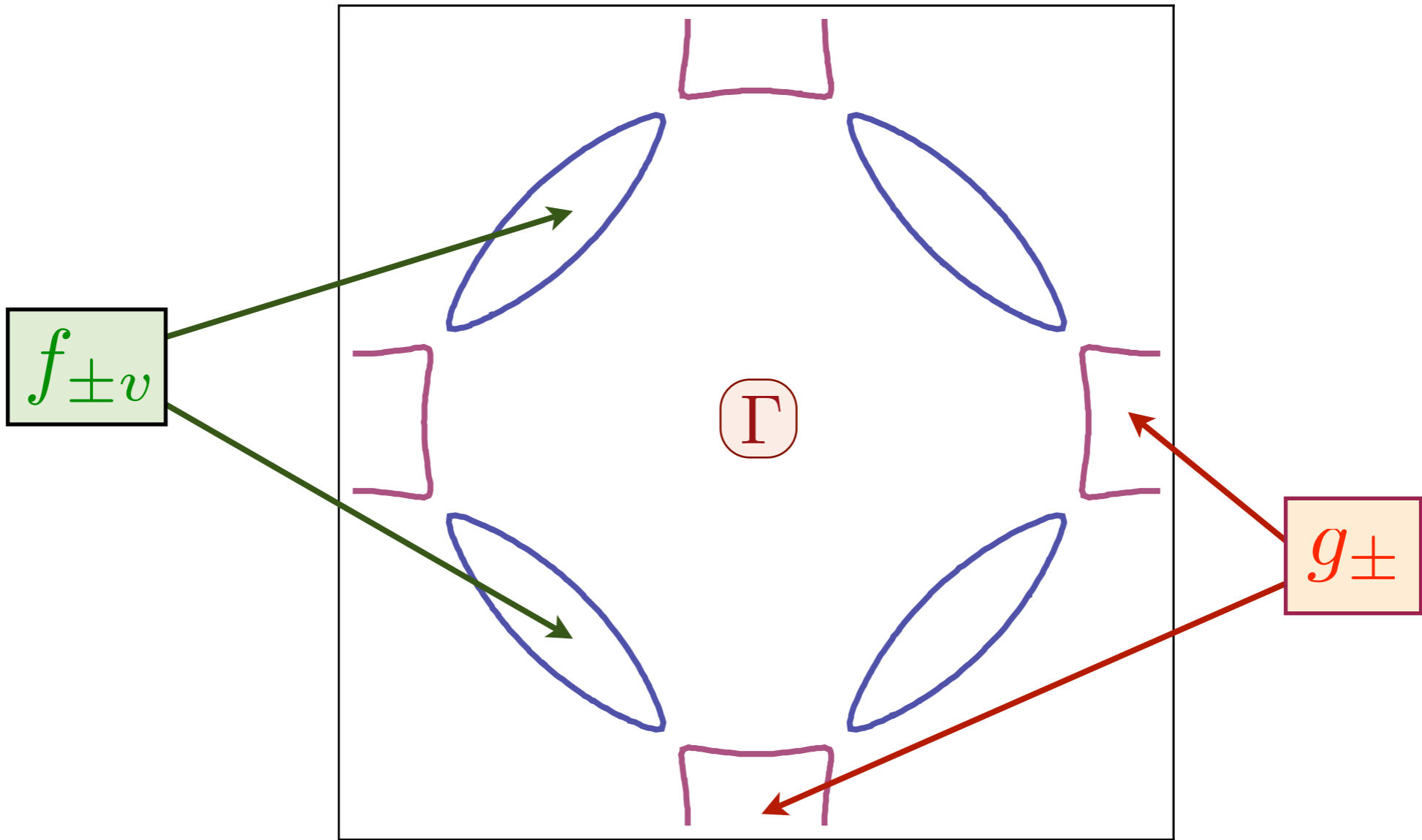
$$\frac{eH_{p2}(0)}{m^*c} = \frac{\pi^2 k_B T_{p0}^2}{\gamma_E \hbar T_F}$$

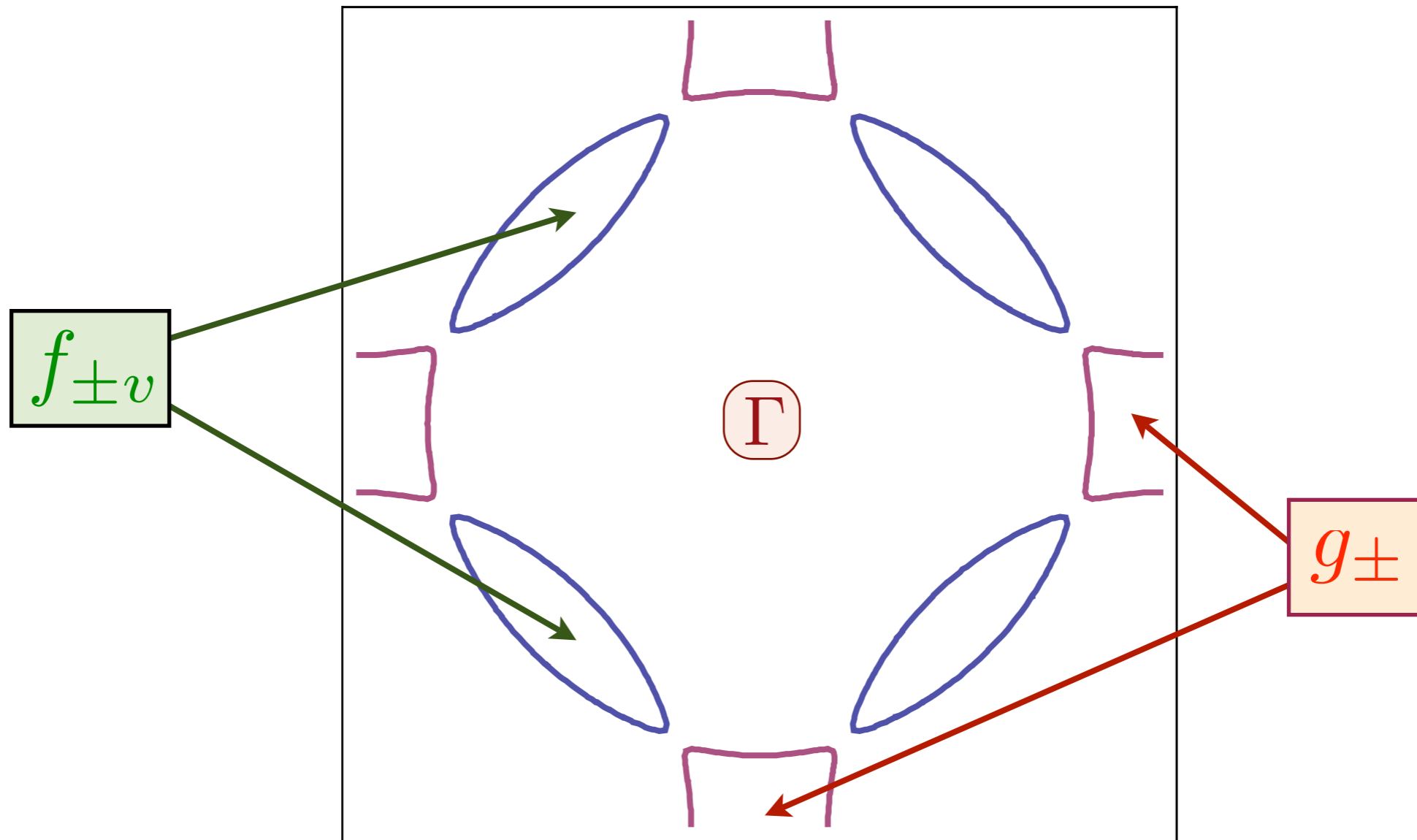
- This leads to the pairing temperature of order

$$T_{p0} \text{ K} \approx \sqrt{\frac{0.24m_e}{m^*} [T_F \text{ K}][H_{p2}(0) \text{ T}]} \sim 100 \text{ K} \text{ or } 2\Delta \sim 400 \text{ K}$$

Strong e-pocket pairing removes Fermi surface signatures from $H=0$ photoemission experiments







Low energy theory for spinless, charge $+e$ fermions $f_{\pm v}$:

$$\mathcal{L}_f = \sum_{v=1,2} \left\{ f_{+v}^\dagger \left[(\partial_\tau - iA_\tau) - \frac{1}{2m^*} (\nabla - i\mathbf{A})^2 - \mu \right] f_{+v} + f_{-v}^\dagger \left[(\partial_\tau + iA_\tau) - \frac{1}{2m^*} (\nabla + i\mathbf{A})^2 - \mu \right] f_{-v} \right\}$$

Weak pairing of the f_{\pm} hole pockets

$$\mathcal{L}_{\text{Josephson}} = iJ [g_+ g_-] \left[f_{+1} \overleftrightarrow{\partial}_x f_{-1} - f_{+1} \overleftrightarrow{\partial}_y f_{-1} + f_{+2} \overleftrightarrow{\partial}_x f_{-2} + f_{+2} \overleftrightarrow{\partial}_y f_{-2} \right] + \text{H.c.}$$

V. B. Geshkenbein, L. B. Ioffe, and A. I. Larkin, Phys. Rev. B **55**, 3173 (1997).

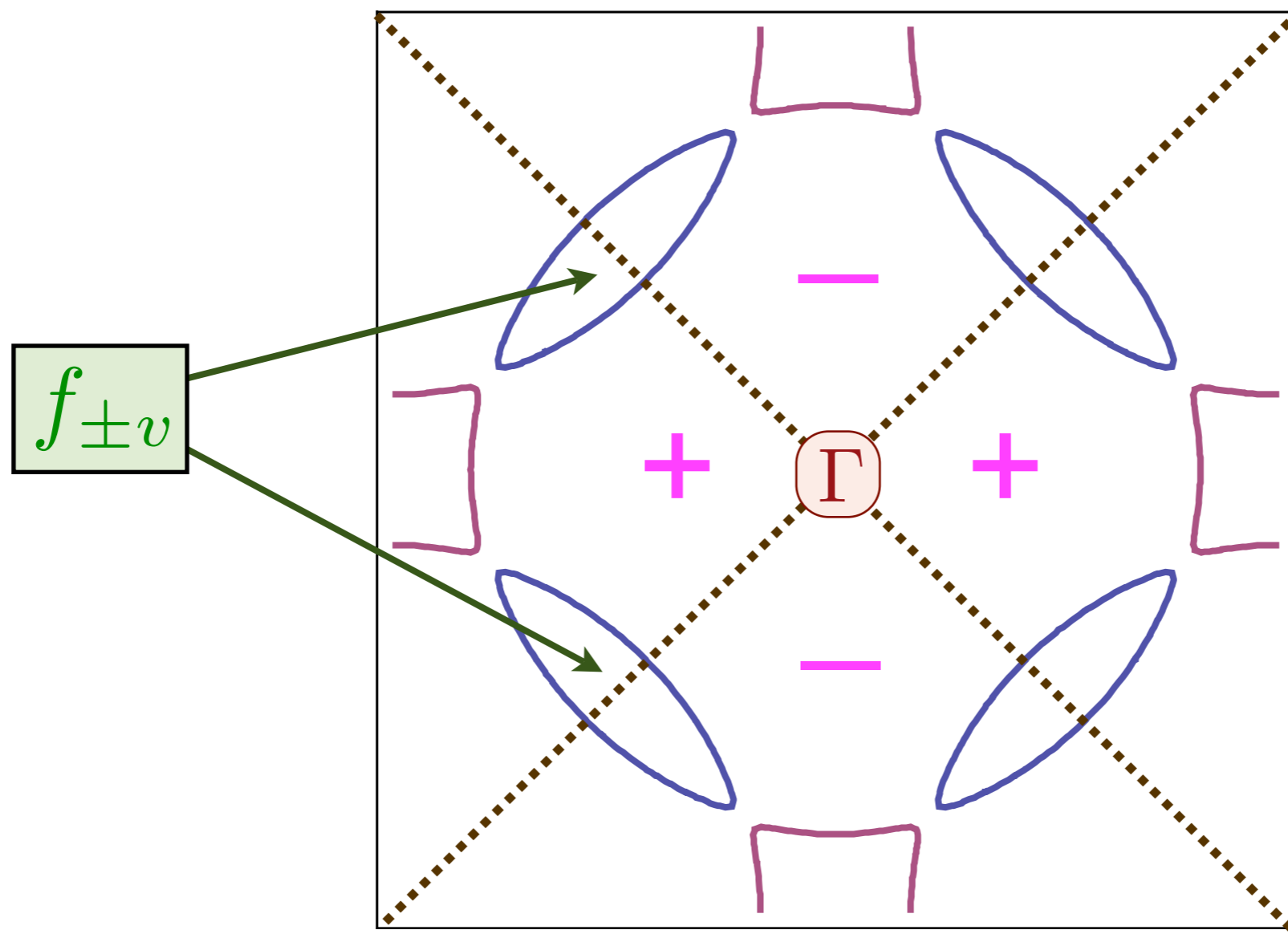
Proximity Josephson coupling J to g_{\pm} fermions leads to p -wave pairing of the $f_{\pm v}$ fermions. The A_{μ} gauge forces are pair-breaking, and so the pairing is weak.

$$\langle f_{+1}(\mathbf{k}) f_{-1}(-\mathbf{k}) \rangle \sim (k_x - k_y) J \langle g_+ g_- \rangle;$$

$$\langle f_{+2}(\mathbf{k}) f_{-2}(-\mathbf{k}) \rangle \sim (k_x + k_y) J \langle g_+ g_- \rangle;$$

$$\langle f_{+1}(\mathbf{k}) f_{-2}(-\mathbf{k}) \rangle = 0,$$

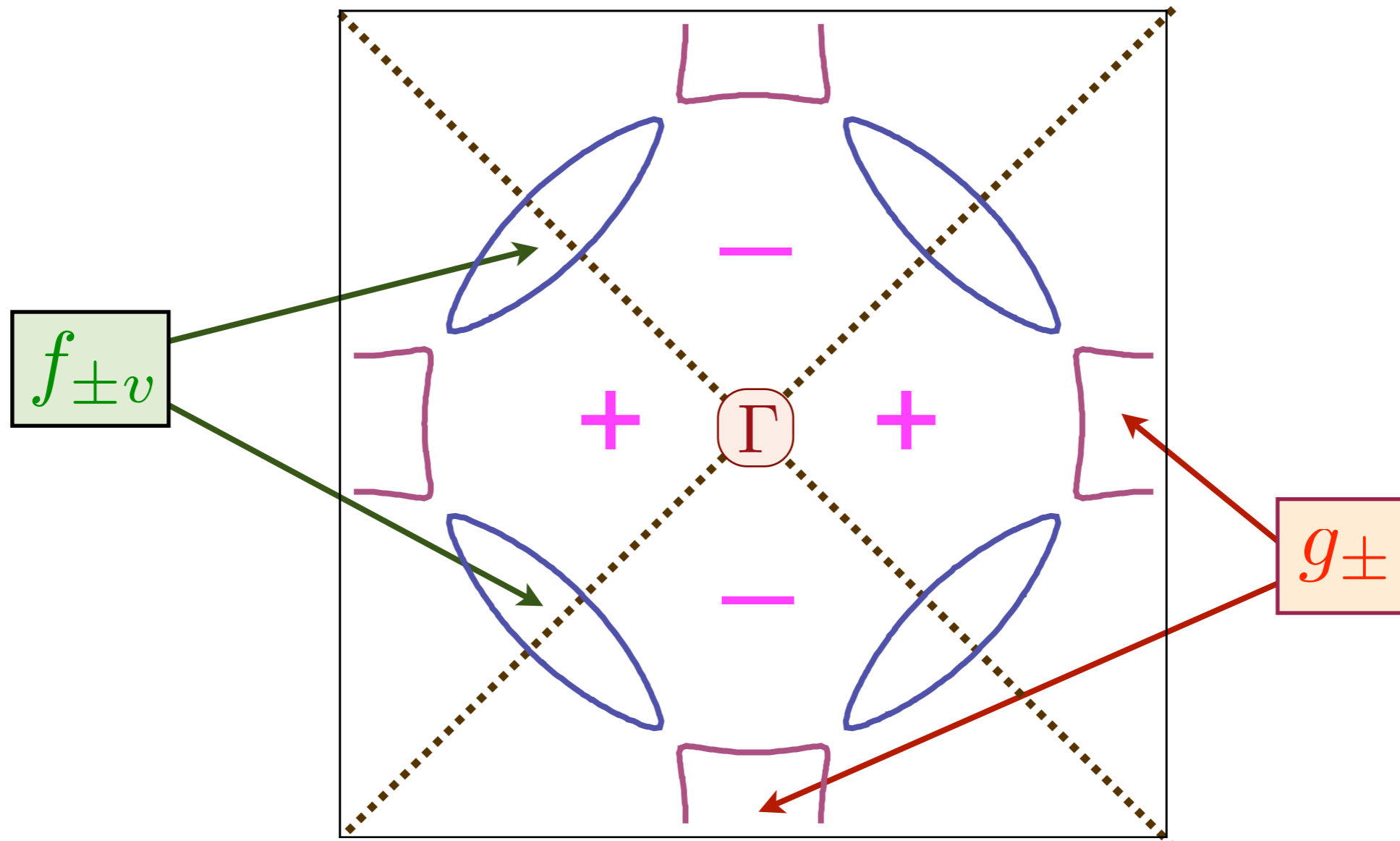
Weak pairing of the f_{\pm} hole pockets



$$\langle f_{+1}(\mathbf{k}) f_{-1}(-\mathbf{k}) \rangle \sim (k_x - k_y) J \langle g_+ g_- \rangle;$$

$$\langle f_{+2}(\mathbf{k}) f_{-2}(-\mathbf{k}) \rangle \sim (k_x + k_y) J \langle g_+ g_- \rangle;$$

$$\langle f_{+1}(\mathbf{k}) f_{-2}(-\mathbf{k}) \rangle = 0,$$



d -wave pairing of the electrons is associated with

- **Strong s -wave** pairing of g_{\pm}
- **Weak p -wave** pairing of $f_{\pm v}$.

Conclusions

- ★ Non-Landau-Ginzburg theory for loss of spin density wave order in a metal

Conclusions

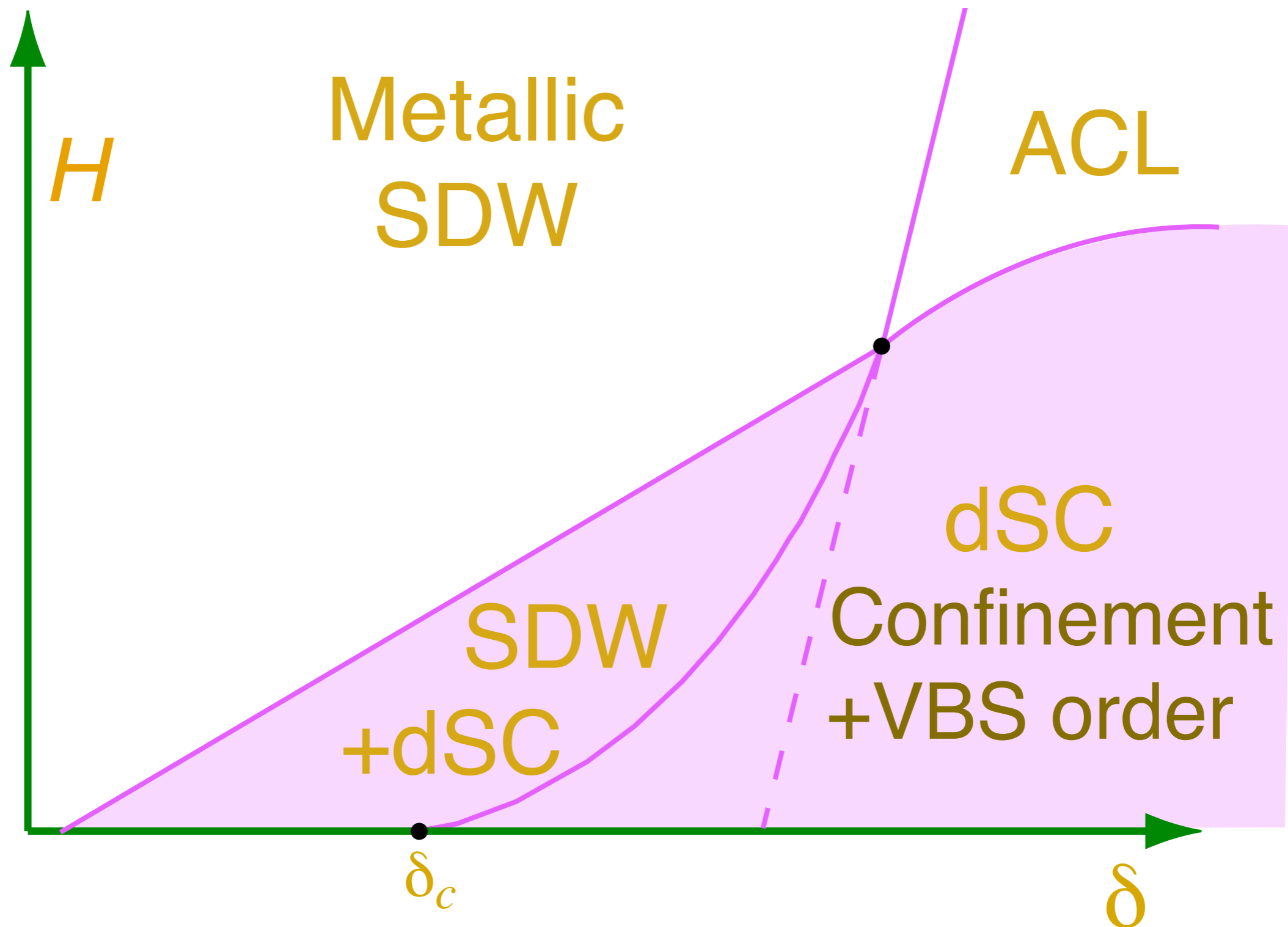
- ★ Non-Landau-Ginzburg theory for loss of spin density wave order in a metal
- ★ Natural route to d -wave pairing with strong pairing at the antinodes and weak pairing at the nodes

Conclusions

- ★ Non-Landau-Ginzburg theory for loss of spin density wave order in a metal
- ★ Natural route to d -wave pairing with strong pairing at the antinodes and weak pairing at the nodes
- ★ New metallic state, the ACL with “ghost” electron and hole pockets, is a useful starting point for building field-doping phase diagram

Phase diagram

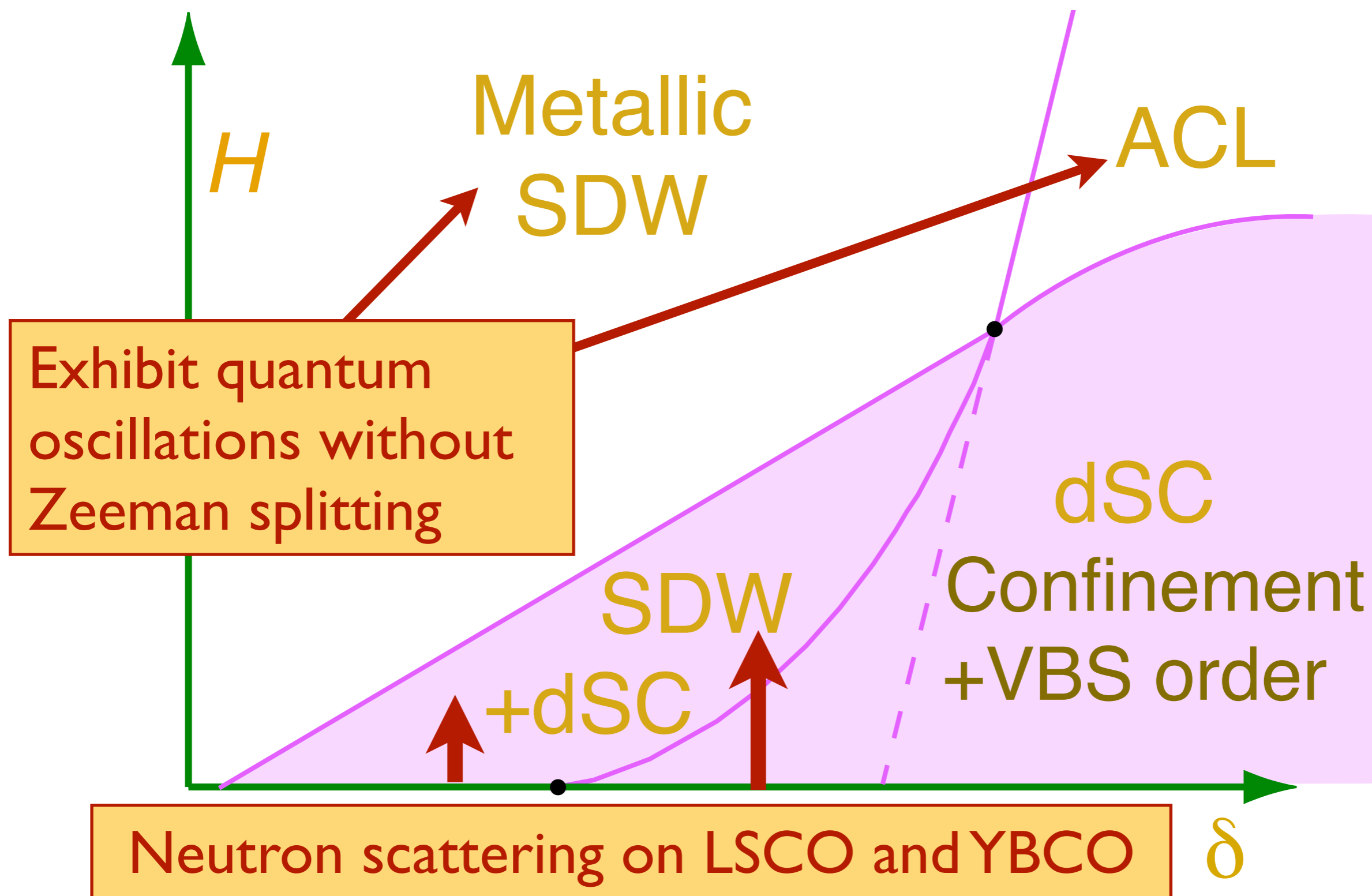
as a function of hole density $\delta \sim t$ and magnetic field H .



Interplay of dSC and SDW order is similar to theory of competing orders

Phase diagram

as a function of hole density $\delta \sim t$ and magnetic field H .



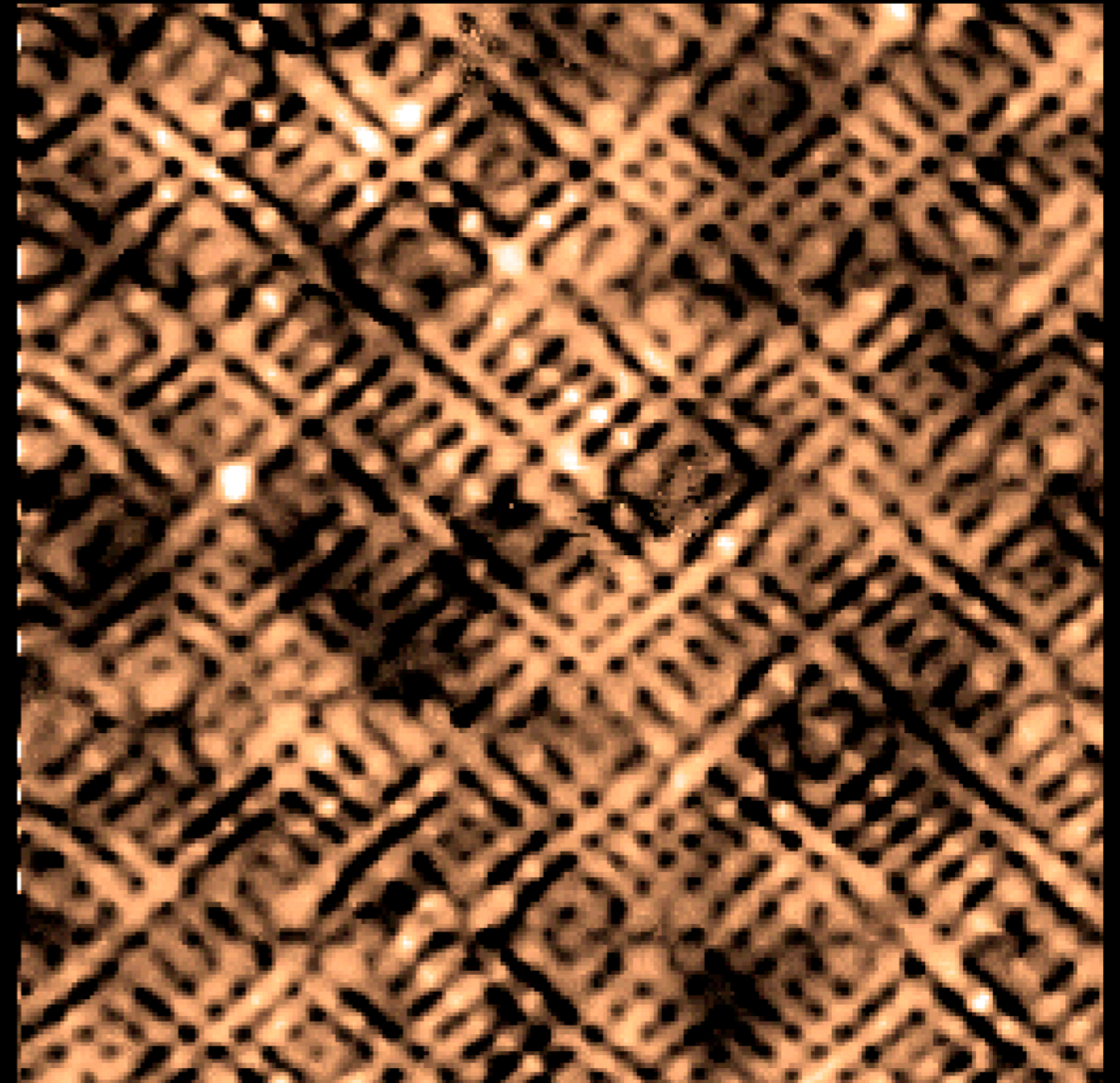
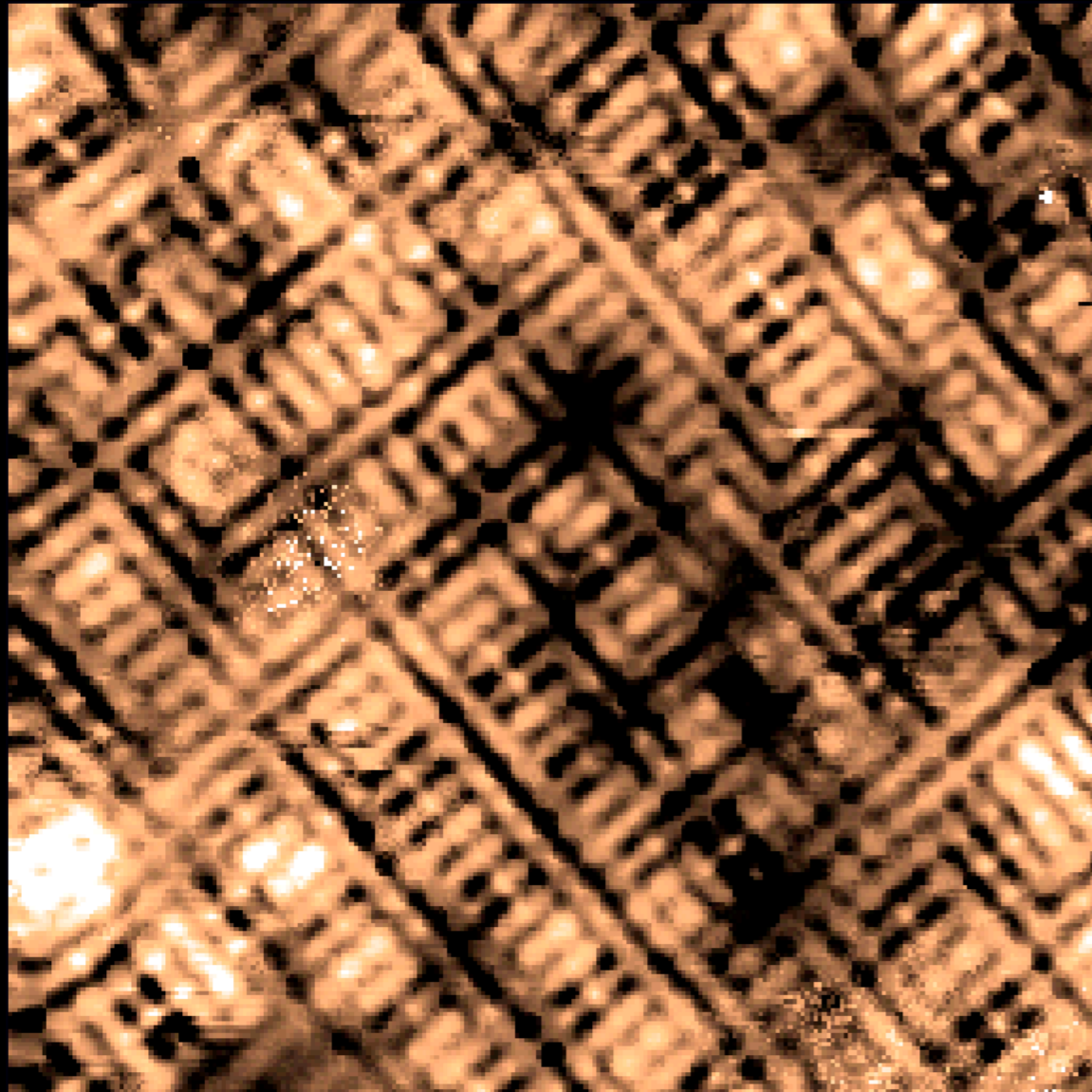
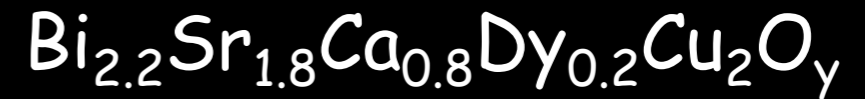
Conclusions

- ★ Non-Landau-Ginzburg theory for loss of spin density wave order in a metal
- ★ Natural route to d -wave pairing with strong pairing at the antinodes and weak pairing at the nodes
- ★ New metallic state, the ACL with “ghost” electron and hole pockets, is a useful starting point for building field-doping phase diagram

Conclusions

- ★ Non-Landau-Ginzburg theory for loss of spin density wave order in a metal
- ★ Natural route to d -wave pairing with strong pairing at the antinodes and weak pairing at the nodes
- ★ New metallic state, the ACL with “ghost” electron and hole pockets, is a useful starting point for building field-doping phase diagram
- ★ Paired electron pockets are expected to lead to valence-bond-solid modulations at low temperature

Tunneling Asymmetry (TA)-map at $E=150\text{meV}$



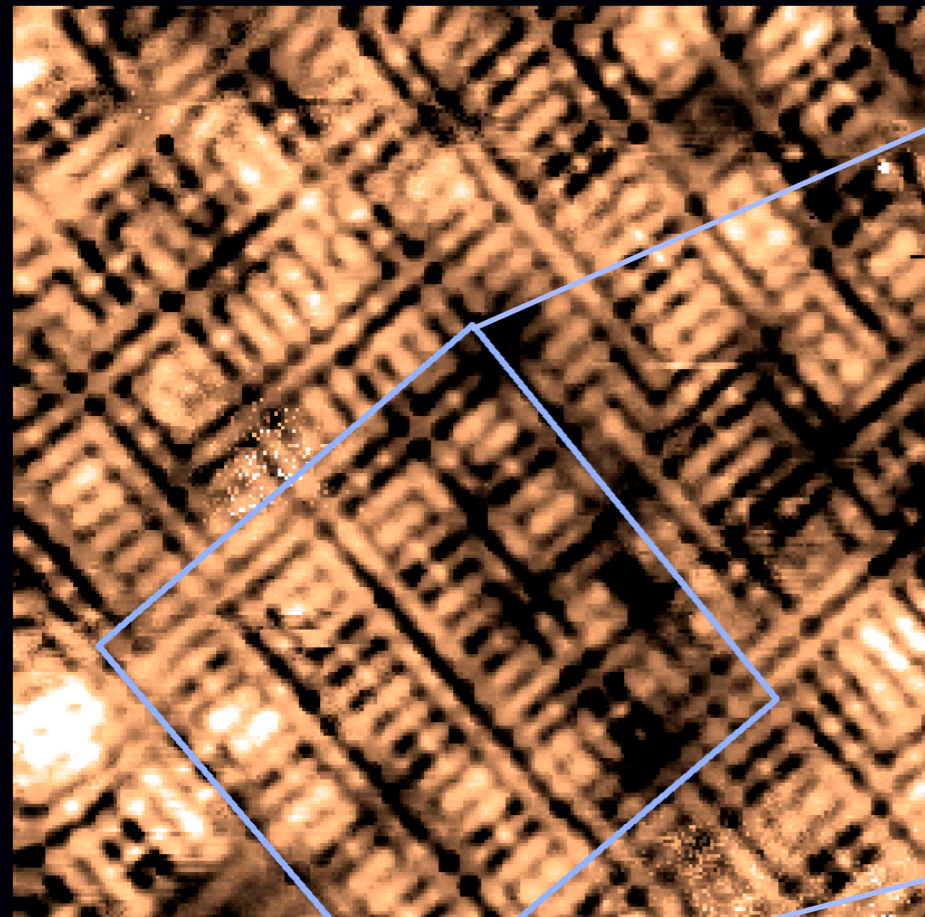
12 nm

Indistinguishable bond-centered TA contrast
with disperse $4a_0$ -wide nanodomains

Y. Kohsaka et al. *Science* 315, 1380 (2007)

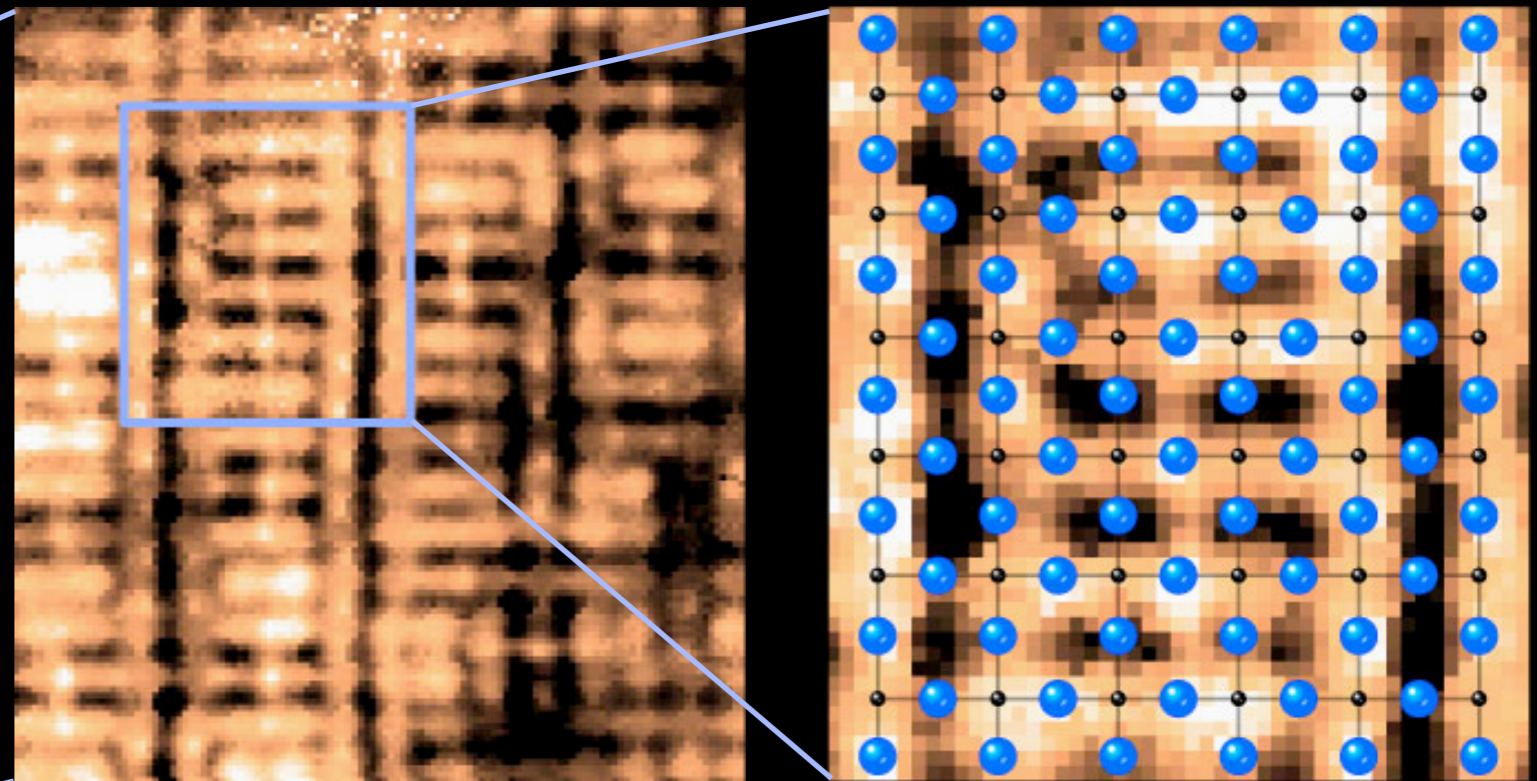
TA Contrast is at oxygen site (Cu-O-Cu bond-centered)

R map (150 mV)



← 12 nm →

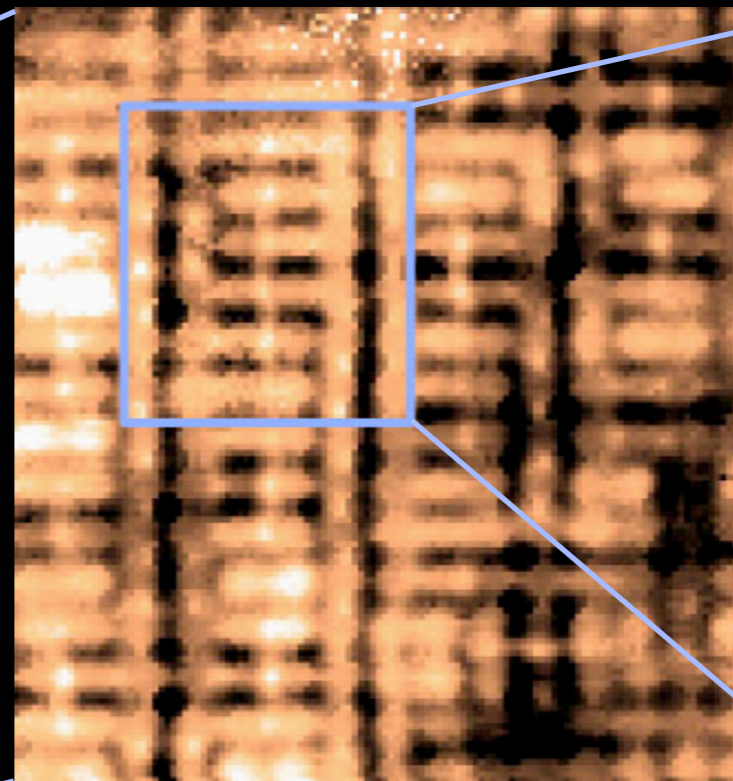
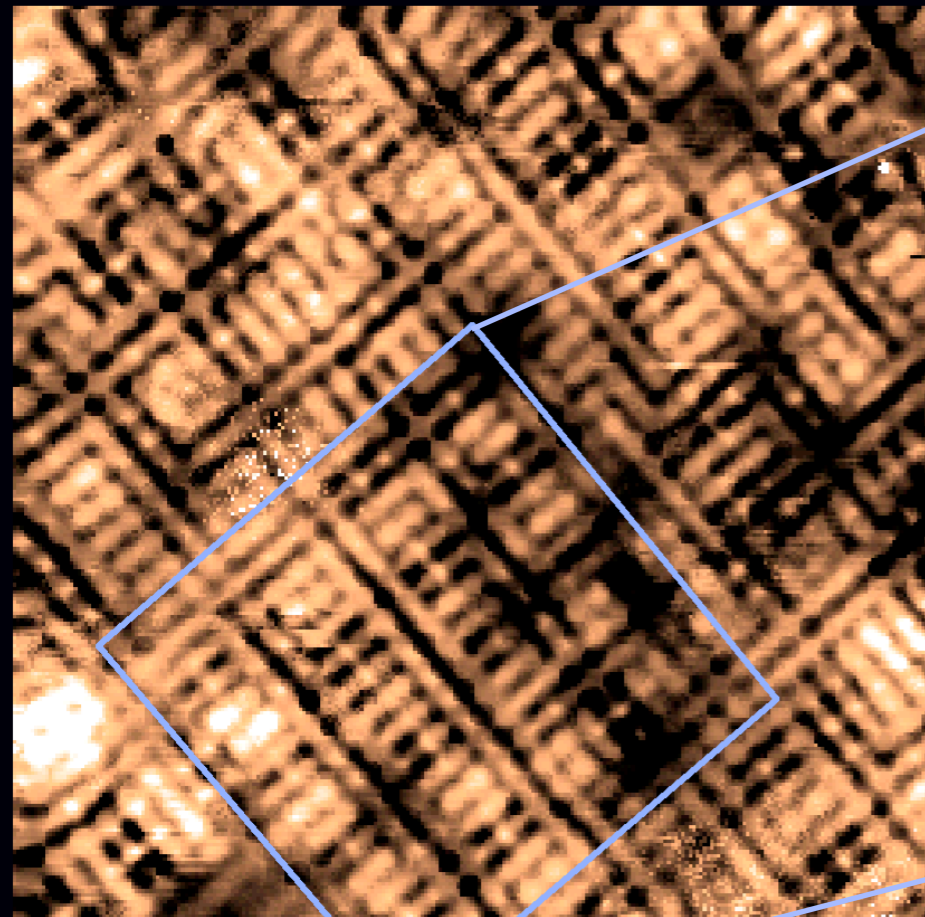
$\text{Ca}_{1.88}\text{Na}_{0.12}\text{CuO}_2\text{Cl}_2$, 4 K



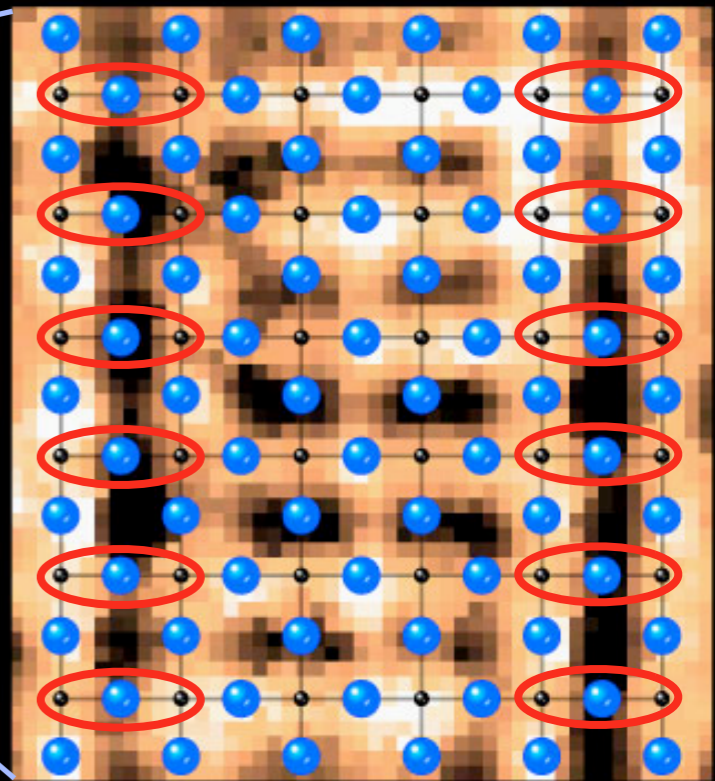
← $4a_0$ →

TA Contrast is at oxygen site (Cu-O-Cu bond-centered)

R map (150 mV)



$\text{Ca}_{1.88}\text{Na}_{0.12}\text{CuO}_2\text{Cl}_2$, 4 K



← 12 nm →

← $4a_0$ →

Evidence for a predicted valence bond supersolid

S. Sachdev and N. Read, *Int. J. Mod. Phys. B* **5**, 219 (1991).

M. Vojta and S. Sachdev, *Phys. Rev. Lett.* **83**, 3916 (1999).

Conclusions

- ★ Non-Landau-Ginzburg theory for loss of spin density wave order in a metal
- ★ Natural route to d -wave pairing with strong pairing at the antinodes and weak pairing at the nodes
- ★ New metallic state, the ACL with “ghost” electron and hole pockets, is a useful starting point for building field-doping phase diagram
- ★ Paired electron pockets are expected to lead to valence-bond-solid modulations at low temperature

Conclusions

- ★ Non-Landau-Ginzburg theory for loss of spin density wave order in a metal
- ★ Natural route to d -wave pairing with strong pairing at the antinodes and weak pairing at the nodes
- ★ New metallic state, the ACL with “ghost” electron and hole pockets, is a useful starting point for building field-doping phase diagram
- ★ Paired electron pockets are expected to lead to valence-bond-solid modulations at low temperature
- ★ Needed: theory for transition to “large” Fermi surface at higher doping